ÉCOLE POLYTECHNIQUE
FÉDÉRALE DE LAUSANNE

MES Semester Project

WIRE Laboratory

Prediction and Comparison of low-Reynolds Airfoil Performance

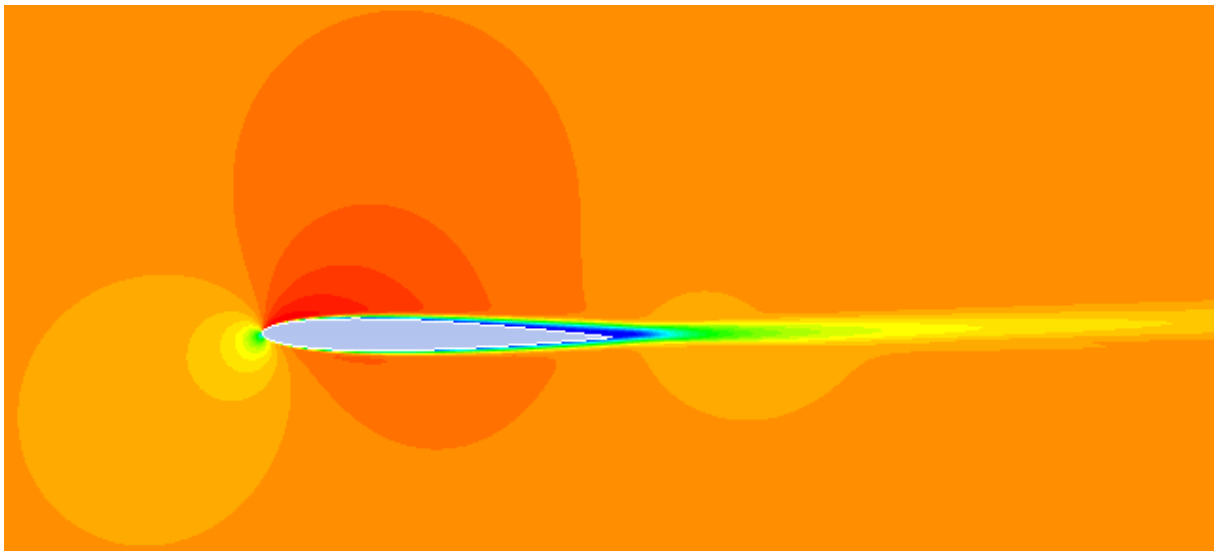

Eric Sauvageat

Tutor:

Vincent Rolin

Professor:

Fernando Porté-Agel

Autumn 2016

Abstract

This semester project is aiming to compare different airfoils in order to select the most promising one as blade shape for scaled the straight-bladed giromills used in wind tunnel experiments. For this matter, a large amount of steady-state CFD-simulations have been performed trying to characterize aerodynamic airfoil's performance at low Reynolds number. It is a continuation of a previous semester project which already selected the numerical model to use for the simulation and developed an automation process for batching several simulations which facilitated the creation of the dataset presented in this report.

In total, thirteen profiles have been investigated through various angles of attack and for chord Reynolds numbers of $1 \cdot 10^4$, $2 \cdot 10^4$ and $4 \cdot 10^4$. The airfoils chosen consist of five symmetrical NACA profiles of different thicknesses (NACA 0005 to NACA 0021), three modified NACA with sharp leading edge (NACA 0005-05, NACA 0009-05 and NACA 0012-05), two 5% cambered NACA profiles (NACA 5505 and NACA 5510) and three specific airfoils for low Reynolds number (E387, S1223 and BW3). Based on the tangential force coefficients of the airfoils, NACA 5505 and BW3 showed the overall best performances at this range of Reynolds which is in accordance with the existing studies on the subject as they are both thin airfoils with around 5% maximum camber at mid chord.

Contents

List of Figures

List of Tables

1 Introduction

Today maybe more than ever, the management of the Earth's resources calls for a rethinking of the energy production and distribution. The fossil fuels era is globally recognised to run the world's population into a stone wall and new technologies have now to emerge to fill the predictable energetic gap.

The wind conversion to electricity has been exploited for a long time and is now an integral part of the world's landscape mostly in the form of Horizontal Axis Wind Turbines (HAWTs). These devices have benefited from a large volume of research which has lead to significant progress in the domain during the past decades. However, the improvements on these devices are getting more incremental which lead to an increased interest in less common technologies such as the Vertical Axis Wind Turbines (VAWTs).

This type of wind turbines has gained a growing interest in the recent years and they are offering some interesting advantages compared to the horizontal devices. For instance, they are insensitive to the wind direction which is simplifying their designs as they do not require any yaw equipment. They have a better capacity to withstand high winds and could provide potential improvement to the power density in wind farms.

However, the studies on the VAWTs are scarce and there is a large margin for improvements if one can overcome the difficulties linked with this technology. Amongst them, we can mention the difficulty to self-start and to predict their global performance correctly due to their more complex aerodynamic than the HAWTs. In fact, the blades of such turbines are experiencing large variation in the incoming flow direction which makes the prediction of their aerodynamics performance difficult.

The present report is focusing on the study of the scaled VAWTs used for wind tunnel experiments. It is aiming to predict and compare the performance of different airfoil profiles that could be used as blade shapes in such turbines. Furthermore, it is part of a bigger project which expands from the study of the airfoil's aerodynamic performance alone (subject of the present report) to the simulation of these airfoils as part of a VAWT and finally to the selection of the most promising profile for an experimental testing in the wind tunnel at EPFL.

2 Vertical Axis Wind Turbines

There are different types of VAWTs, and they can be categorised whether they are actuated by the lift (Darrieus rotor) or the drag force (Savonius rotor). During this project, we will study a specific type of Darrieus rotor; the three straight-bladed type, also called giromill.

Giromills are using straight vertical blades attached to the middle axis and arranged symmetrically around it. They can have different number and shape of blades and an example of a two-bladed turbine is presented in Figure 1. For practical and economical reasons, the most widely used shapes for such turbines are the conventional NACA profiles well known in aerodynamics.

As said previously, the performance's prediction of such turbines is not an easy task, mostly because of their operating principle which is involving some complex aerodynamic

behaviour. This principle will be presented briefly in the section 2.1.

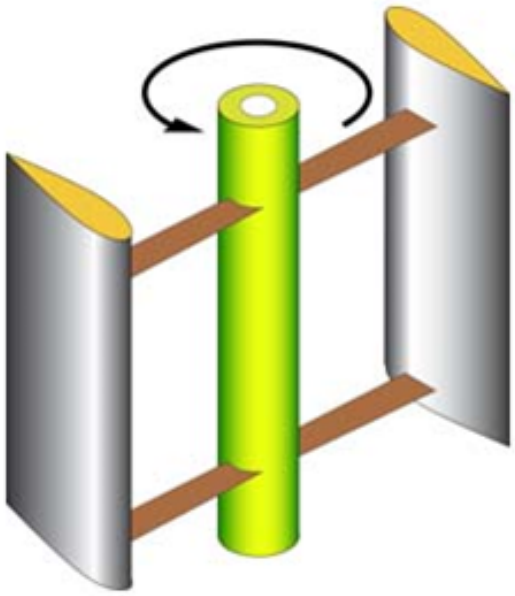

Figure 1: Example of a straight two-bladed Vertical Axis Wind Turbine. Image taken from: `http://www.thefullwiki.org/Darrieus_wind_turbine`

2.1 Operating principle of a VAWT

Similarly to the airplane's wings, the operating principles of these turbines relies on the lift and drag forces occurring on the blade when it is facing the air flow. These forces depend on the wind speed, the blade profile and the angle at which it is facing the wind (called angle of attack and designated as α). The forces acting on a single blade of a giromill are presented in Figure 2 and their effects will be further detailed in section 2.2. On a VAWT, the difficulty is that the blades are rotating which means they are subject to some continuous changes in wind direction (even reaching α higher than stall). In the case of giromills with more than one blade, the downwind part of the turbine will be subject to disturbed incoming flow velocity after the crossing of the upwind blade and this phenomena is also participating to difficulties that occur for modelling the performance of such turbines.

The angle at which the blade is facing the wind is depending not only on the azimuth angle θ, but also on the tip-speed ratio λ (TSR). This ratio is a key parameter for the study of a VAWT and is defined as the ratio between the ground speed of the blade's tip and the wind velocity:

$$\lambda = \frac{\omega R}{U_\infty} \tag{1}$$

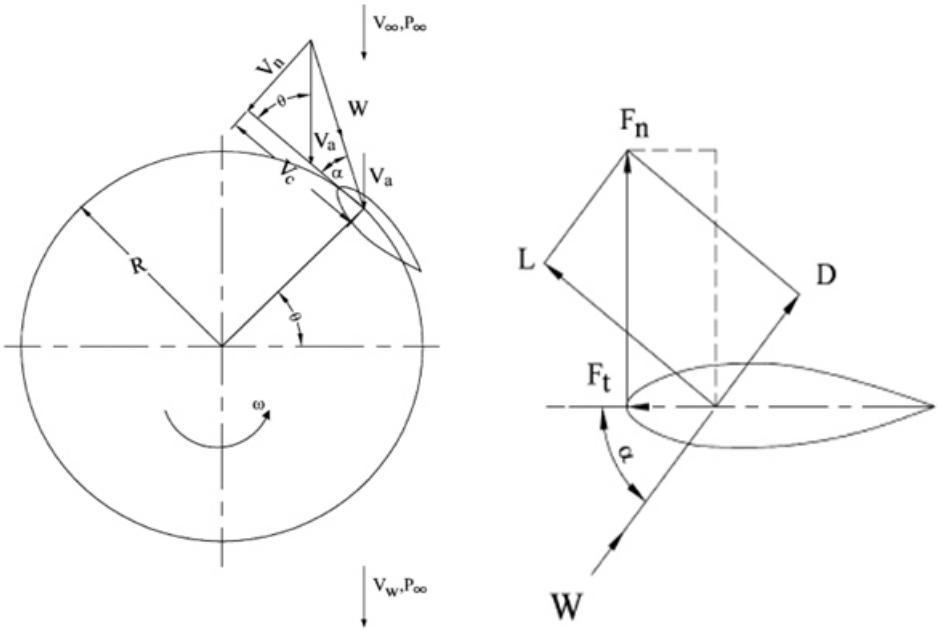

Figure 2: Flow velocities and force diagram on a single blade [1]

In fact, the relation between the angle of attack α and the TSR can be deduced from the force and velocity diagram from Figure 2:

$$\alpha = \tan^{-1}\left(\frac{\sin(\theta)}{\cos(\theta) + \lambda}\right) \tag{2}$$

It means that, for a given TSR, the angle of attack of an airfoil in a VAWT is oscillating at a certain amplitude in function of the azimuth angle θ. This phenomena is represented in Figure 3 for a complete revolution of the turbine and has the consequence that a large range of angles of attack have to be studied in order to characterized the performance of airfoils operating in such turbines.

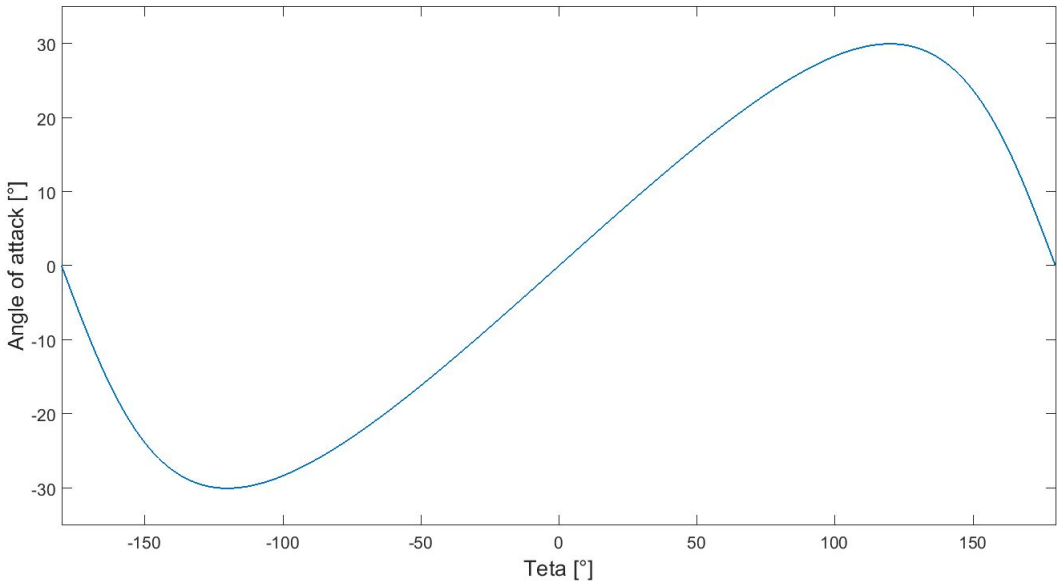

Figure 3: Variation of angle of attack over θ for $\lambda = 2$

2.2 Power extraction from a VAWT

From Figure 2, we can see that the main force that will create a torque and cause the turbine to turn is the **tangential force** F_t. This instantaneous force can be described with the lift (L) and drag (D) forces for each angle of attack as:

$$F_t = L\sin(\alpha) - D\cos(\alpha) \tag{3}$$

Similarly, this expression can be written with normalized coefficient for each of the force. The **tangential force coefficient** is defined as:

$$C_t = C_l\sin(\alpha) - C_d\cos(\alpha) \tag{4}$$

With C_l and C_d being the lift and drag coefficients that are generally used for describing airfoil's performance in aerodynamics. They are defined as:

$$C_l = \frac{L}{\frac{1}{2}\rho S v_\infty^2} \tag{5}$$

$$C_d = \frac{D}{\frac{1}{2}\rho S v_\infty^2} \tag{6}$$

$\frac{1}{2}\rho v_\infty^2$ being the dynamic pressure of the inflow and S the surface of the blade that can be described by its chord length c and its height h.

This tangential force coefficient enable to characterize the **instantaneous torque** Q_i which can be expressed with the radius of the rotor and the relative velocity of the wind arriving on the blade (respectively R and W on Figure 2) by:

$$Q_i = \frac{1}{2}\rho W^2 hcC_t R \tag{7}$$

This torque is a function of α and consequently of azimuthal angle θ. Therefore it can be averaged for the complete rotation of the turbine and multiplying it by the number of blades is giving the **total torque (Q)**. The **total power output (P)** from the turbines will be then the multiplication of this torque with the rotational speed of the turbine ω:

$$P = Q \cdot \omega \tag{8}$$

The goal for a VAWT is therefore to maximize this coefficient of tangential force in order to maximize the torque created by the wind and consequently the power output from the turbine. Practically, we can already consider the ratio between the lift and drag coefficient (lift-to-drag ratio) as being a good indicator of the performance of a given blade. The higher is this ratio, the higher should be the power extraction of the turbine.

3 Definition of the project

The main purpose of this project is to predict and compare the performance of different airfoil profiles for a use as blade shapes in scaled VAWTs.

More specifically, the goal is to deal with the three-bladed scaled VAWTs that are used for experimental testing in the wind tunnel of the WIRE lab at EPFL. As seen before, the efficiency of a VAWT depends highly on the tangential force that will occur on the blades of the turbines. It is described by its coefficient of tangential force which depends on the lift-to-drag ratio. The idea is then that, knowing the lift-to-drag ratio of a given profile over the range of angle of attack occurring during the rotation of the turbine, we should be able to estimate the power production of a VAWT using such blade shape.

Studying the aerodynamics performance of the blade itself could then be sufficient to study and predict the performance of the turbine in its whole. Practically, a large range of numerical steady-state simulations will be performed on different airfoil profiles in order to compare them on their basis of their tangential force coefficient. The commercial software Ansys Fluent will be used for this task. On the long term, it should enable to create a database of airfoil's performances at low Reynolds numbers in order to select the most promising profile for an experimental testing.

In term of scale, we are dealing with blade chord of 5 cm and radius rotor of around 8 cm. A study with this kind of scaled VAWT has already been performed at the WIRE Laboratory and the parameters of the simulations will be chosen according to the ones used in reference [2]:

- The chord Reynolds number[1] is in the range of $2 \cdot 10^4$. In fact the simulations will be performed with three different Reynolds number; $Re_c = 1 \cdot 10^4$, $2 \cdot 10^4$ and $4 \cdot 10^4$.
- The Tip Speed Ratio is set to $\lambda = 2$ which means the study will have to consider angle of attack ranging from approximately $-30°$ to $30°$ (see Figure 3). In fact, it has now been shown in various studies that stall delay occurs on VAWT and therefore, a dynamic stall model will be applied to compute the lift and drag coefficients for the bigger range of angle (especially surpassing stall). We are then considering only angle of attack ranging from 0 to $14°$ with an increment of $2°$.

Considering the number of simulations to perform in order to characterize one profile (24 in total), an automation of the process has been created by Emile Piccoli in a previous semester project [3] at the WIRE Laboratory and this is represented schematically in Figure 4. Basically, this process is enabling the launch of multiple simulations in series on Fluent. After importing the geometry and creating the mesh in ANSYS, launching the Fluent solver is writing a "Setup Output case file" that can be extracted from the Fluent folder and stored for each airfoil. Journal files are then automatically generated with Python using the specific airfoil's setup case file for each angle of attack and each Reynolds number. A main command program is then used to run all the journal files directly in Fluent until all the files have been launched. For the results, Fluent have been configured to write down the history of lift and drag coefficients for each case and it is additionally writing a case and a data file for the solution. All the scripts used for this

[1] For practical reasons, we will speak only about "Reynolds number" in the rest of the report

report are available in Emile's report (see [3]) as well as their detailed description. For this report, only the post-process file written in Matlab will be presented in Appendix D.

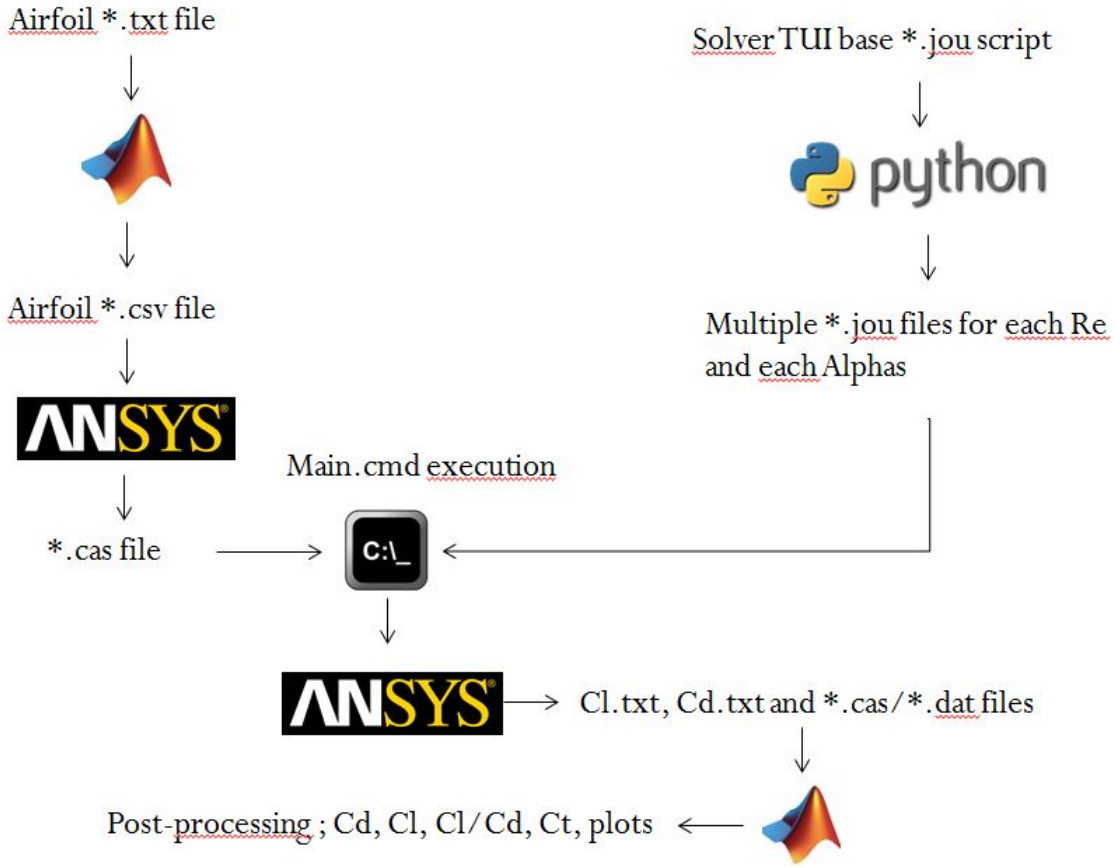

Figure 4: Automation process for the simulations (by E. Piccoli)

3.1 Challenges

Low-Reynolds aerodynamic

The main challenge in this project is linked to the simulation of the flow around the airfoil alone. In fact, we are dealing here with the low-Reynolds aerodynamic in which the viscous effect are of primary importance for the right modelling of the air flow. More specifically, we are not located in fully laminar nor turbulent regime, but in a transition mode between both which is responsible for the complexity of the calculations that we have to deal with. In fact, the potential flow theories that can be applied for higher Reynolds do not seem to be valid anymore for the calculation of the lift force and transition models have to be considered (well summarized in [4]).

Several transition models are offered by commercial software like Ansys Fluent but the choice between them is not obvious as it relies mostly on previous experiences which are really scarce in this range of Reynolds number. This aspect has mainly be addressed by the previous semester project, especially regarding the choice of the model that will enable the best prediction of the flow features around the airfoil. Particularly, it was paid a great attention to the Laminar Separation Bubble (LSB) phenomena as it seems to have significant impact on the calculated aerodynamic forces at this range of Reynolds number

(see [5] for more details). The model chosen and the validation performed by Emile will be presented in section 3.2 but the complete process for the model's choice will not be repeated in this report (see [3]).

Meshing and convergence of non-symmetrical airfoils

The previous semester project focused on finding the best model for the simulations and automating the process in order to enable the simulations of many different airfoils. Therefore, it has only performed simulations on symmetrical NACA 0012 and NACA 0018 profiles and it appeared that the mesh chosen for this matter was not suitable anymore when dealing with non-symmetrical ones. A previous semester project at the WIRE Lab was found to be dealing with that kind of mesh but it used a meshing software (GAMBIT) which was no longer available and it was not possible to reproduce the exact same mesh on Fluent. The building of a new mesh was then necessary and it finally appeared to be very time consuming in this project. After trying large amounts of meshes, an acceptable mesh has been found and is presented in section 3.2.

Still, even if this mesh seemed visually acceptable, it could not provide good convergence for the non-symmetrical airfoils. In fact, very few cases have reached convergence and there is still some improvements needed in this domain if we want some more reliable results for the non-symmetrical profiles (see section 6).

3.2 Numerical setup

Symmetrical profiles

For symmetrical profiles, the numerical setup was already described and validated in the previous report and after re-writing all the files, the automation process worked nicely and the simulations gave good results. As only few corrections have been added to his work, only few details will be given about the setup for symmetrical airfoils in this report.

Simulations were launched using a typical C-Mesh with a 12.5 chord length radius for the front section and a square of size $s = 12.5$ m for the past section. This mesh can be seen in the previous report [3]. A mesh convergence had also been performed in the previous report in order to ensure a good capture of the flow patterns near the airfoil. The Y+ value had been studied and the size of the first cell has been adapted in order to get some Y+ values close to one.

The boundary conditions were defined on three different groups of edges:

- Inlet: Defined as velocity components applied on the main x and y axis for the simulations of the three different chord Reynolds numbers and angles of attack. Chord length was set to 1 m and the properties of the fluid were the default ones in Fluent. Therefore the velocity magnitude was applied for each of the three chord Reynolds numbers as:

$$U_\infty = \frac{Re_c \cdot \nu}{c} \tag{9}$$

  And then simply projected on the main axis in order to simulate the angle of attack

α as:

$$U_x = \cos(\alpha) \cdot U_\infty$$

$$U_y = \sin(\alpha) \cdot U_\infty$$

- Outlet: Defined as a pressure boundary condition, set as the value of the static pressure
- Airfoil: Treated as a no-slip wall.

Regarding the solver, two-dimensional with double precision and with second order upwind difference scheme for velocity has been chosen by Emile. Pressure-velocity coupling was performed by the default SIMPLE algorithm. He tested different turbulence models for low-Reynolds regimes on his simulations and evaluated the k-epsilon and the sst-transition against the datasets from Kumar et al. [6] for the NACA0018 symmetrical profile (CFD-simulations with Fluent as well). The sst-transition model was found to perform better and after a visual inspection of the flow patterns and a comparison with extrapolated experimental data from Sheldahl [7], this model was chosen for the rest of the project. In term of convergence, Emile judged it on the basis of the residuals and on the lift and drag coefficient's histories. He let the simulations run for 10'000 iterations for each case and found good convergence for low angle of attack (below 10^{-6} for continuity equation). For higher angles of attack, he had to lower the under-relaxation factor in order to avoid oscillatory behaviour on the lift and drag coefficient (0.35 for momentum and 0,2 for pressure) and sometimes launch recalculation when there was no convergence reached in 10'000 iterations.

Other variations of parameters have been tried by Emile such as varying the size of the domain or the mesh resolution. All these can be found in detail in his report [3] as well as his results and validation with existing data.

We kept globally the same setup for our symmetrical profiles' simulations but with an addition of convergence factor for all residuals at 10^{-5} in order to gain some computing time when the convergence of the solution was reached before.

Non-symmetrical profiles

Numerical simulations of non-symmetrical profiles have not been performed by Emile and, as said before, the mesh built for the symmetrical ones was not working anymore. The mesh built for the simulations of non-symmetrical airfoils is presented in Figure 5. It consists of the same C-mesh used for the symmetrical simulations but includes a circle of radius $R = 2 \cdot chord$ centered around the airfoil. The cell's size is set at 0.3 m in the domain and refined at 0.03 m for the inside circle. An inflation layer (10 layers with 1.3 growth rate) as well as an edge sizing (130 divisions with smooth transition bias of 1.2) are then applied around both sides of the airfoil in order to capture the viscous effects and to refine the elements at the leading and trailing edges. After a new grid convergence, the size of the first cells have been reset to $1.8 \cdot 10^{-3}$ m in order to keep the Y+ value around one. As an example, the Y+ for E387 airfoil at $Re = 10^4$ and $\alpha = 8°$ is presented in Figure 6. Similar graphs can be found for all non-symmetrical cases.

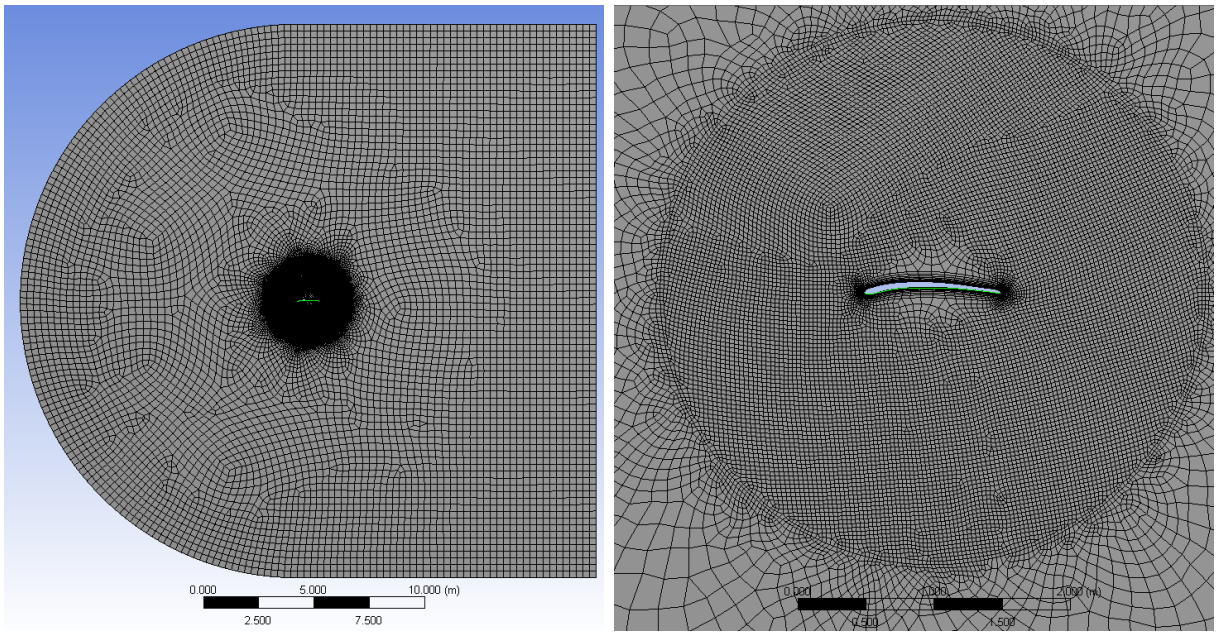

(a) Mesh (b) Mesh, zoomed

Figure 5: Mesh for non-symmetrical airfoils

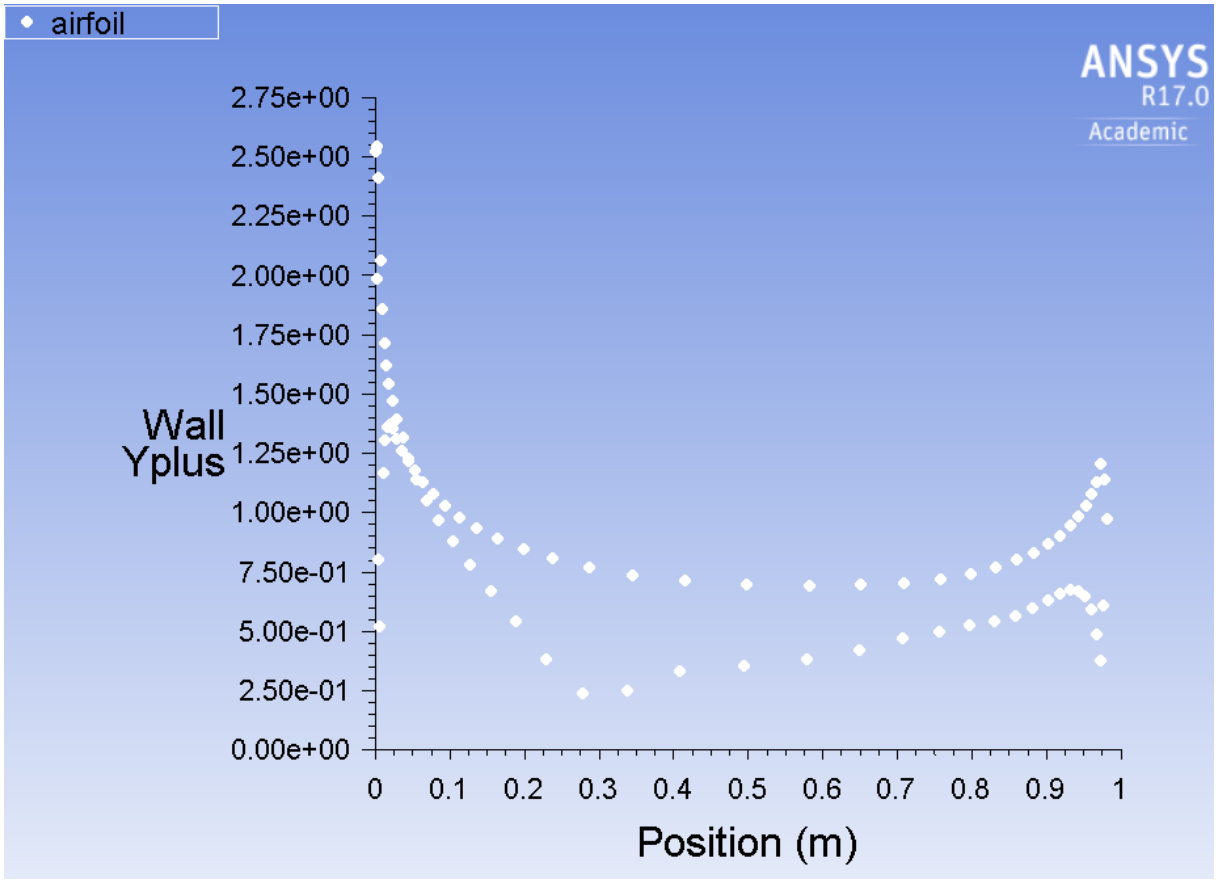

Figure 6: Y+ values on the surface of the E387 airfoil

As we saw before, the convergence for the non-symmetrical airfoils is still a big issue in this project and it will have to be addressed seriously in the next semester report. In fact,

the minimum orthogonal quality of this mesh is really poor ($2.6 \cdot 10^{-5}$) and the need for a new design is important. Improvements on the mesh has been addressed by my tutor V. Rolin and a new mesh for this kind of profile is under creation. Simulations should be run on this new mesh soon in order to potentially get better convergence on non-symmetrical airfoils.

3.3 Expected results

As said before, the studies in this range of Reynolds are scarce as the focus has mainly stayed on $Re \geqslant 10^6$ which is the order of magnitude at which are operating big aeroplanes. The research focusing on low-Reynolds numbers are often limited to $Re \geqslant 10^5$ and for this reason, only few studies concerning small wind turbines or small aircraft (drones) are offering results for $Re \approx 10^4$. Additionally, the measurements of aerodynamic forces at this regime are particularly difficult as they are generally smaller than at bigger Reynolds numbers (which means their relative uncertainties are much higher) and they are more sensitive to the model geometry and roughness which make it hardly repeatable (see [4]). Modelling the flow pattern at this low Reynolds regime is also a complex matter (as briefly discussed in section 3.1). For all these reasons, the data presented below must be treated with great care. The results available for the range of Reynolds that interests us can be classified in 4 categories:

1. Experimental data:

   These are not easy to find but, for $Re = 4 \cdot 10^3$, there is a paper from 1997 which tested the influence of different airfoils shape (camber, thickness, ...) on aerodynamic characteristic [8]. They found that, added separately, the airfoil with the best performance at this Reynolds should be thin, have a sharp-leading edge and have a camber of about 5% at about mid chord. It is important to note that these recommendations has been formulated on conditions added separately and on small sample.

   Some results are also available for $Re = 6 \cdot 10^4$ from both the University of Illinois at Urbana-Champaign (UIUC) and Princeton University. Actually, the second is not available on-line but the tests from UIUC are resumed in two books [9] that are really extensive. They have tested different types of airfoils which are promising for the model-aviation at different Reynolds, including $Re = 6 \cdot 10^4$ and even lower for some airfoils (NACA 0009 for example has been tested at $Re = 4 \cdot 10^4$). All the detailed results will not be presented here but this book has been very interesting to make a first selection of airfoils for our simulations.

2. CFD-results:

   The main results in this domain are provided by Kumar et al. in a study on the implementation of VAWT on Mars [6]. They are the results of CFD simulations of NACA 0018 profile with Fluent at Reynolds number between 1000 and 160'000 using both free transition and fully turbulent model with the introduction of a self-designed intermittency function which is modifying the effective viscosity. They have compared their results with both experimental data at $Re = 160'000$ and with the extrapolated ones of Sheldahl and have found that the S-A free transition model seemed to predict more accurately the aerodynamic forces of NACA 0018.

3. Extrapolation of experimental data:

   Another way of validation used by Emile was the dataset created by Sheldahl et al. [7]. These are experimental data for four different symmetrical airfoils tested at bigger Reynolds ($\approx 0.5 \cdot 10^6$), with angle of attack ranging from 0 to 180°. These data have then been extrapolated to Reynolds number down to 10'000 and are to consider with great attention as they contains, for example, some negative lift value for positive angle of attack (see in the Results section).

4. Xfoil predictions:

   On Internet (for example; `http://www.airfoiltools.com`), it is possible to find some basic lift and drag polar computed with Xfoil. They do not have great values in term of accuracy but their predictions for $Re = 50'000$ are pretty close to the ones found in our simulations for $Re = 40'000$ and it is particularly true for the results of the comparison between airfoils. Therefore, it has also been used for the choice of the airfoils to simulate in our project.

As a quick conclusion, even if the results are scarce at this Reynolds regime, they are existing data that are of interests not too far from our Reynolds range or some that could potentially help to find the right model to perform our simulations. At least, some will be used for a comparison with our results in order to improve their reliability. Based on the four types of results presented before and on the literature, the awaited results for our range of Reynolds should pretty similar to the conclusions of Sunada [8] and the thin, cambered (around 5%) airfoils should show good aerodynamics performance in our simulations.

4 Airfoils selection

Until now, a total of thirteen different airfoils have been simulated during the semester. This project is not over and more have to be tested in the following months in order to get the most diversified range of airfoils possible. For this semester, the airfoils simulated can be classified in two categories whether they are symmetrical or not.

4.1 Symmetrical profiles

All the symmetrical profiles are shapes developed by the National Advisory Committee for Aeronautics (NACA). They include classical and modified NACA 4 digits' profiles. The modifications are introducing a sharp leading edge for three of the profiles. It is represented by the addition of 2 digits preceded by an hyphen after the classical NACA 4 digits' writing. The first one represents the shape of the leading edge (0 being "sharp") and the second one specifying the location of the maximal thickness. All these profiles are drawn in Figure 7.

The classical NACA profiles are the most common ones used in the domain of research of VAWT and that is almost the only ones that can be compared with existing data. That is especially true for NACA 0012 and NACA 0018 and the choice to begin with these two was then pretty logical. Regarding the sharp leading edges, the purpose was to see if the prevision from Sunada regarding this parameter [8] was justified or not.

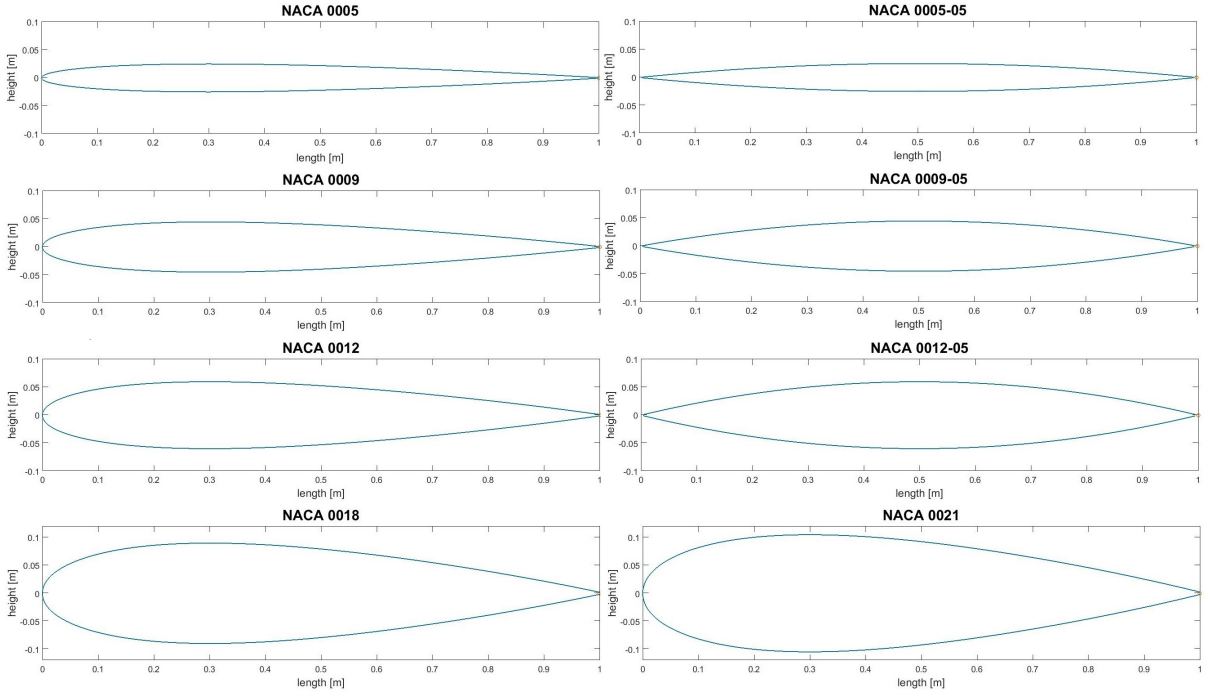

Figure 7: NACA symmetrical profiles

4.2 Non-symmetrical profiles

Regarding the non-symmetrical profiles, they have been selected on two basis. Firstly, as the NACA 0005 and 0009 had performed pretty well and as their profiles is pretty easy to draw, the goal was to apply them a camber of 5% at mid-chord and see if they would perform better than the classical ones. Note that, for practical reason, the thickness of NACA 0009 has been changed to 10% for its cambered version. Then, for the three last profiles, a literature review of high lift-to-drag ratio for low-Reynolds aerodynamics airfoils was made and pointed them as potentially interesting profiles. They are presented in the following list:

- E387

  This airfoil is typical high-lift airfoil designed in the early 1960s by Richard Eppler. The choice for this airfoil in particular is linked to the fact that it is very often used for wind-tunnel experiments which means that possibly, we could get some comparison data to evaluate our simulations for this profile.

- S1223

  The S1223 is an airfoil designed to have a very high lift force at $Re \approx 200'000$ (in fact the highest according to ref. [9]). Looking at other references, it seemed that this airfoil could potentially also perform pretty good in our range of Reynolds and that is why it has been chosen.

- BW-3

  The Bergey BW-3 profile was basically developed for wind turbines. In fact, his shape (5% max. thickness and 5.7% max. camber at 45.4% chord) is pretty close

to the description of Sunada [8] for what should be the best airfoil choice for low-Reynolds and additionally, its performance seemed pretty promising according to the Xfoil prediction on `http://www.airfoiltools.com`.

All the non-symmetrical profiles simulated during this project are shown in Figure 8:

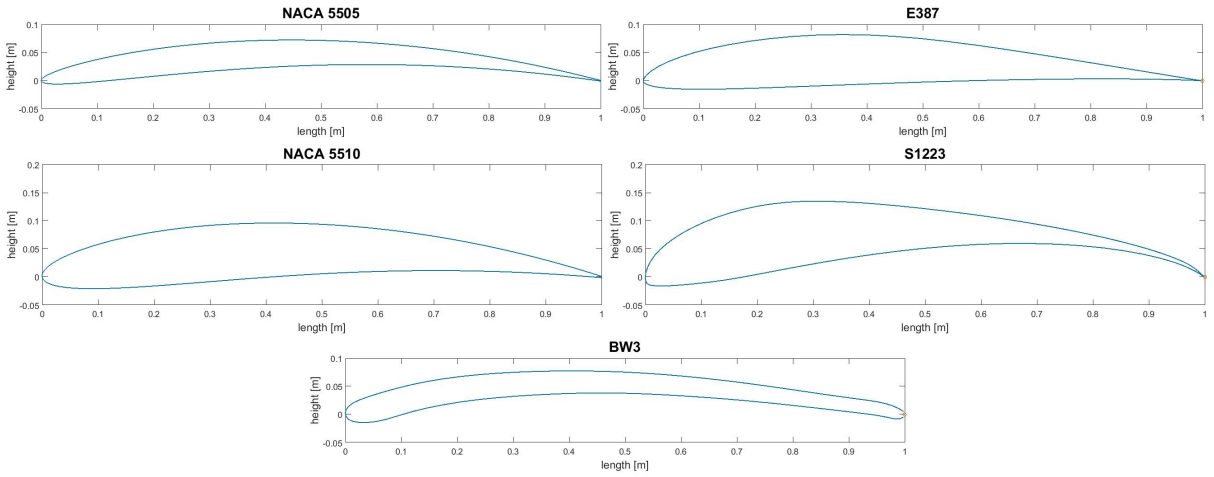

Figure 8: Non-symmetrical profiles

5 Results

Preliminary remark: The main goal of this project being the comparison of the aerodynamic performances of a large range of different airfoils, it is important to note that the focus of this project was less to compute some very accurate polars of the lift and drag coefficients than have sufficiently accurate data for airfoils comparisons. However, as a comparison can only make sense if the results are quite realistic, we have tried to perform a maximum of comparisons with existing experimental and/or simulated data.

All the results presented in this chapter come from CFD-simulations performed for the WIRE Laboratory at EPFL during the autumn semester 2016. The simulations were launched in parallel on 11 cores on the workstation available to students in the WIRE Laboratory. Each of them lasted more less 30 minutes and the complete study of one airfoil was generally taking around one night (8 different angles of attack for 3 Reynolds numbers each time). For each simulation, the C_l and C_d coefficients were written at each iteration in two different text files by Fluent. Matlab was used for the post processing in order to get the number of iterations, the C_l and C_d values after convergence of the solution, the lift-to-drag ratios and the tangential force coefficients for each angle of attack and each Reynolds number. All these data were stored in Excel files which are given in Appendix A for each airfoil. The lift and drag polars were then created with Matlab as well as the lift-to-drag ratio and the coefficient of tangential force over the angle of attack for each Reynolds. Considering the amount of data, only the lift and drag polars at Reynolds $2 \cdot 10^4$ and its range of convergence will be presented in this section for each airfoil. All the complete results (Tables of values and polars for all three Reynolds) can be found in Appendix A. A discussion on the reliability of the results will be presented in section 6 and the comparison between airfoils will then be performed in section 7 based on the lift-to-drag ratios and the coefficients of tangential force.

5.1 Symmetrical NACA 00xx profiles

NACA 0005

Converged for $\alpha = [0; 2; 4; 6; 8]$

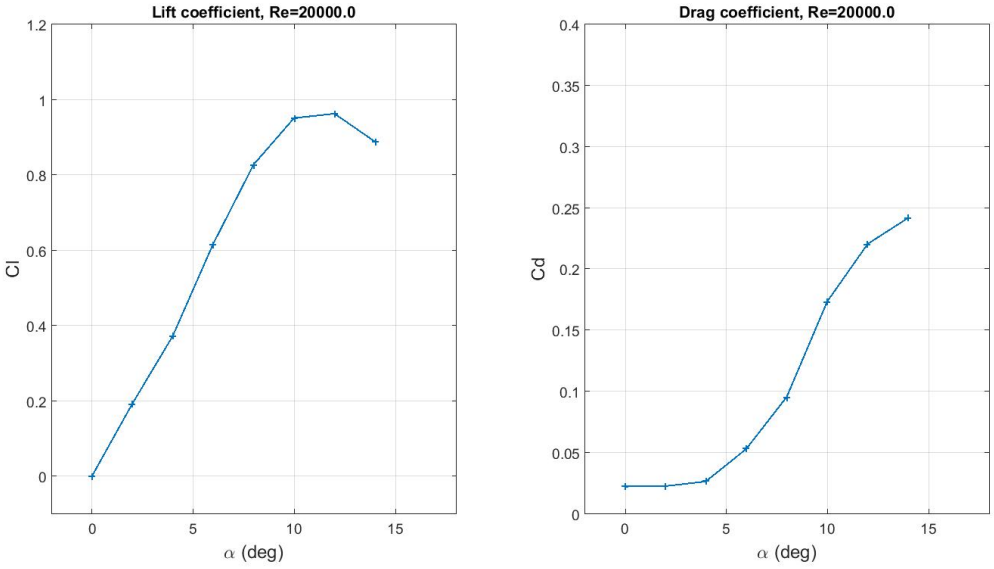

Figure 9: Polars for NACA 0005, $Re = 2 \cdot 10^4$

NACA 0009

Converged for $\alpha = [0; 2; 4; 6; 8; 10]$

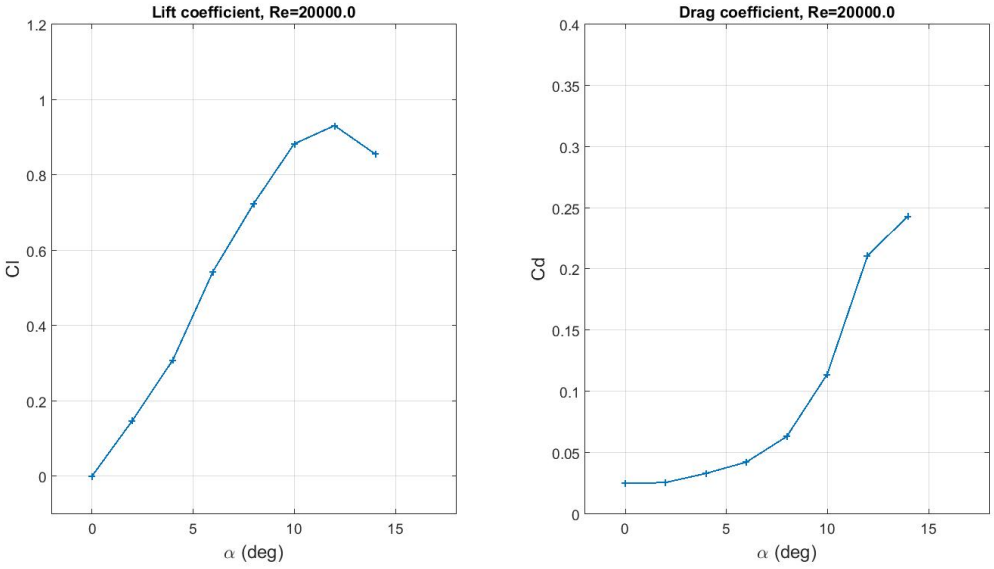

Figure 10: Polars for NACA 0009, $Re = 2 \cdot 10^4$

NACA 0012

Converged for $\alpha = [0; 4; 6; 8; 10]$

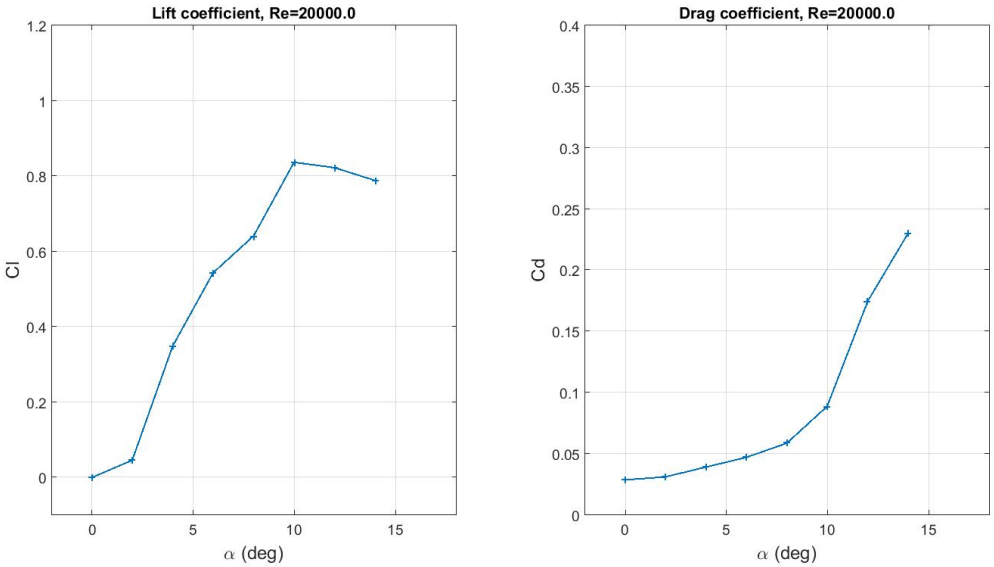

Figure 11: Polars for NACA 0012, $Re = 2 \cdot 10^4$

NACA 0018

Converged for $\alpha = [0; 2; 4; 6; 8; 10]$

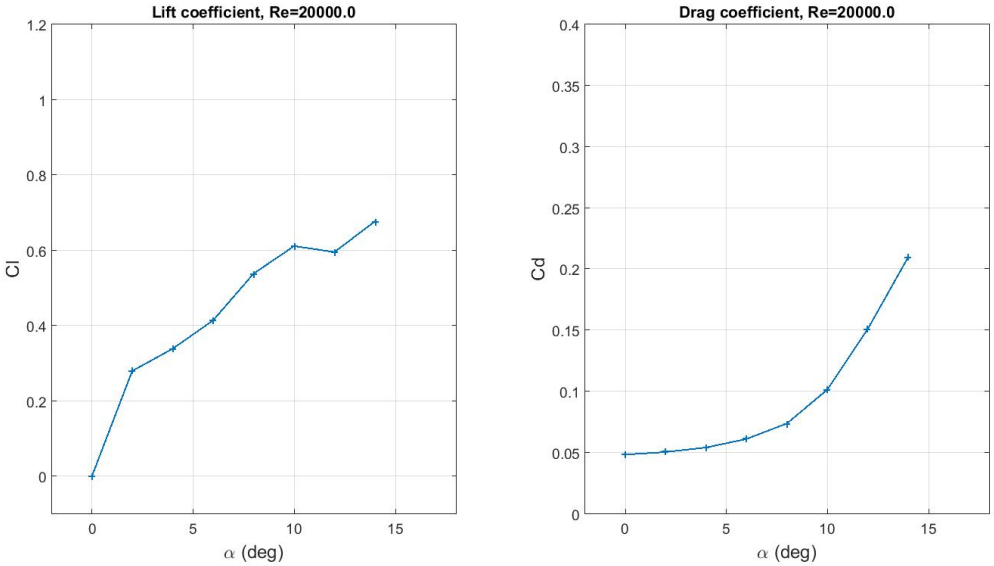

Figure 12: Polars for NACA 0018, $Re = 2 \cdot 10^4$

NACA 0021

Converged for $\alpha = [0; 2; 4; 6; 8]$

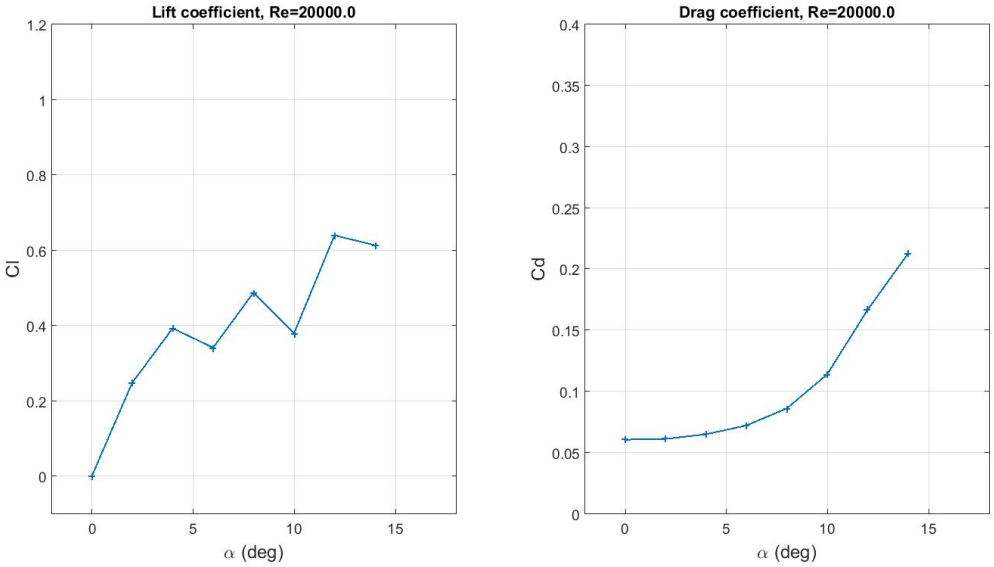

Figure 13: Polars for NACA 0021, $Re = 2 \cdot 10^4$

5.2 NACA 00xx-xx profiles with sharp leading edge

NACA 0005-05

Converged for $\alpha = [0; 2; 4; 6; 8]$

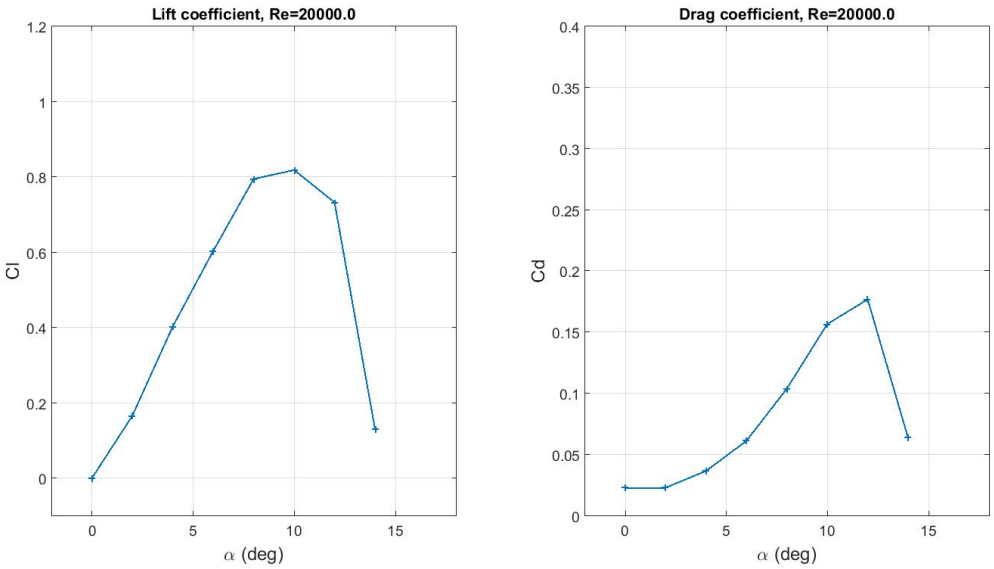

Figure 14: Polars for NACA 0005-05, $Re = 2 \cdot 10^4$

NACA 0009-05

Converged for $\alpha = [0; 2; 4; 6; 8; 10]$

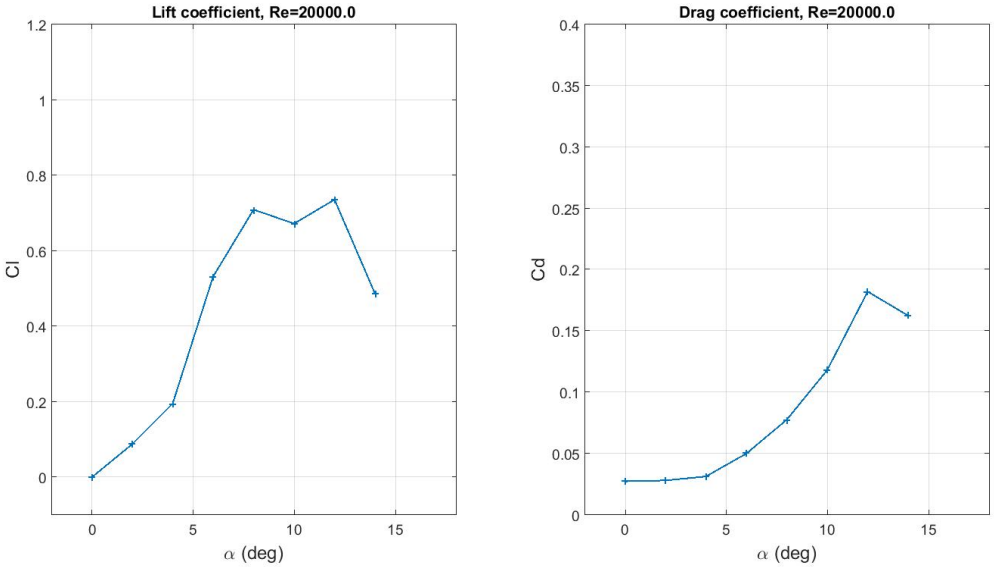

Figure 15: Polars for NACA 0009-05, $Re = 2 \cdot 10^4$

NACA 0012-05

Converged for $\alpha = [0; 6; 8; 10]$

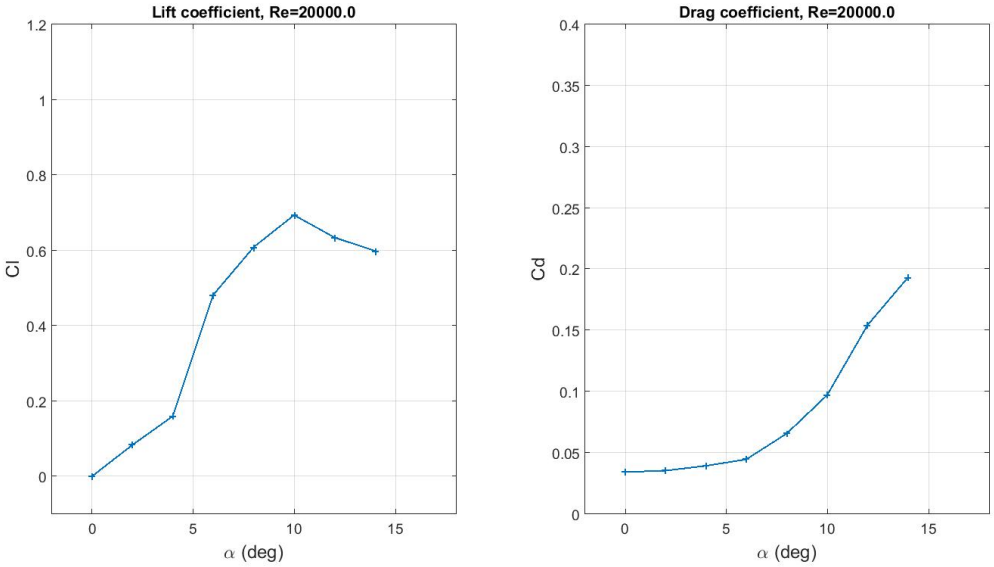

Figure 16: Polars for NACA 0012-05, $Re = 2 \cdot 10^4$

5.3 NACA 55xx profiles

NACA 5505

Converged or considered valid[2]for $\alpha = [0; 2; 4; 6]$

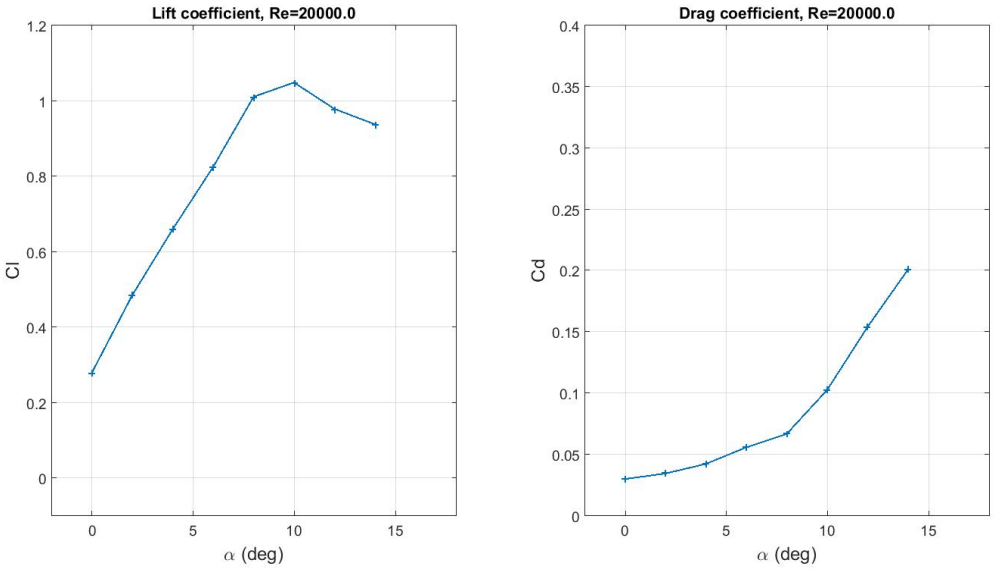

Figure 17: Polars for NACA 5505, $Re = 2 \cdot 10^4$

NACA 5510

Converged or considered valid for $\alpha = [0; 2; 4; 6]$

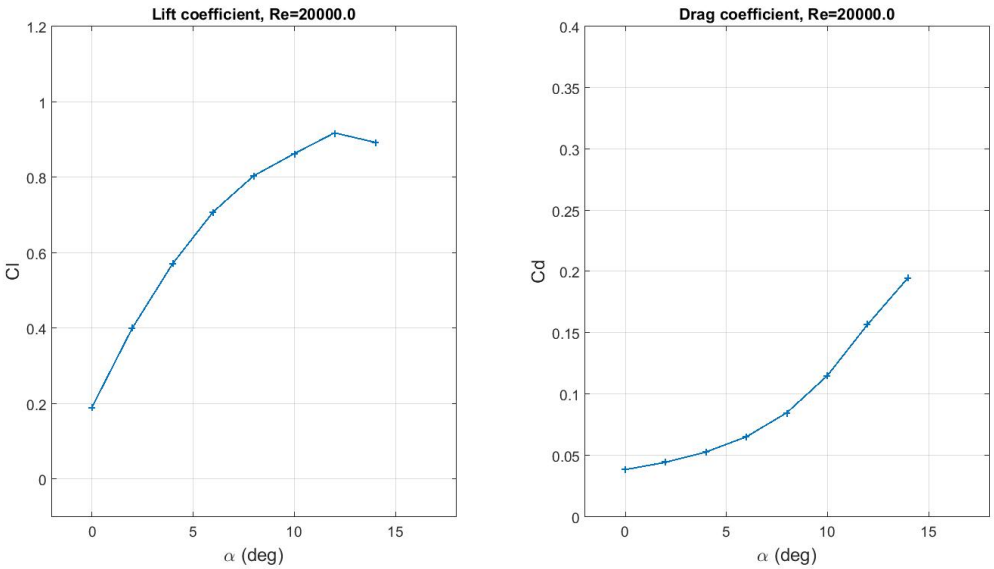

Figure 18: Polars for NACA 5510, $Re = 2 \cdot 10^4$

[2] See section 6

5.4 Other profiles

E387

Converged or considered valid for $\alpha = [0; 2; 4; 6; 8]$

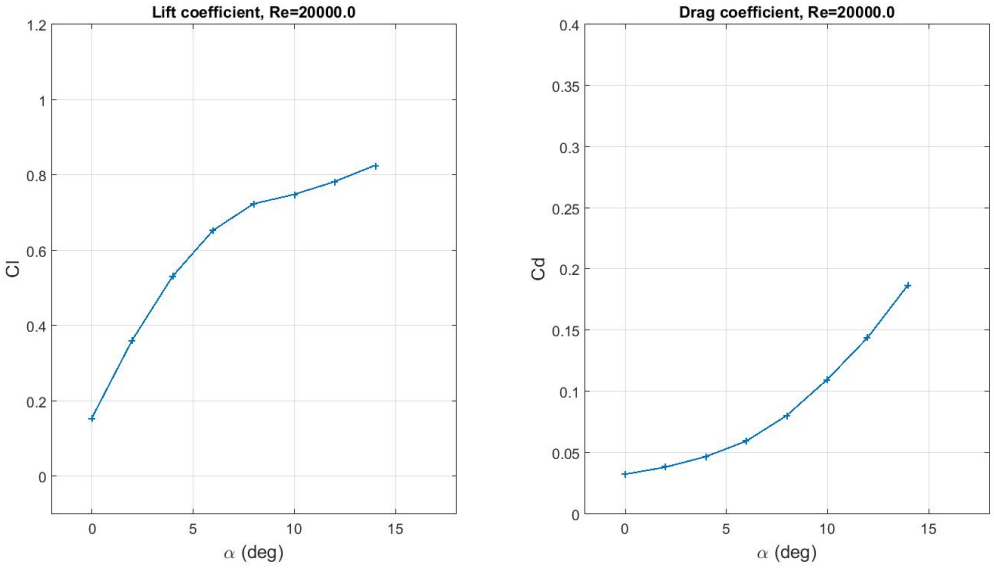

Figure 19: Polars for E387, $Re = 2 \cdot 10^4$

S1223

Converged or considered valid for $\alpha = [0; 2; 4; 6]$

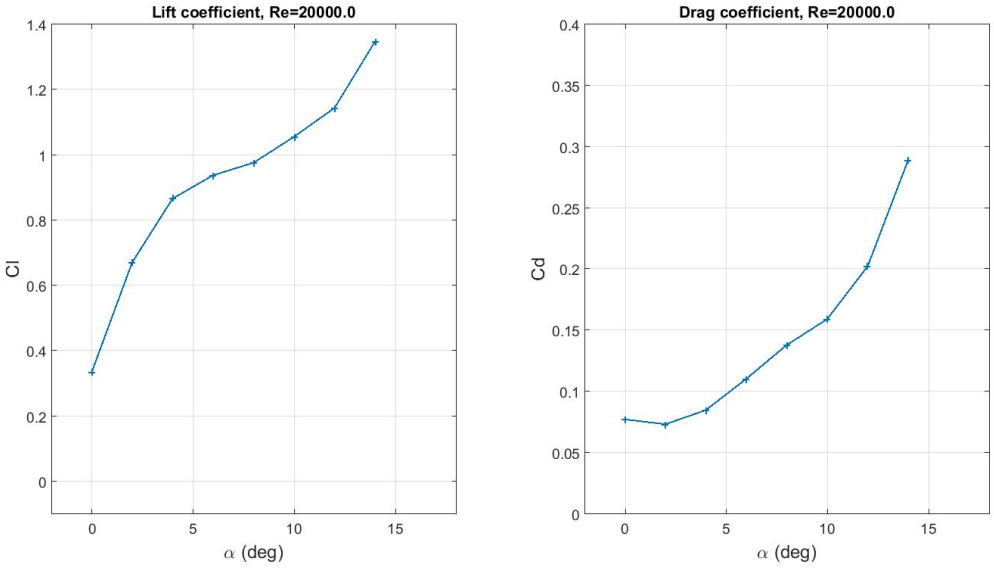

Figure 20: Polars for S1223, $Re = 2 \cdot 10^4$

BW3

Converged or considered valid for $\alpha = [0; 2; 4; 6; 8]$

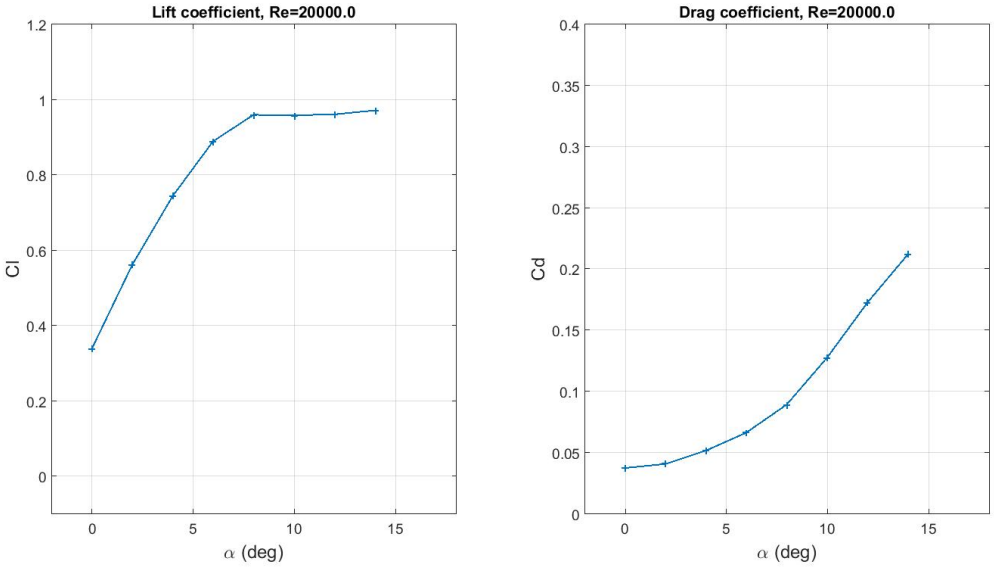

Figure 21: Polars for BW3, $Re = 2 \cdot 10^4$

6 Reliability of the results

Globally speaking, the results obtained with our simulations are similar to ones that could have been expected from such simulations. The lift and drag polars have classical patterns in most cases (rise of lift and low drag until stall angle, then drop of lift and rise of drag). In general, we got convergence for low angles of attack for most symmetrical airfoils but hardly any for angles approaching stall (more complex behaviour of the flow).

Concerning non-symmetrical airfoils, this was a bit different as we got almost no convergence at all during our simulations. Still the polars have nice patterns but without further investigations, they were not usable directly. After study of the lift and drag histories, it was noticed that some cases presented some completely stabilized coefficients (study on the last 1'000 iterations). Moreover, a study of the residuals revealed that they were already very low and stable in some cases (see for example Figure 22). It was of course not sufficient for using the results but, after a careful visual inspection of the flow patterns for each of the case, it has been decided that the results that would present stabilized lift and drag coefficients, low residuals and a regular flow pattern at the same time, could be used for a global comparison with the other airfoils.

An example of two different flow patterns is presented in Figure 23. One can clearly see that Figure 23b is presenting very weird flow pattern and this kind of case was directly considered as non valid while the velocity contours in Figure 23a, if coming along with stabilized residuals and coefficients, was considered valid for a comparison. All the results that did not converged but were considered valid for the following comparisons are highlighted in green in the tables of results in Appendix A.

In fact, one more time, only low angles of attack were able to satisfy both conditions and even if all range of α are presented in the results, it is of utmost importance to keep that in mind in order to realize meaningful comparisons.

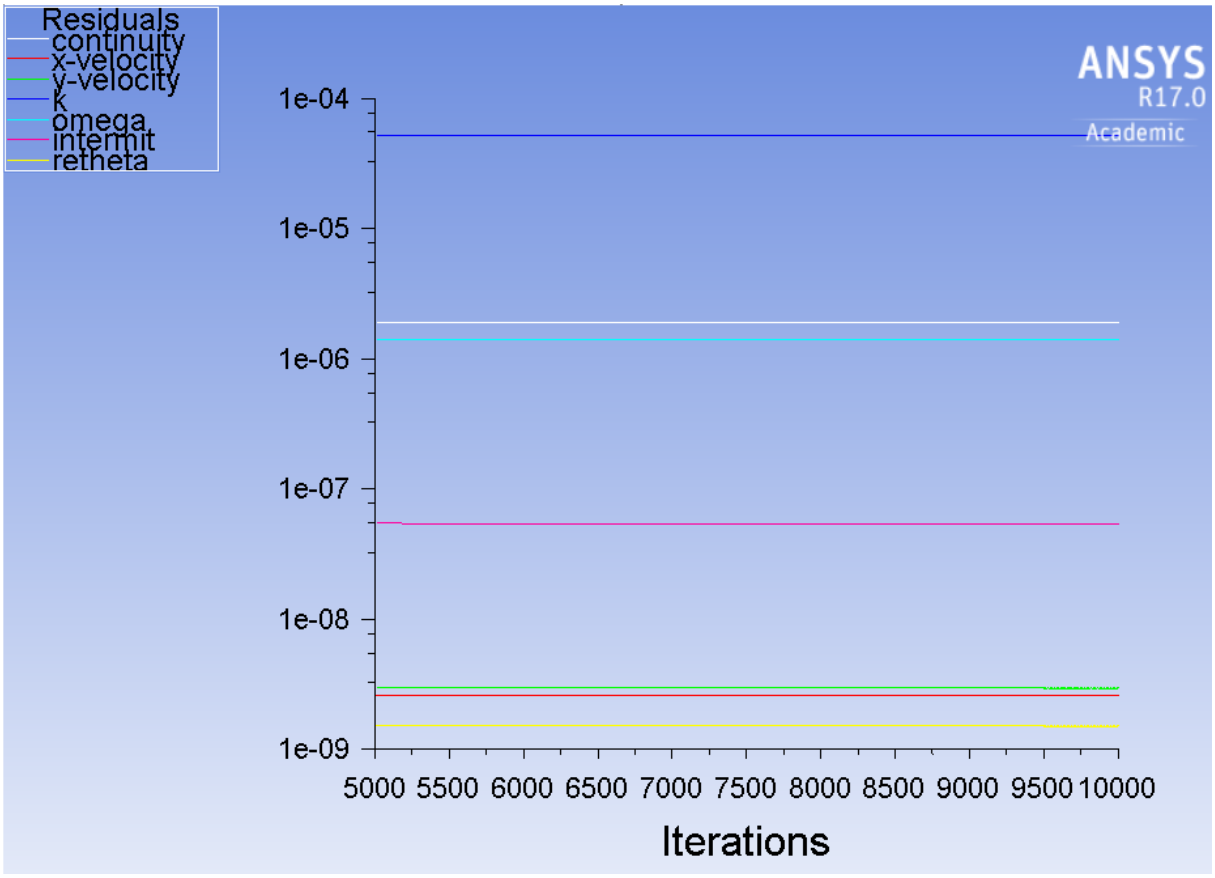

Figure 22: Residuals for E387 at $Re = 10^4$ and $\alpha = 4°$

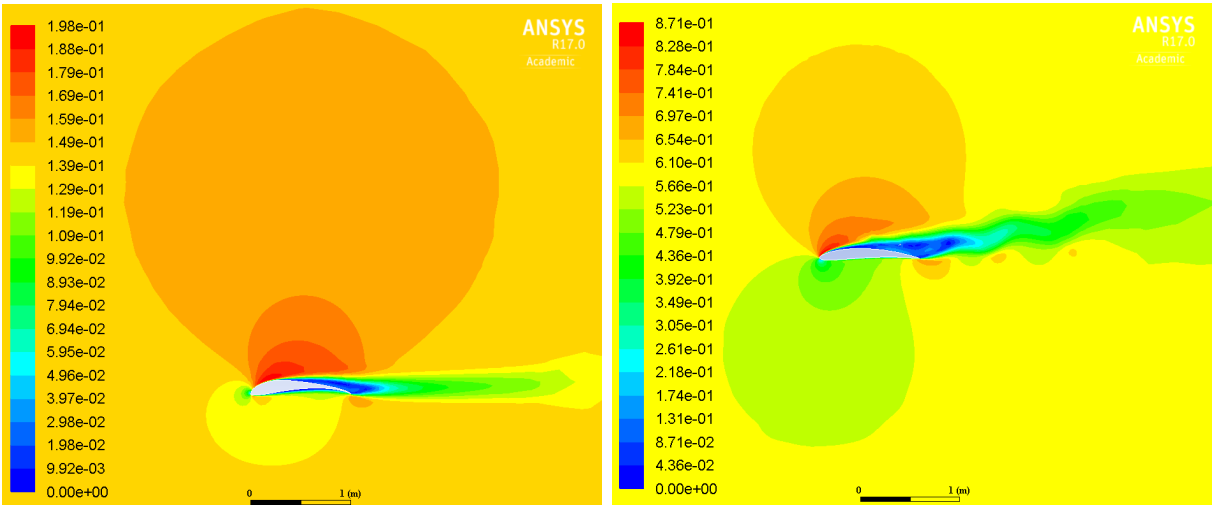

(a) Velocity contour for S1223 at $Re = 10^4$ and $\alpha = 4°$

(b) Velocity contour for NACA 5510 at $Re = 4 \cdot 10^4$ and $\alpha = 12°$

Figure 23: Example of 2 velocity contours

7 Discussion and comparison between airfoils

7.1 Comparison with existing data

In this section are presented some comparisons with existing data (experimental or CFD-simulations) in order to judge the model used for our simulations. As said, data on the low-Reynolds number aerodynamic are pretty scarce and only few airfoils have already been tested in the exact same conditions. In the symmetrical ones, NACA 0018 and NACA 0012 are probably the most tested and compared airfoils. The previous semester project used these two airfoils as validation for the numerical model by comparing it to the data from Kumar [6] for NACA 0018 and from Sheldahl [7] for NACA 0012. Sunada [8] is also providing some experimental data for NACA 0006, NACA 0009 and NACA 0012 but only for $Re \leqslant 4 \cdot 10^3$. The wind tunnel of the University of Illinois at Urbana-Champaign (UIUC) also tested a large range of airfoils at different Reynolds number and their result for NACA 0009 at $4 \cdot 10^4$ is the only one which is really matching our range of Reynolds. Finally, it will not be detailed here but a global comparison have been done with `http://www.airfoiltools.com` as it seemed that their own comparison tool was giving similar results than ours. Depending on the results found, the comparison method will globally stay the same, studying the lift and drag coefficients mostly.

Comparison with experimental results

As said before, UIUC tested a large range of airfoils and NACA 0009 has been tested at $Re = 4 \cdot 10^4$. The comparison with our own simulation for this Reynolds is presented in Figure 24 (error bars of 10% have been added on the experimental data):

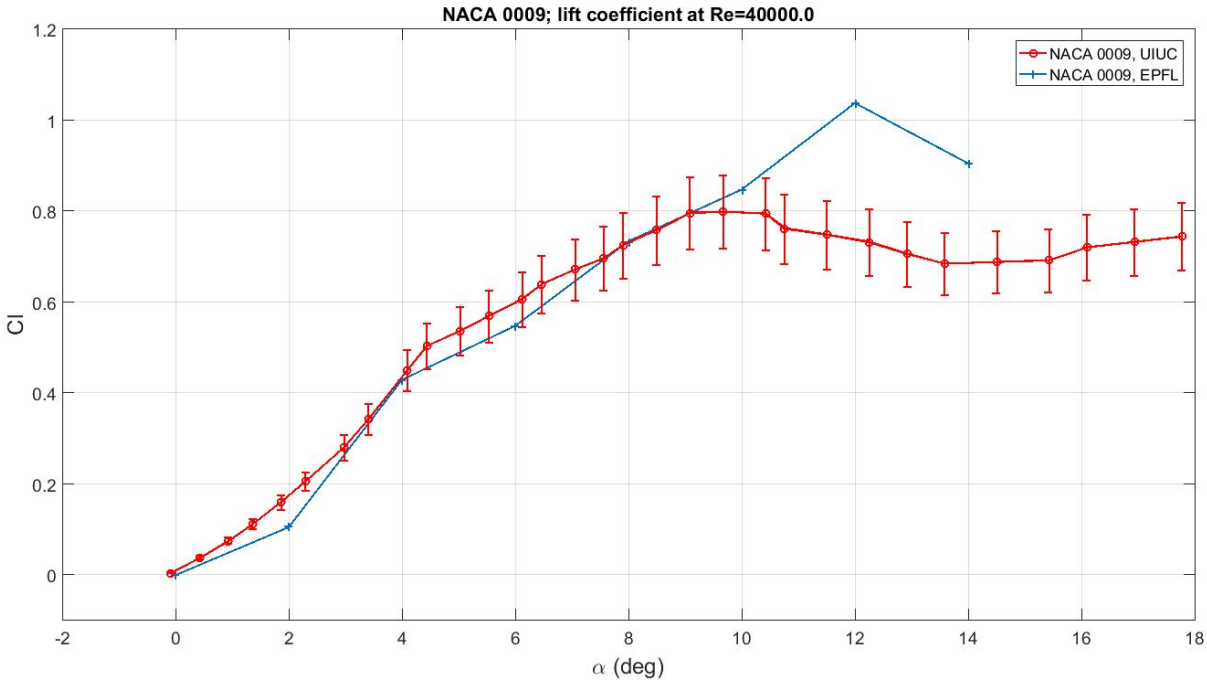

Figure 24: Comparison of lift coefficients of NACA 0009, $Re = 4 \cdot 10^4$

These results for low angles of attack are pretty satisfactory, at least until stall happens

($\approx 8°$ for this case according to the experimental data and to `http://www.airfoiltools.com/`). We note as well that, according to Table A.6, the cases $\alpha = [2, 10, 12, 14]$ did not converged in our simulations and it is precisely the data that present the more difference with the experimental ones. Therefore, we can say that our simulation is pretty accurate in this case.

CFD-results from Kumar

The data from Kumar et. al [6] have been simulated for the study of the implementation of VAWT on Mars. Therefore, due to the atmosphere and the wind speed on this planet, they are dealing with low Reynolds numbers typically in the range that interests us. NACA 0018 was chosen for their simulations and it then provides a good comparison tool for our own simulations. Emile already performed a comparison for his results and used it in order to validate his use of the sst-transition model in Fluent. He found that his own results were mostly in a reach of a 20% error with the ones for Kumar for low angles of attack. In our case, error bars have been set to 25% on the data from Kumar and only two Reynolds tested are presented here because the case $Re = 10^4$ got almost no angle of attack converged (see Table A.10) and is therefore not relevant for a comparison. Figure 25 and 26 are presenting the comparison of our simulations with the ones from Kumar at $Re = 2 \cdot 10^4$ and $Re = 4 \cdot 10^4$.

We can note first that our simulations didn't converged for $\alpha \geqslant 12°$ and that more cases converged for $Re = 2 \cdot 10^4$ (see Table A.11 and A.12). Keeping that in mind, we can globally say that our simulations overestimated the ones from Kumar but that the similarity between the two dataset is not so bad until stall happens. Still the difference is consequent and it shows one more time the difficulty of CFD-analysis in this range of Reynolds number.

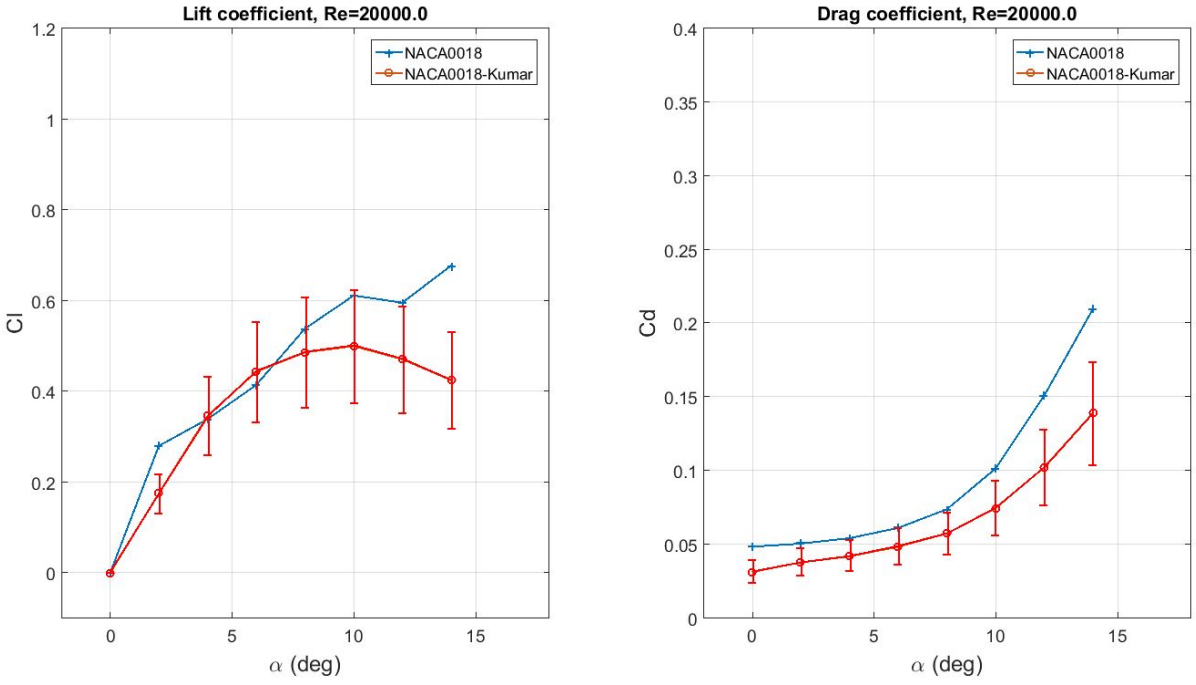

Figure 25: Comparison of lift coefficients of NACA 0018 with Kumar, $Re = 2 \cdot 10^4$

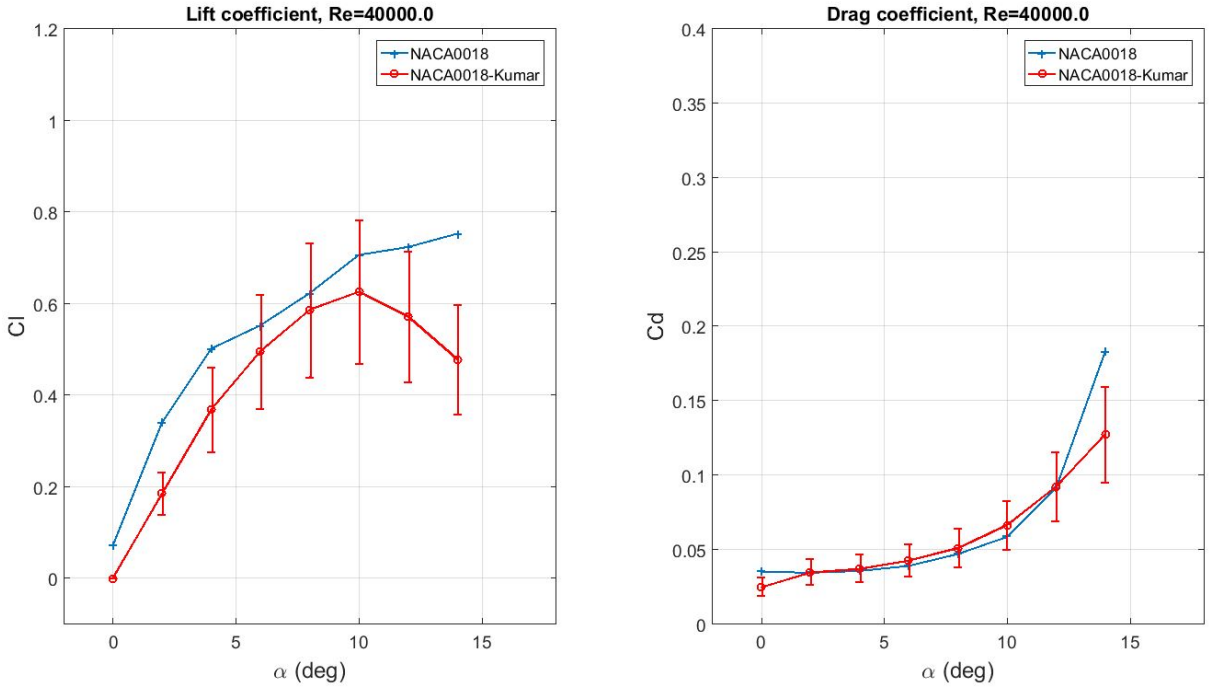

Figure 26: Comparison of lift coefficients of NACA 0018 with Kumar, $Re = 4 \cdot 10^4$

Extrapolated data from Sheldahl

In this section, we will present the comparison of three airfoils (NACA 0012, 0018 and 0021) with the extrapolated data from Sheldahl [7]. As a consequence of the extrapolation, some data from Sheldahl are typically non relevant (for example $C_l \leq 0$ for symmetrical airfoils at $\alpha \geqslant 0$). Only $Re = 4 \cdot 10^4$ will be presented in this section as the convergence of our simulations at this Reynolds is pretty good and therefore our results can be considered relevant.

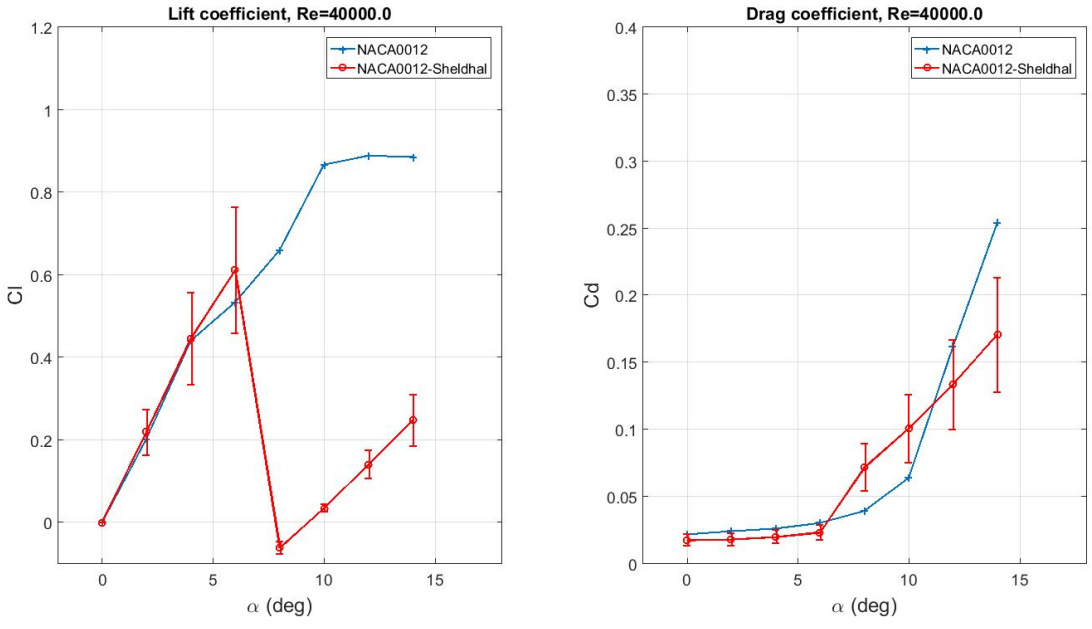

Figure 27: Comparison of lift coefficients of NACA 0012 with Sheldahl, $Re = 4 \cdot 10^4$

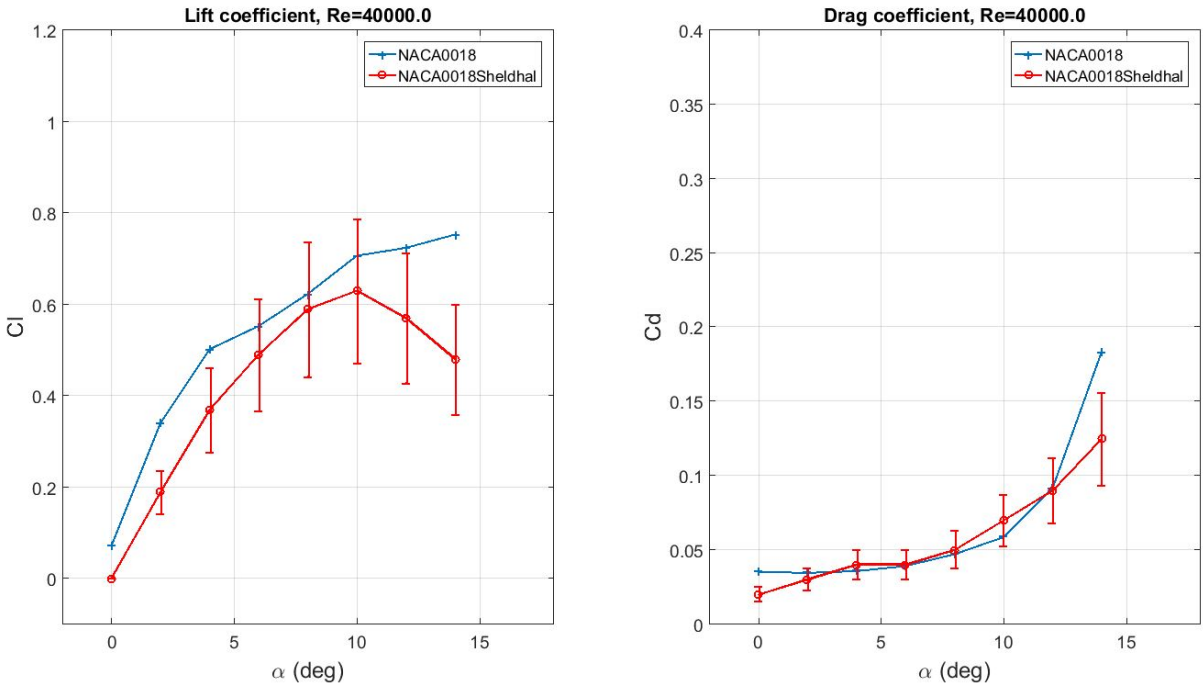

Figure 28: Comparison of lift coefficients of NACA 0018 with Sheldahl, $Re = 4 \cdot 10^4$

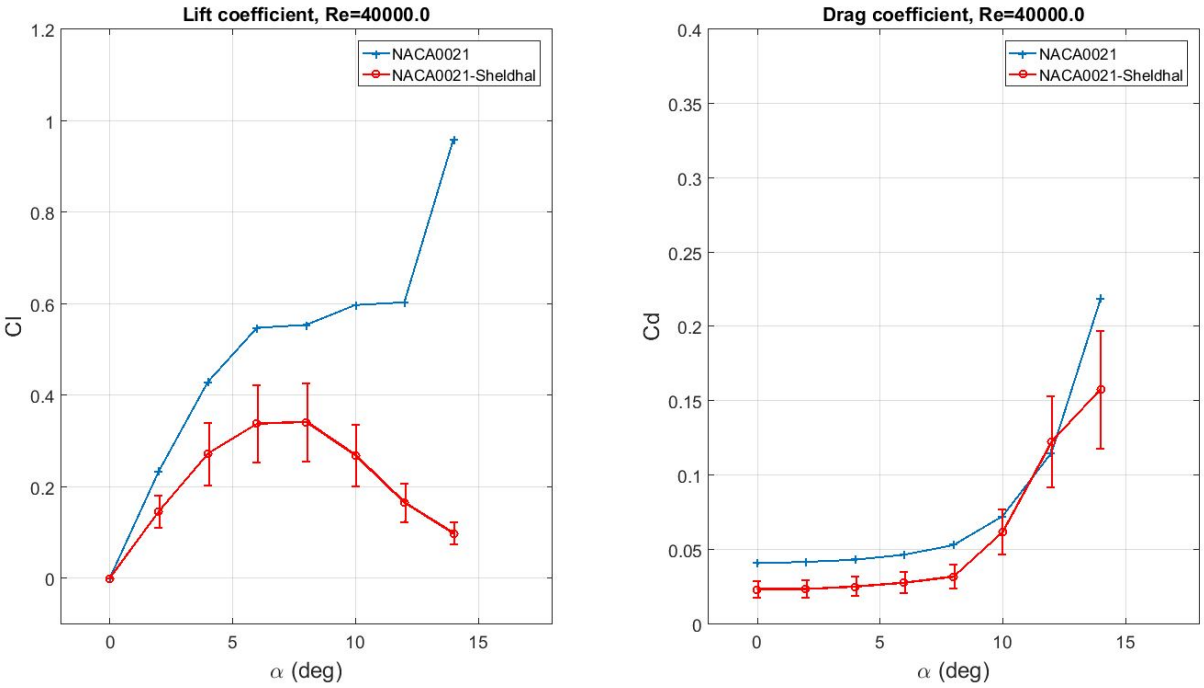

Figure 29: Comparison of lift coefficients of NACA 0021 with Sheldahl, $Re = 4 \cdot 10^4$

This three comparison are showing one more time the limitations of both simulations and extrapolations. Lift coefficient in Figure 27 is a typical example of what extrapolation can lead to but overall, these data show a good similarity with our simulations at low angles of attack. Here as well we can note that our simulations tend to overestimate the lift and drag coefficients from Sheldahl. The rest of the comparison performed with the extrapolated data can be found in Appendix B and shows globally the same results.

7.2 Discussion of the results

Thickness

In this section, the results of our simulations are presented, discussed and comparisons amongst them are performed.

The first parameter to study in our project was the effect of the thickness on the performance of airfoils at low Reynolds numbers. Looking at the results for the symmetrical airfoils, thinner airfoils generally have higher lift at this range of Reynolds than thicker ones. They also seem to have a smaller drag at low angles of attack but this one seems to be growing faster with angle of attack than for thicker airfoils. To assess on this parameter, five symmetrical airfoils with different thickness have been simulated and the comparison based on their lift-to-drag ratios and their coefficients of tangential force at Reynolds $Re = 10^4$, $Re = 2 \cdot 10^4$ and $Re = 4 \cdot 10^4$ are presented in Figure 30, 31 and 32.

The effect of the thickness seems to induce some consequent variations depending on the Reynolds number. In fact, for the two lowest Reynolds, thinner profiles (NACA 0005, NACA 0009 and NACA 0012) definitely performs better than the two thicker ones (NACA 0018 and NACA 0021) but this tendency is less clear for $Re = 4 \cdot 10^4$ as the thicker profiles are closer and even better at some angles of attack than the thinner ones. Focusing on the relevant angles of attack (where convergence occurred for all airfoils namely $\alpha \leqslant 8°$), the three thinner airfoils are still performing slightly better at the highest Reynolds and therefore, we can express the conclusion that thinner airfoils are generally performing better at this range of Reynolds. As a consequence of the fast rising drag on really thin airfoils (NACA 0005), we have to note that the performances of such profiles seem to drop pretty quickly after angle of attack around $6 - 8°$.

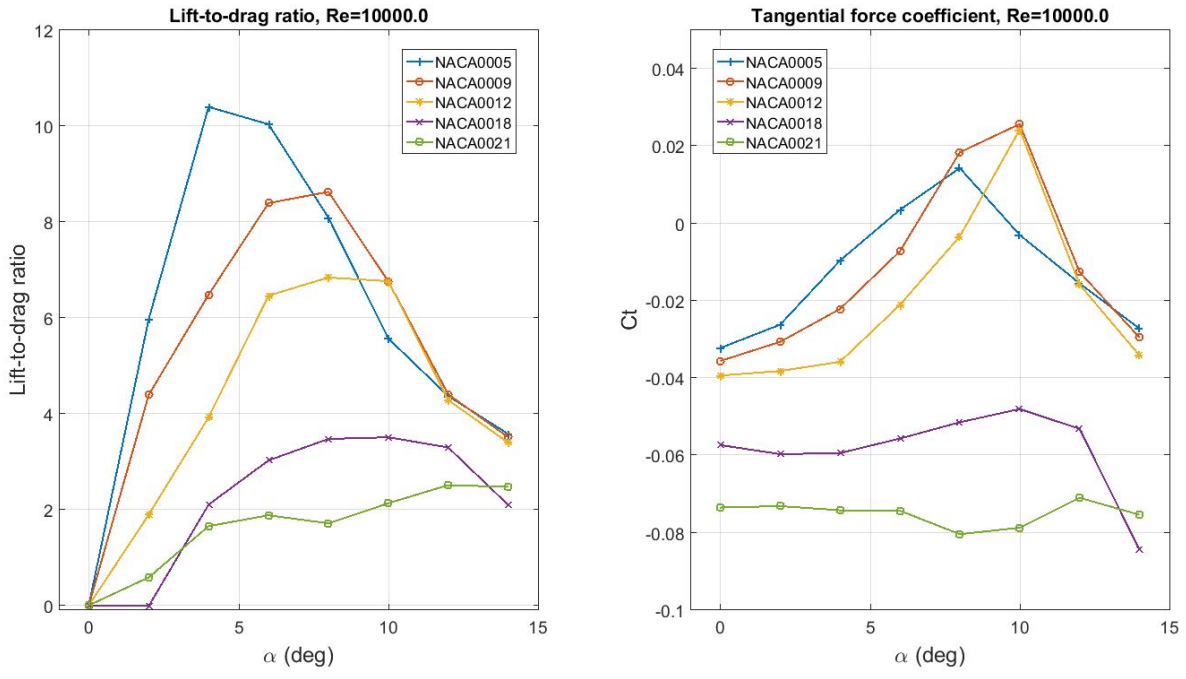

Figure 30: Comparison between symmetrical airfoils, $Re = 10^4$

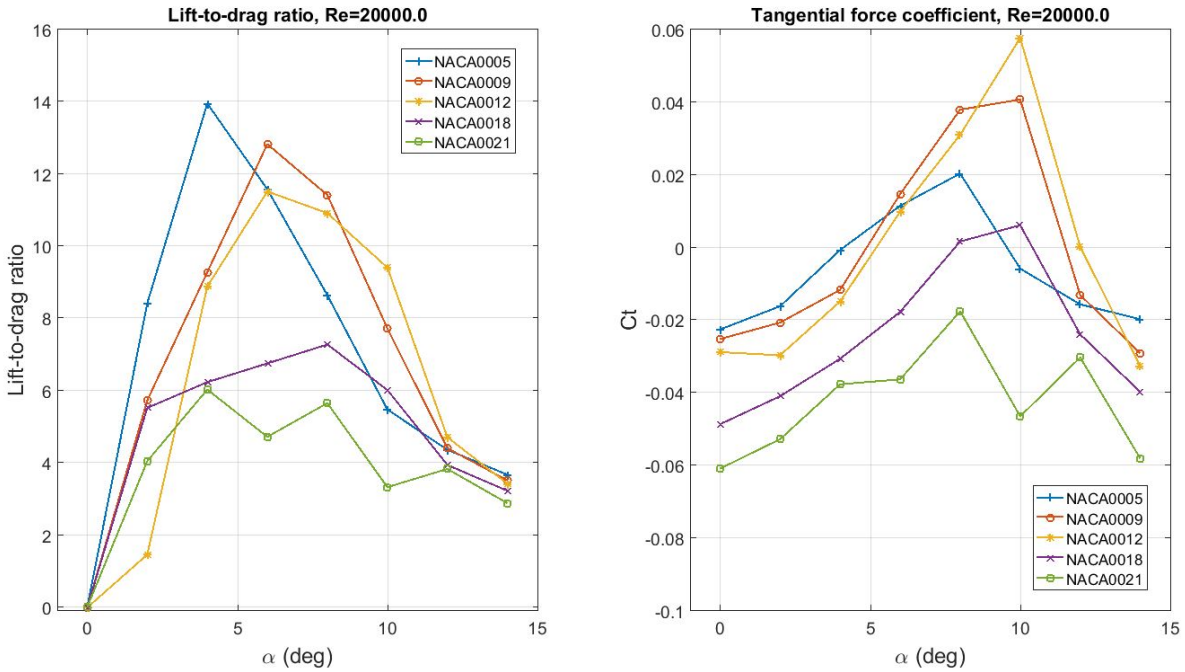

Figure 31: Comparison between symmetrical airfoils, $Re = 2 \cdot 10^4$

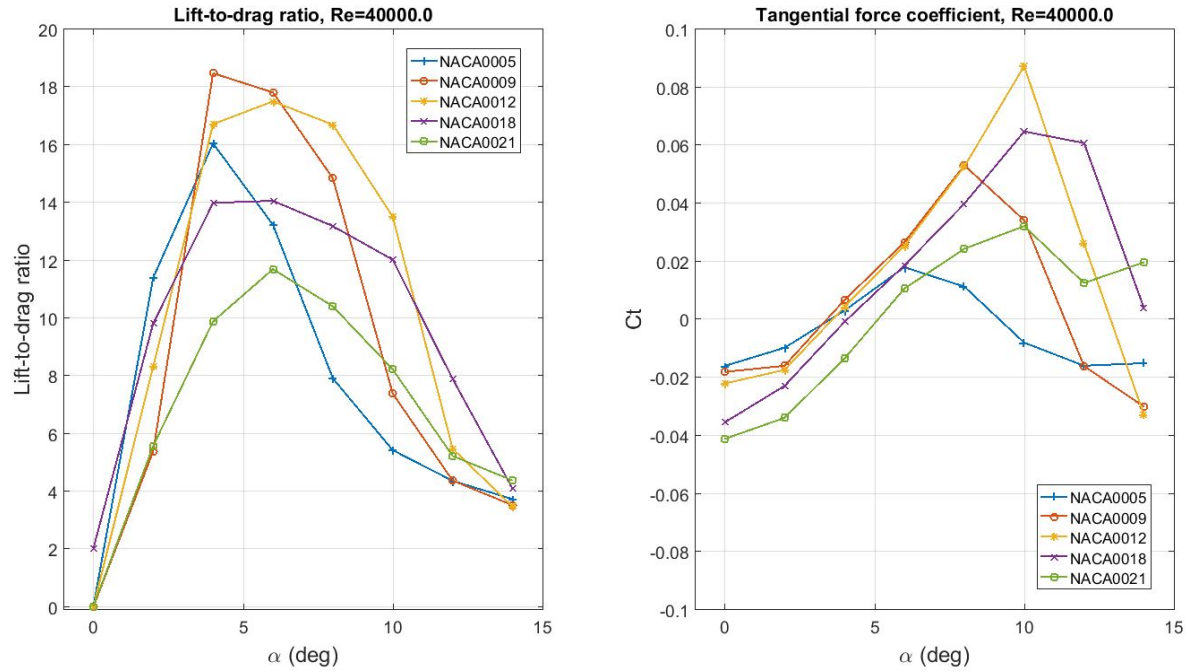

Figure 32: Comparison between symmetrical airfoils, $Re = 4 \cdot 10^4$

Addition of a sharp leading edge

One of the parameter to study in this project was the addition of a sharp leading edge. Having a look at the raw results, it does not seem to improve the performance of the airfoils. In fact it generally lowers the lift coefficient while keeping the drag more less constant. Three symmetrical profiles (NACA 0005, NACA 0009 and NACA 0012) have

been added a sharp leading edge and their comparison in term of lift-to-drag ratios with the classical profiles at different Reynolds numbers are presented in Figure 33, 34 and 35:

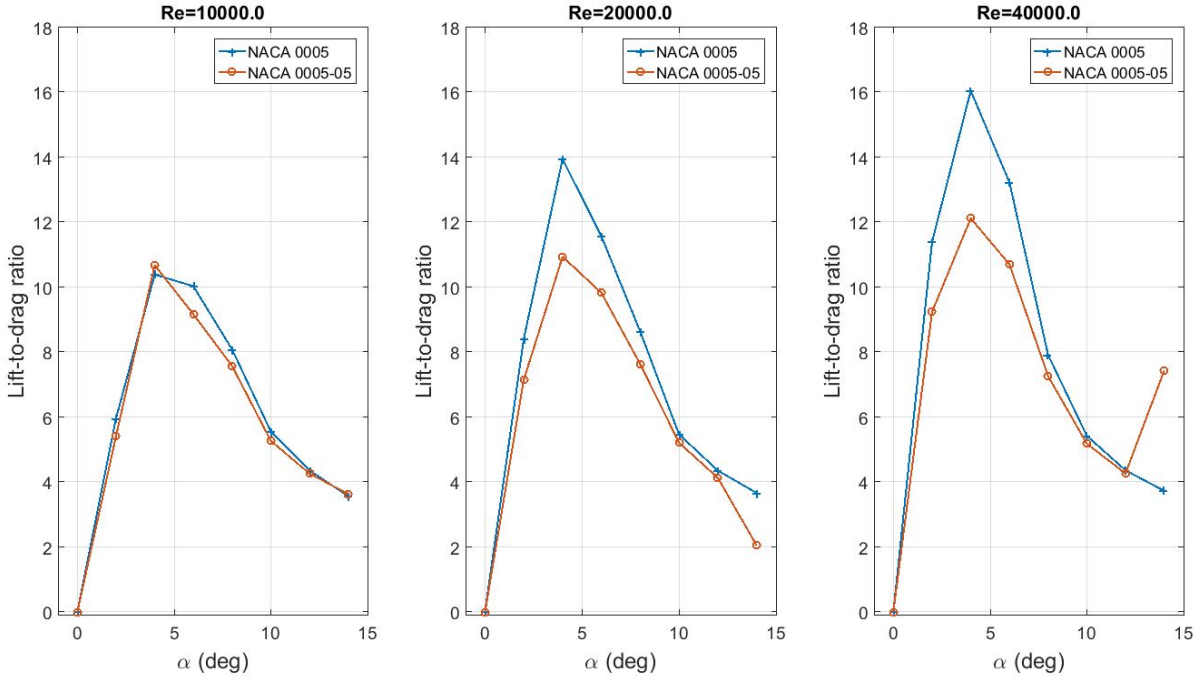

Figure 33: Effect of the sharp leading edge on NACA 0005

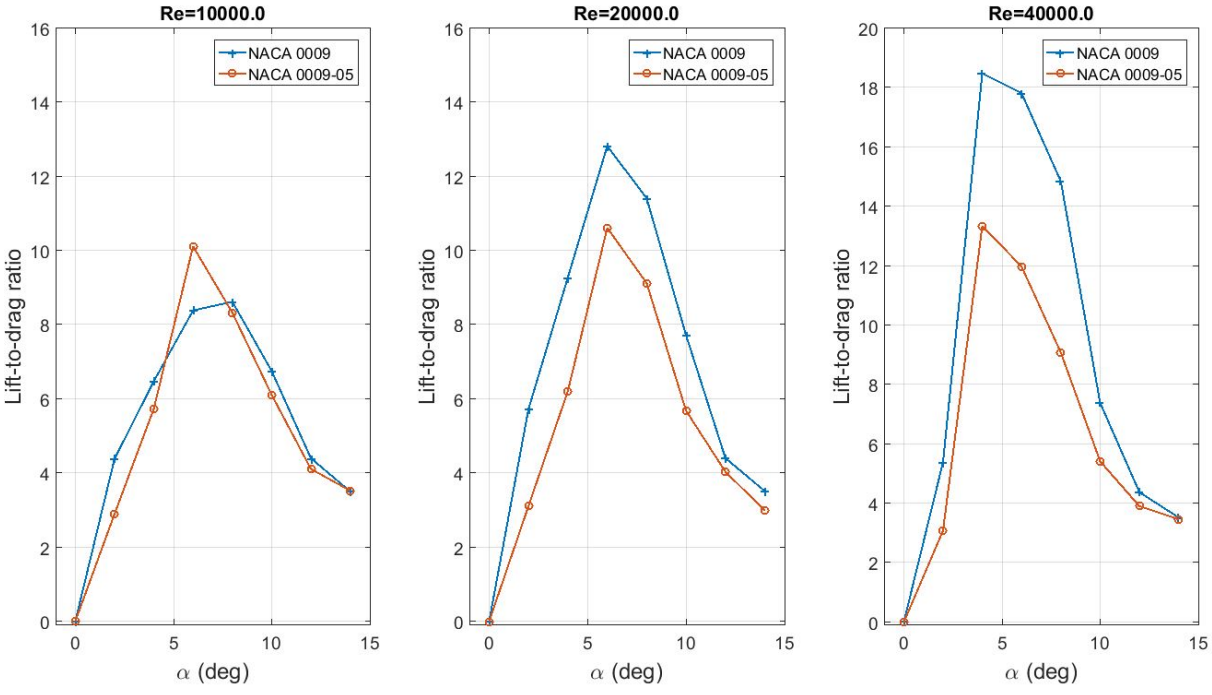

Figure 34: Effect of the sharp leading edge on NACA 0009

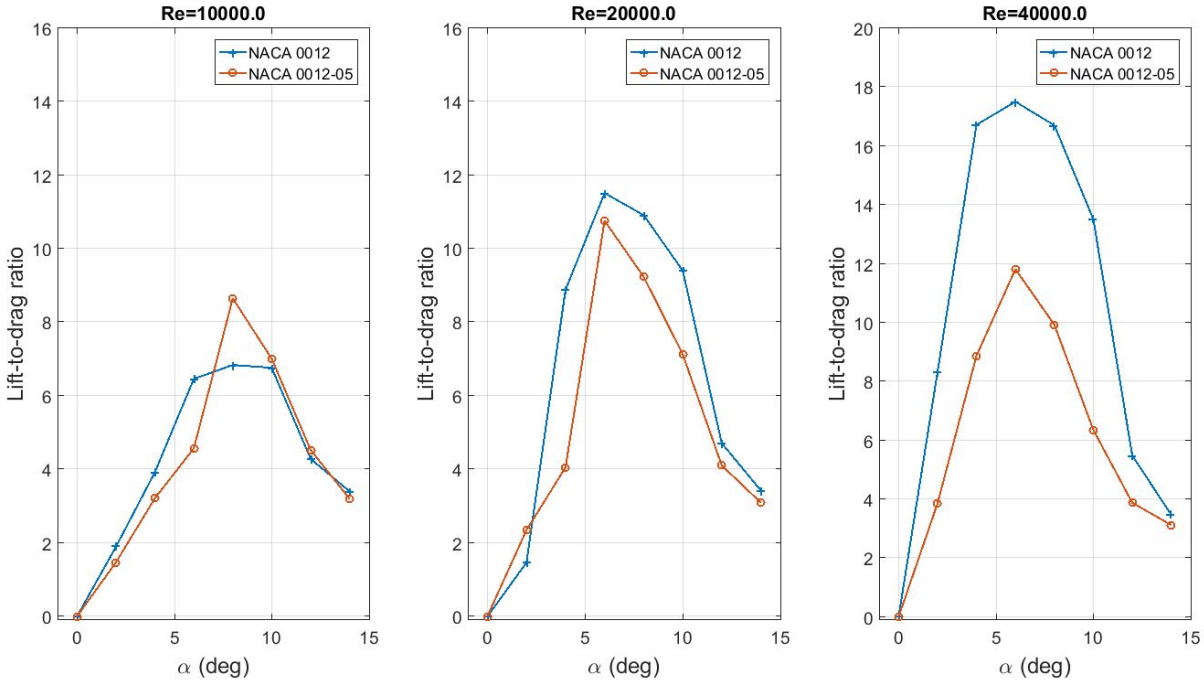

Figure 35: Effect of the sharp leading edge on NACA 0012

It seems that the addition of a sharp leading edge on symmetrical profiles have clearly a negative effect on airfoil's performance at $Re = 2 \cdot 10^4$ and $Re = 4 \cdot 10^4$. For $Re = 10^4$, the effect is more neutral and it seems that the smaller is the Reynolds, the better is the effect of the addition of a sharp leading edge. Therefore, our results could be in accordance with the ones of Sunada [8] as his conclusion was made on Reynolds $\leqslant 4 \cdot 10^3$ but generally speaking, the effect of a sharp leading edge is recognized to have a positive impact even at $Re \geqslant 10^3$ and that is not the case in our results.

Addition of a camber

According to Sunada [8], the addition of a camber should improve the low Reynolds performance of airfoils at very low Reynolds. In our simulation, the results showed that the addition of a 5% camber was improving a lot the lift coefficient but also resulted in an increase of the drag at low angles of attack. Therefore, a comparison have been done on NACA 0005 to see which increase would have the more impact on the general performance. The comparison of NACA 0005 and NACA 5505 is presented in Figure 36. The result of this comparison is pretty clear and match the previsions that have been made on the addition of camber at low Reynolds.

Even if they are not exactly the same thickness, it is interesting to note that the comparison between NACA 0009 and NACA 5510 is not so clear as we can see in Figure C.8 in Appendix C. Still the camber is at least equaling the performance of the classical airfoils and we can say that globally, the addition of a camber is slightly improving the low Reynolds' performance of airfoils.

In addition, the effect of the thickness can one more time be pointed out with Figure 37. Similarly to symmetrical profiles, the thinner cambered profiles seem to perform better at low Reynolds while the results are more mitigated for $Re = 4 \cdot 10^4$.

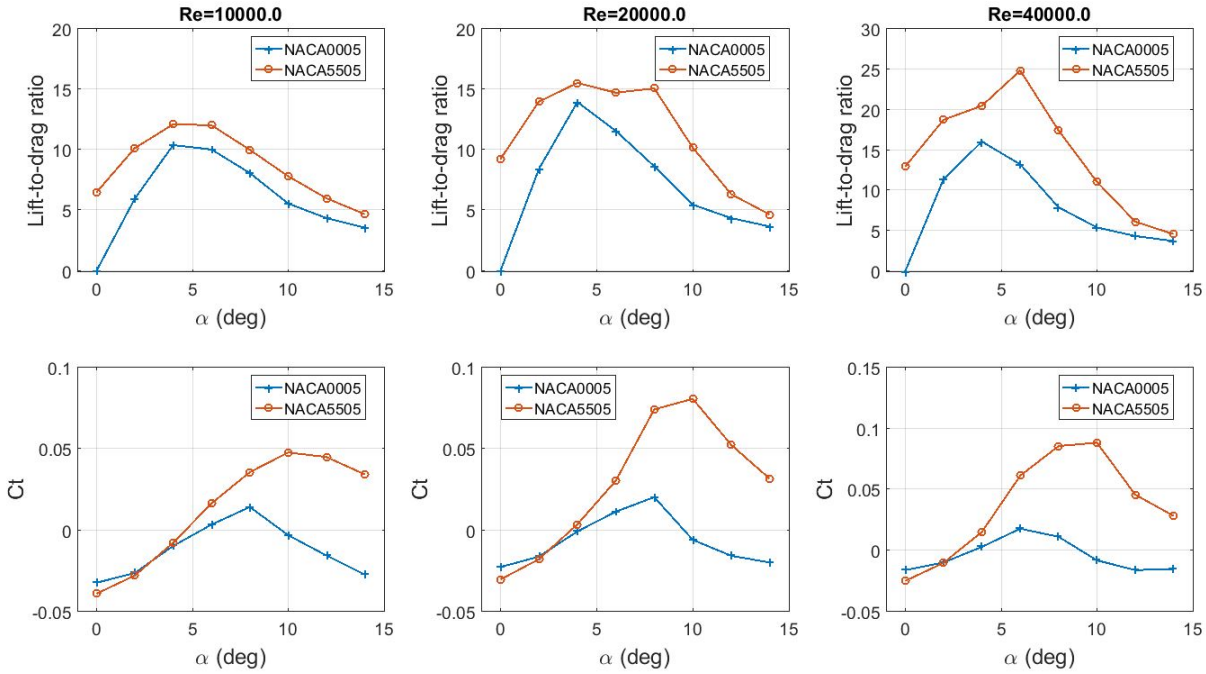

Figure 36: Effect of the 5% camber on NACA 0005

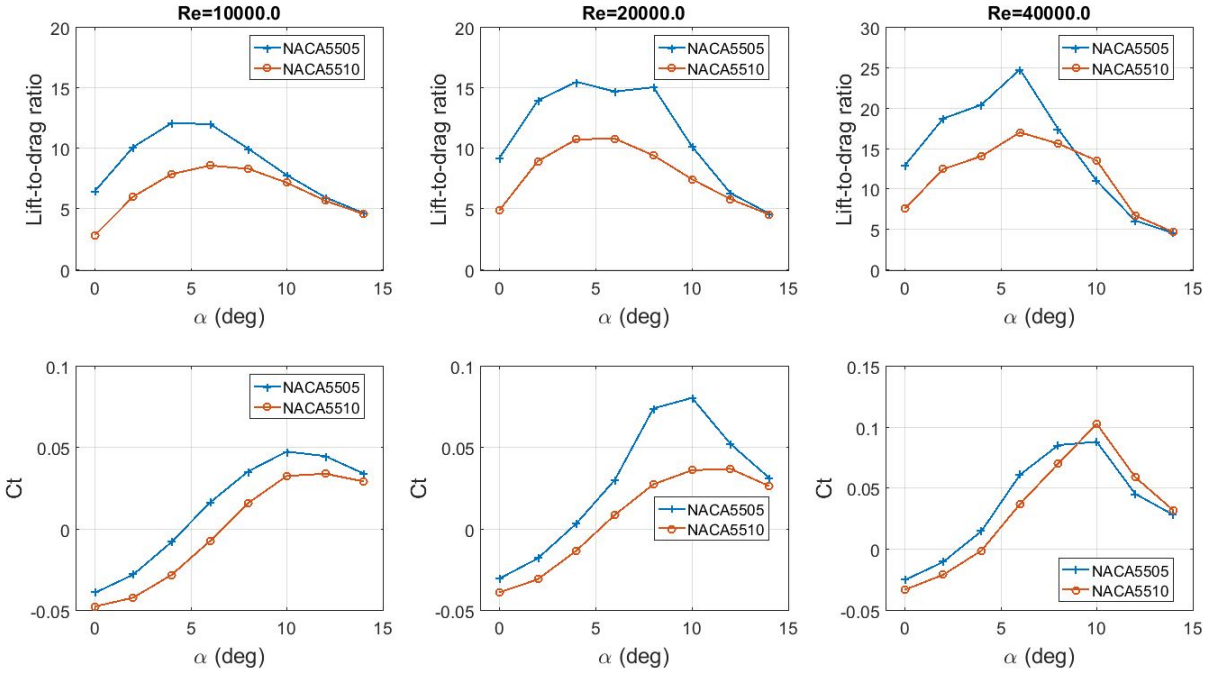

Figure 37: Comparison of NACA 5505 and NACA 5510

Searching for better performance

In reality, the research of airfoils showing high performances at low Reynolds is not limited to NACA profiles. In fact, the existing results in this domain have shown that they were better profiles to maximize lift-to-drag ratio in this range of Reynolds. Based on the literature, we have then selected three special airfoils all dedicated for maximizing low Reynolds airfoils' performance. These are profiles E387, S1223 and BW3 and looking

at the raw results, their lift coefficient is effectively higher than the classical symmetrical NACA profiles. Their drag is also higher and it will be interesting to see if they are really improving the performance at such low Reynolds (these airfoils are generally considered for Reynolds around $10^5 - 10^6$. As said before, all the results for the non-symmetrical profiles have to be considered with care as the simulations have shown poor convergence for most of the cases.

A comparison of these three specific airfoils at $Re = 4 \cdot 10^4$ is presented here. It will then enable a visual comparison with the site `http://www.airfoiltools.com` which simulated them with Xfoil at $Re = 5 \cdot 10^4$. Keeping in mind that the results are considered valid with $\alpha \leqslant 8°$ for E387 and BW3 and $\alpha \leqslant 4°$ for S1223, this comparison is presented in Figure 38 and is pretty similar to what was predicted by Xfoil. Namely, a very fast drop in lift-to-drag ratio for S1223 (stall at $\approx 4°$) and a overall best performance of BW3 at this range of Reynolds. The comparison for lower Reynolds are presented in Appendix C and are confirming the good performance of BW3.

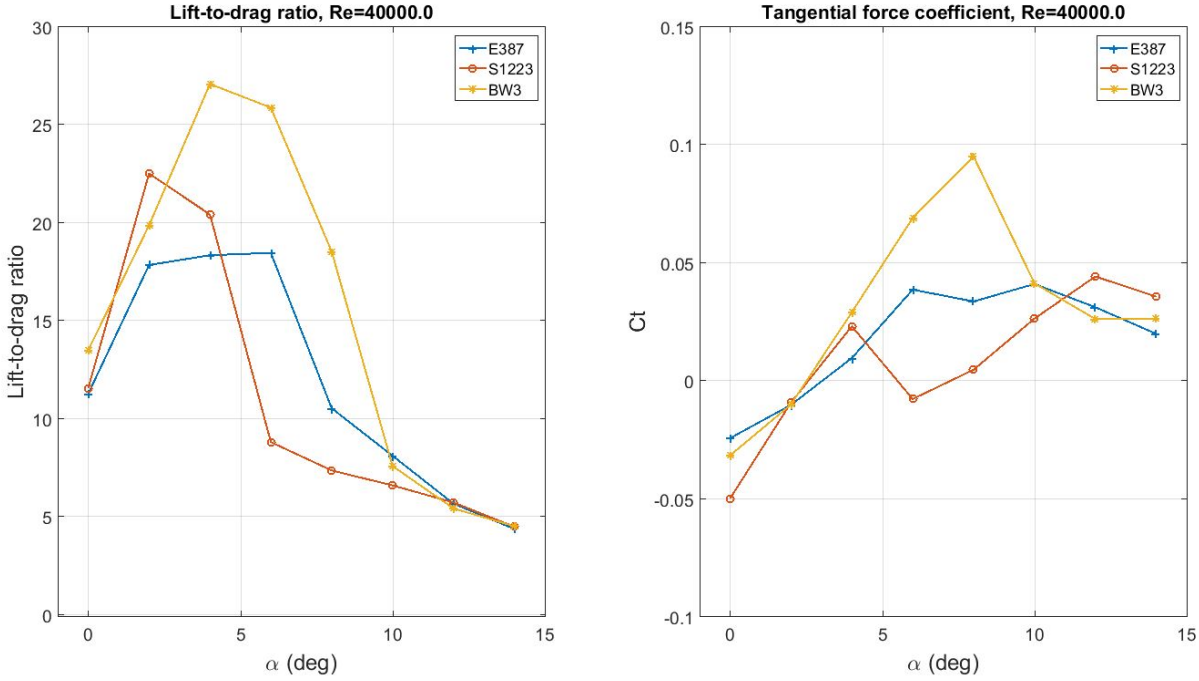

Figure 38: Comparison of E387, S1223 and BW3 at $Re = 4 \cdot 10^4$

Final comparison

Now, considering all the results, one more comparison can be done by selecting the most promising airfoils. In fact, this choice is depending on which Reynolds number we consider and therefore, some airfoils might be chosen just because they show good performance at one given Reynolds. Consequently, the following choice have been made for the final comparison:

- NACA 0012 for its good performance at $Re = 4 \cdot 10^4$
- NACA 5505 because it is surpassing NACA 0005 and NACA 5510 almost on the whole range of Reynolds (and recalling NACA 0005 was showing one of the best overall performance of the symmetrical profiles).

- The two best specific airfoils (E387 and BW3) for their overall good performances. S1223 has a too low stall angle for making sense for use in a VAWT

The comparison of these 4 airfoils is presented in Figure 39 restricting this time at $\alpha = 10°$ as almost none of the simulations converged (or were considered as relevant) at higher angles of attack.

The results are pretty clear and two airfoils in particular seem to perform better at the three Reynolds number tested. It is NACA 5505 and BW3 which are pretty close in term of shape (BW3 has also a maximum thickness of around 5% with a max camber of 5.7% around mid-chord). It is then pretty logical that these two have approximately the same performances and the fact that they are overall better goes in the direction of Sunada's conclusions [8] for low Reynolds airfoils' performances.

One more time, we can also note the similarity with the prediction from Xfoil; even if the absolute values are different and the profile NACA 5505 is not available, the comparison presented on `http://www.airfoiltools.com` have some similarities with our comparison for $Re = 4 \cdot 10^4$. Though, forgetting the others airfoils would be precipitated and not realistic as more tests have to be designed with (hopefully) a better convergence of the solutions. It is also important to keep in mind that these simulation are not entirely representative of the performance of the VAWT that will use these airfoils as blade shapes and this has to be simulated further (see section 8).

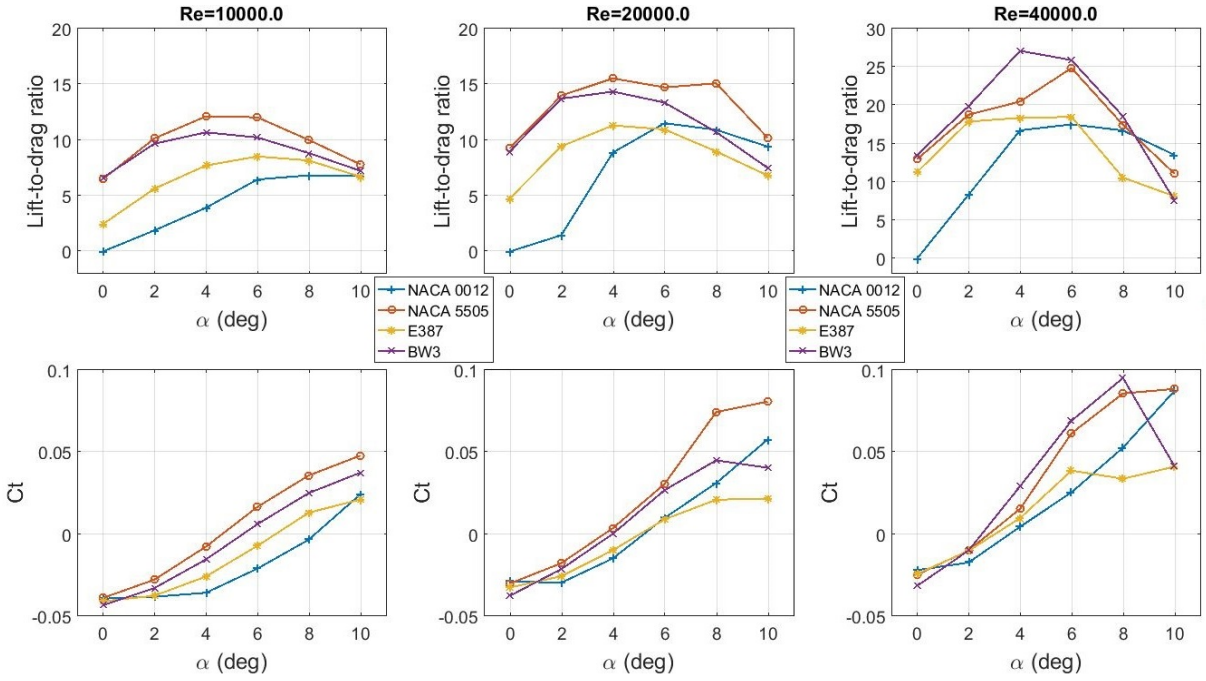

Figure 39: Comparison of NACA 0012, NACA 5505, E387 and BW3

8 Continuation of the project

As said before, this report is presenting the first part of a bigger project with is aiming to predict the performance of VAWTs using these airfoils as blade shape (see section 8.1). Additionally, more work is needed in order to have really relevant results on the non-symmetrical airfoils due to the low convergence of our solutions and more airfoils have to be simulated to get a better panel of the shapes possible. According to Xfoil predictions (which worked pretty well until now), AH6407 would definitely be a good choice for further research in shapes and looking at the literature on the subject, the simple 5% cambered plate seems to offer very interesting performance while having low complexity (see for example [10]). Another type of airfoils that could be investigated are the two-parts' airfoils, with a flexible trailing edge for example. It seems that this type of modification can improve interestingly the aerodynamics' performances for low TSR although it rises the level of complexity of the blades.

8.1 Simulation of the airfoils as part of a VAWT

Modelling the airfoils as part of a scaled VAWT will be performed by applying the Double Multiple Stream Tube (DMST) model. It will be very briefly introduced here in order to get a better understanding of the work presented in this report. This model has basically been developed by I. Paraschivoiu [11] for the Darrieus wind turbines and further described among others by Islam et al. [1] or by H. Beri and Y.Yao [12].

This model is basically dividing the domain into parallel "stream tubes" in which will be considered a certain wind velocity. Each of this tube will be then separated in two, with an upwind and a downwind half (see Figure 40a taken from [12]). The velocity at rotor level is calculated for each half tube using the actuator theory (see Figure 40b also taken from [12] used as well for horizontal axis wind turbines. In fact, the airfoils rotating are represented by two actuators having an induction factor a (upwind) and a'(downwind) on which the air will apply aerodynamic forces. According to this theory (and assuming complete expansion from upwind wake before reaching the second actuator), the downstream equilibrium velocity between the two blades is:

$$V_e = V_\infty(1 - 2a) \tag{10}$$

And the induced velocity hitting the downwind blade is then described by:

$$V_{ad} = V_e \cdot (1 - a') = V_\infty(1 - 2a)(1 - a') \tag{11}$$

With a and a' being the induction factor of the actuators which are expressed by:

$$a = \frac{V_\infty - V_{au}}{V_\infty} \tag{12}$$

$$a' = \frac{V_e - V_{ad}}{V_e} \tag{13}$$

V_{au} and V_{ad} being respectively the upstream- and downstream-induced velocities arriving on the actuators and V_∞ being the incoming wind speed before the turbine.

Using the local wind velocity and the aerodynamic coefficients of the airfoils, it can then compute the aerodynamic forces acting on the blades and model the thrust applied on the airfoils by the upcoming wind (and therefore its thrust coefficient). At the same time, the equation for the conservation of momentum is solved with the actuators theory for assumed induction factors and the corresponding thrust coefficient is computed.

It is then using an iterative process for adjusting the induction factors for each of the tube until the solution for both thrust corresponds in each tube. Note that the thrust of the airfoils on the incoming wind also influences the aerodynamics condition and is therefore modifying the induced flow velocity and its effect on the blade.

For this matter, it is important to note that the aerodynamic performances of the airfoils are needed at angles of attack bigger that 14° (see section 2.1). It has been shown that dynamic stall is present on VAWT and therefore this model is also implementing a dynamic stall model for $\alpha > 14°$ in order to compute the aerodynamic performances on the whole rotation of the turbine.

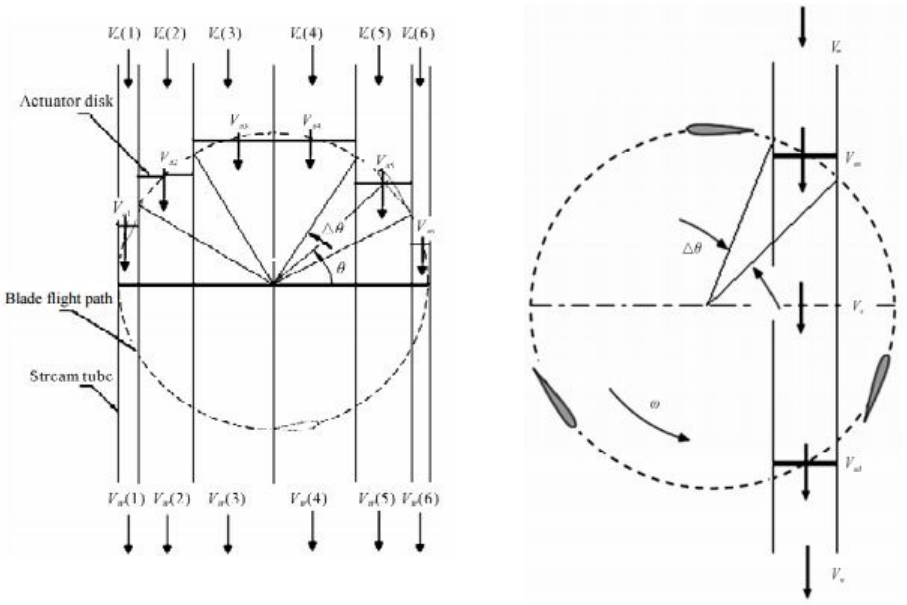

(a) Stream tubes ($\Delta\theta$ constant) (b) Actuator model applied on VAWT

Figure 40: Double Multiple Stream Tube model for VAWT

This model is globally recognized to show some good agreements between calculations and experimental results and it can already give an idea of the power production for a given airfoil. This part of the project is done in parallel by V.Rolin also in the WIRE Laboratory, having as a long term objective to study which airfoil would have the best theoretical performance as part of a VAWT and launch an experiment in the wind tunnel at EPFL.

9 Summary

The low Reynolds aerodynamics is definitely a difficult domain to study and the results presented in this report are to be considered with care. Obviously, the convergence problems on the non-symmetrical simulations have to be addressed and the research for higher performances' airfoils have to go on. However, the results obtained during this project are already interesting and it seems that they should be sufficiently accurate for the main purpose of this work which is the comparisons between airfoils and the selection of the most promising one(s).

From our simulations, two airfoils seem to show overall better performances than the rest; NACA 5505 and BW3. Based on their tangential force coefficients, both should be able to generate positive torque when used as blade shape in a scaled VAWT. It confirms mostly what can be found in the literature as they are both thin airfoils with a camber of around 5% and that already shows that these simulations make sense at this level.

The addition of a sharp leading edge has also been investigated in this project and it seems that such modification is not really improving aerodynamics performances at Reynolds numbers bigger than 10^4. Though, the literature seem to think the contrary and it is maybe worth continuing the study of this parameter to understand how such a difference can appear.

Except those uncertainties on the results, we can highlight the fact that the automation process created in the previous semester project and completed with this one is now working nicely and it offers a real opportunity for the creation of large dataset of airfoil's performances at this range of Reynolds numbers. Especially if we consider the new mesh created recently for the non-symmetrical profiles which should definitely improve the convergence of the solutions for a large range of new airfoils.

References

[1] Mazharul Islam, David S.-K. Ting and Amir Fartaj, *Aerodynamic models for Darrieus-type straight-bladed vertical axis wind turbines.*

Renewable and Sustainable Energy Reviews 12, pp.1087–1109, Elsevier Ltd, 2008

[2] V. Rolin and F. Porté-Agel, *"Wind-tunnel study of the wake behind a vertical axis wind turbine in a boundary layer flow using stereoscopic particle image velocimetry".*

Journal of Physics: Conference Series 625, p.012012, IOP Publishing, 2015

[3] E. Piccoli, *"CFD prediction of low-Reynolds airfoil performance."*

Semester project performed under the supervision of V.Rolin and F. Porté-Agel at the WIRE laboatory at EPFL during the spring semester 2016.

[4] J. McArthur, *"Aerodynamics of wings at low Reynolds numbers"*

Qualifying exam proposal presented at University of Southern California, 2007

[5] H. Sturm, G. Dumstorff, P. Busche, D. Westermann and W. Lang 1,*"Boundary Layer Separation and Reattachment Detection on Airfoils by Thermal Flow Sensors"*

Sensors 2012, 12, pp.14292-14306

[6] V. Kumar, M. Paraschivoiu, I. Paraschivoiu,*"Low Reynolds Number Vertical Axis Wind Turbine for Mars"*

Wind Engineering, 2010 - SAGE Publications

[7] Sheldahl, R.E. and Klimas, P.C.,*"Aerodynamic characteristics of seven symmetrical airfoil sections through 180-degree angle of attack for use in aerodynamic analysis of vertical axis wind turbines"*

Report SAND80–2114, Sandia National Laboratories, 1981

[8] S. Sunada, A. Sakaguchi and K. Kawachi,*"Airfoil Section Characteristics at a Low Reynolds Number"*

Journal of Fluids Engineering, Vol. 119, pp.129-135, March 1997

[9] M. S. Selig, J. J. Guglielmo, A. P. Broeren, C. A. Lyon, C. P. Ninham and P Giguere,*"Summary of Low-Speed Airfoil Data, volume 1 and 2"*

SoarTech Publications, 1995 (volume 1) and 1996 (volume 2)

[10] E. E. Laitone,*"Aerodynamic lift at Reynolds numbers below* $7 \cdot 10^4$*"*

AIAA Journal, Vol. 34, No. 9 (1996), pp. 1941-1942.

[11] I. Paraschivoiu, *"Double-multiple streamtube model for studying vertical-axis wind turbines"*

Journal of Propulsion and Power, Vol. 4, No. 4 (1988), pp. 370-377.

[12] H. Beri and Y. Yao, *"Double Multiple Stream Tube Model and Numerical Analysis of Vertical Axis Wind Turbine"*,

Energy and Power Engineering, 2011, 3, 262-270

Appendices

A Performance of airfoils

A.1 NACA 0005

Reynolds 10'000

Table A.1: Data for NACA 0005, $Re = 10^4$

Reynolds = 10000.0

Alpha	CL	CD	Cl/Cd	Ct	number of iterations
0	2.16E-05	0.032207	0.000671	-0.03221	3715
2	0.19747	0.033087	5.9684	-0.02618	3217
4	0.36591	0.035187	10.3989	-0.00958	4694
6	0.65062	0.064825	10.0365	0.003538	6492
8	0.85514	0.1057	8.0899	0.014337	5788
10	0.91817	0.1649	5.5682	-0.00295	9764
12	0.96821	0.22162	4.3688	-0.01547	10000
14	0.92567	0.25882	3.5764	-0.0272	10000

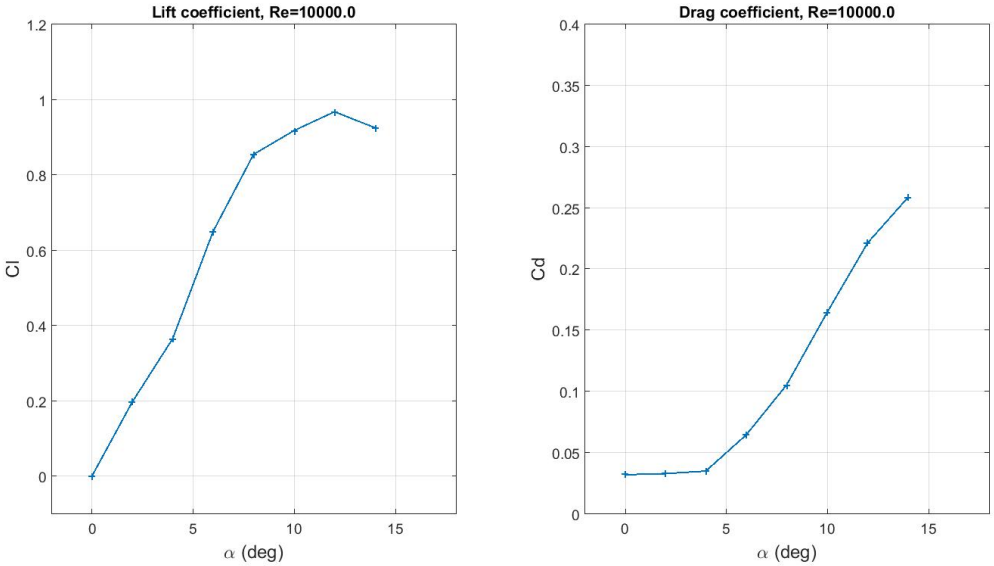

Figure A.1: Polars for NACA 0005, $Re = 10^4$

Reynolds 20'000

Table A.2: Data for NACA 0005, $Re = 2 \cdot 10^4$

Reynolds = 20000.0

Alpha	CL	CD	Cl/Cd	Ct	number of iterations
0	2.23E-05	0.022533	0.000989	-0.02253	2517
2	0.19258	0.022871	8.4202	-0.01614	3096
4	0.37256	0.026703	13.9521	-0.00065	4788
6	0.6172	0.053312	11.577	0.011494	4776
8	0.82786	0.095766	8.6446	0.020382	6215
10	0.95139	0.17363	5.4795	-0.00578	10000
12	0.96309	0.22069	4.3641	-0.01563	10000
14	0.88877	0.24194	3.6736	-0.01974	10000

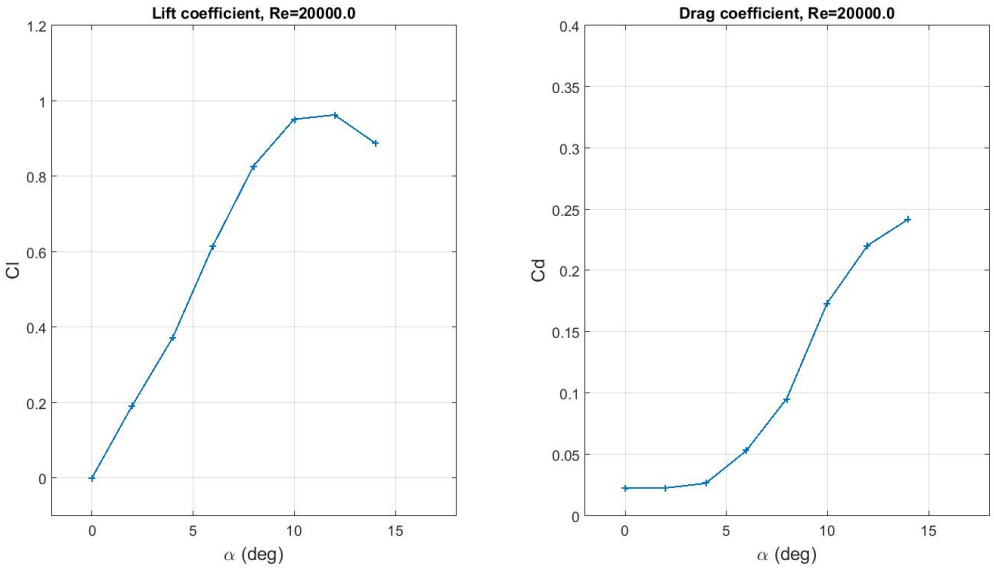

Figure A.2: Polars for NACA 0005, $Re = 2 \cdot 10^4$

Reynolds 40'000

Table A.3: Data for NACA 0005, $Re = 4 \cdot 10^4$

Reynolds = 40000.0

Alpha	CL	CD	Cl/Cd	Ct	number of iterations
0	2.65E-05	0.01594	0.001661	-0.01594	1554
2	0.18319	0.016066	11.4024	-0.00966	3446
4	0.41427	0.025804	16.0546	0.003157	6447
6	0.615	0.04647	13.2341	0.018069	4052
8	0.80739	0.10196	7.9187	0.011399	10000
10	1.031	0.18982	5.4316	-0.0079	10000
12	0.99697	0.22813	4.3702	-0.01586	10000
14	0.85004	0.22737	3.7385	-0.01498	10000

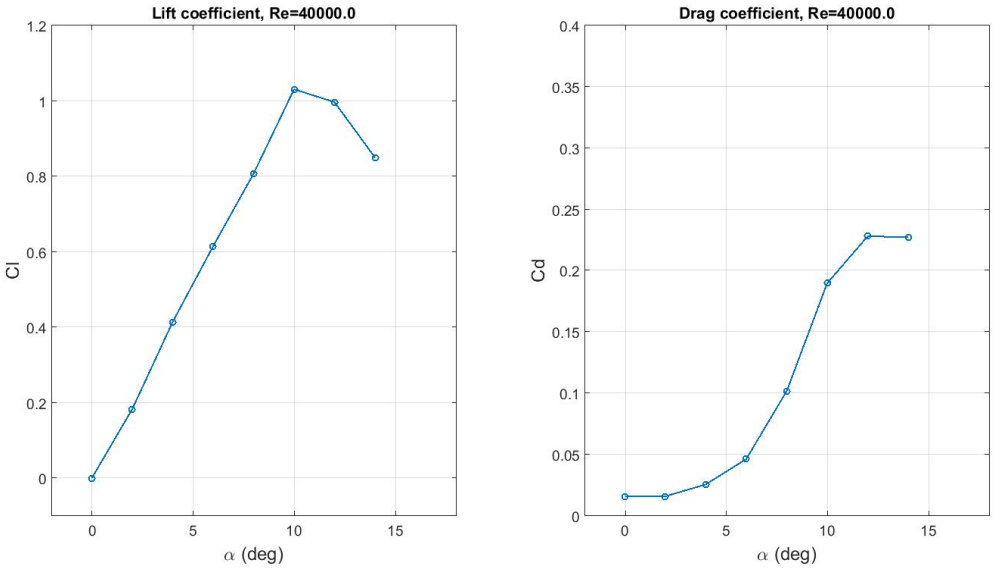

Figure A.3: Polars for NACA 0005, $Re = 4 \cdot 10^4$

A.2 NACA 0009

Reynolds 10'000

Table A.4: Data for NACA 0009, $Re = 10^4$

Reynolds = 10000.0

Alpha	CL	CD	Cl/Cd	Ct	number of iterations
0	-9.02E-05	0.035558	-0.00254	-0.03556	4081
2	0.1588	0.036174	4.3898	-0.03061	4051
4	0.26273	0.040535	6.4816	-0.02211	4783
6	0.51314	0.061146	8.3921	-0.00717	7836
8	0.7551	0.087524	8.6273	0.018417	5472
10	0.91931	0.13599	6.7603	0.025716	7290
12	0.88492	0.20094	4.4039	-0.01256	10000
14	0.85407	0.24332	3.51	-0.02948	10000

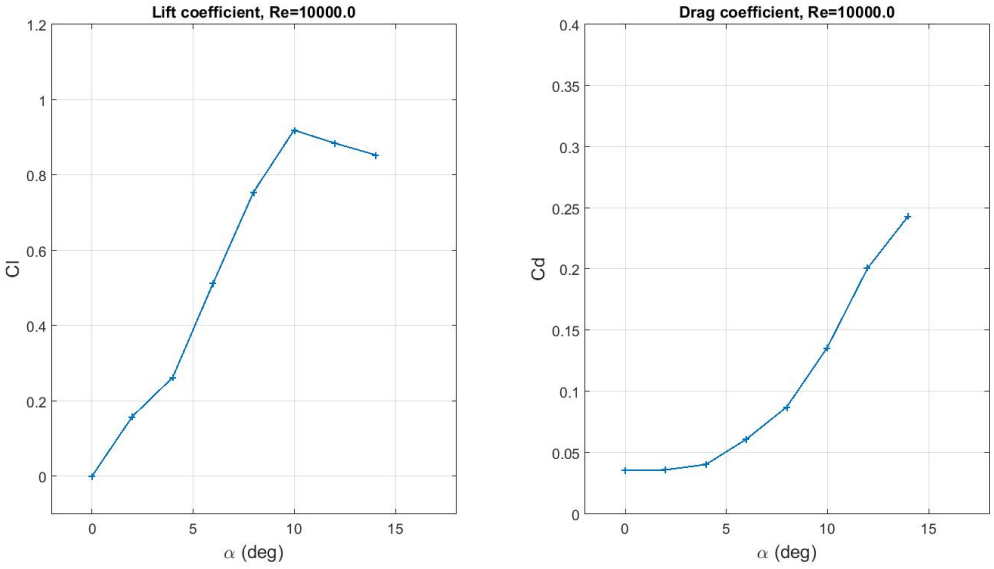

Figure A.4: Polars for NACA 0009, $Re = 10^4$

Reynolds 20'000

Table A.5: Data for NACA 0009, $Re = 2 \cdot 10^4$

Reynolds = 20000.0

Alpha	CL	CD	Cl/Cd	Ct	number of iterations
0	-9.58E-05	0.025156	-0.00381	-0.02516	2858
2	0.14788	0.025806	5.7307	-0.02063	3229
4	0.3084	0.033232	9.2804	-0.01164	4129
6	0.5449	0.04248	12.8273	0.01471	6198
8	0.72384	0.063393	11.4183	0.037963	4757
10	0.88268	0.11427	7.7243	0.040739	7444
12	0.93138	0.21133	4.4071	-0.01307	10000
14	0.8565	0.24351	3.5172	-0.02908	10000

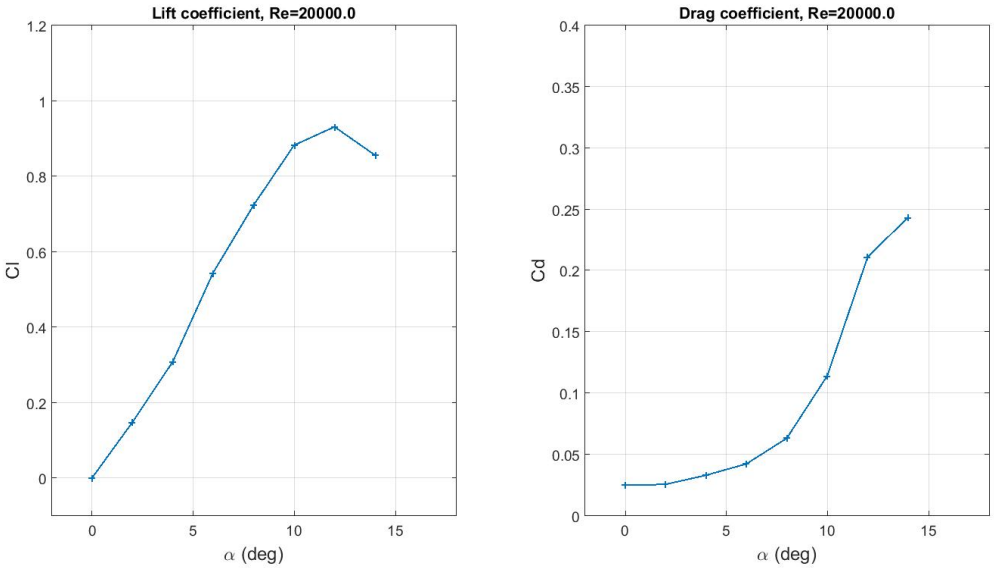

Figure A.5: Polars for NACA 0009, $Re = 2 \cdot 10^4$

Reynolds 40'000

Table A.6: Data for NACA 0009, $Re = 4 \cdot 10^4$

Reynolds = 40000.0

Alpha	CL	CD	Cl/Cd	Ct	number of iterations
0	-8.19E-05	0.018002	-0.00455	-0.018	2093
2	0.1053	0.019545	5.3873	-0.01586	10000
4	0.42932	0.023228	18.4827	0.006776	6809
6	0.54788	0.030748	17.8182	0.026689	5426
8	0.73384	0.049426	14.8473	0.053186	4141
10	0.84761	0.11469	7.3903	0.034236	10000
12	1.0377	0.23694	4.3798	-0.016	10000
14	0.90513	0.25656	3.528	-0.02997	10000

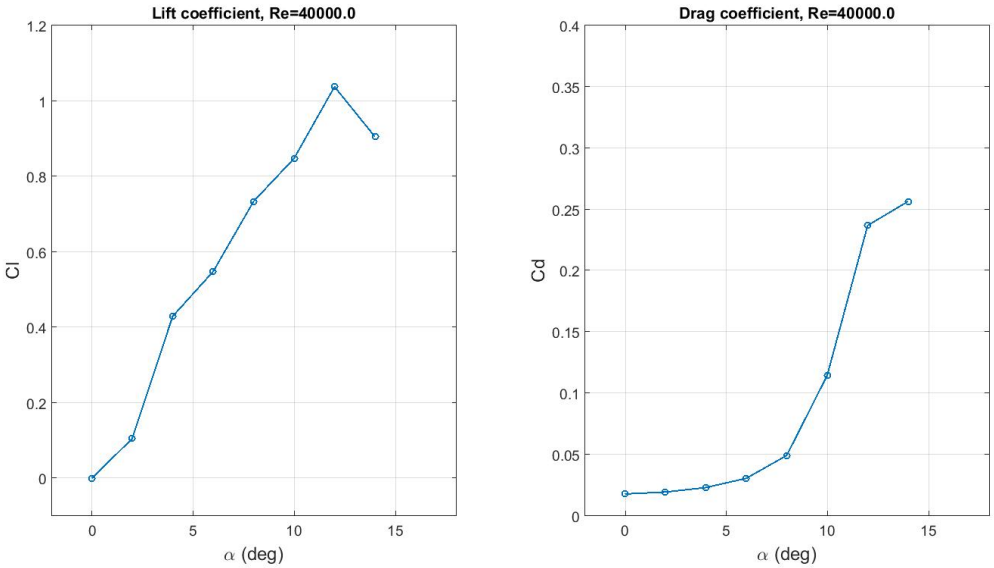

Figure A.6: Polars for NACA 0009, $Re = 4 \cdot 10^4$

A.3 NACA 0012

Reynolds 10'000

Table A.7: Data for NACA 0012, $Re = 10^4$

Reynolds = 10000.0

Alpha	CL	CD	Cl/Cd	Ct	number of iterations
0	-4.83E-05	0.039337	-0.00123	-0.03934	5014
2	0.077304	0.040869	1.8915	-0.03815	4902
4	0.19375	0.049408	3.9213	-0.03577	4734
6	0.42623	0.065967	6.4614	-0.02105	10000
8	0.59562	0.087089	6.8392	-0.00335	8408
10	0.86552	0.12798	6.7631	0.024264	5726
12	0.77158	0.18017	4.2825	-0.01581	10000
14	0.781	0.22989	3.3973	-0.03412	9899

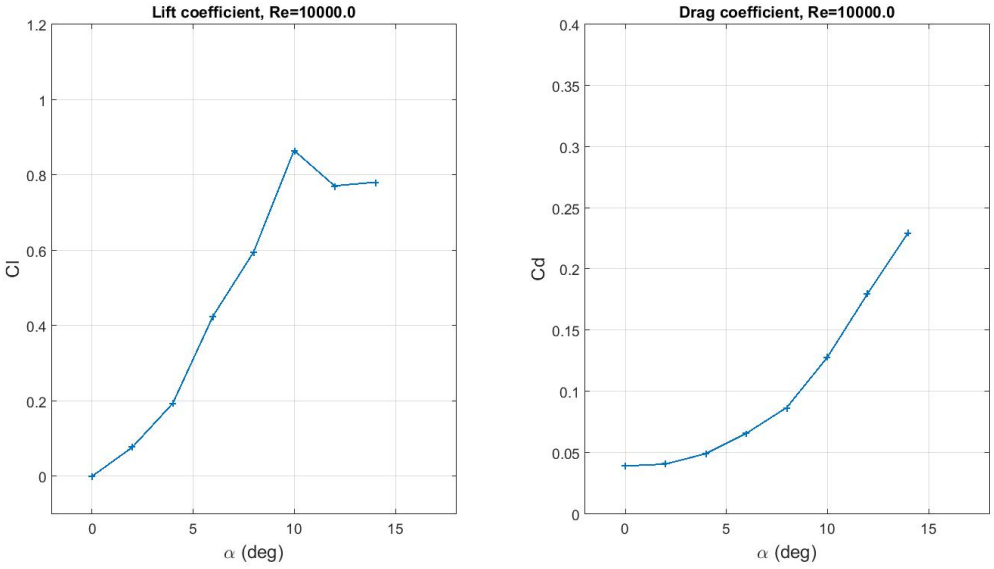

Figure A.7: Polars for NACA 0012, $Re = 10^4$

Reynolds 20'000

Table A.8: Data for NACA 0012, $Re = 2 \cdot 10^4$

Reynolds = 20000.0

Alpha	CL	CD	Cl/Cd	Ct	number of iterations
0	-0.00018	0.028771	-0.00629	-0.02877	4659
2	0.045652	0.031242	1.4612	-0.02963	10000
4	0.34865	0.039246	8.8838	-0.01483	7562
6	0.54321	0.047166	11.5168	0.009873	7086
8	0.64118	0.058735	10.9164	0.031071	5699
10	0.83666	0.08893	9.408	0.057705	5101
12	0.82236	0.17461	4.7098	0.000187	10000
14	0.7885	0.23025	3.4245	-0.03266	10000

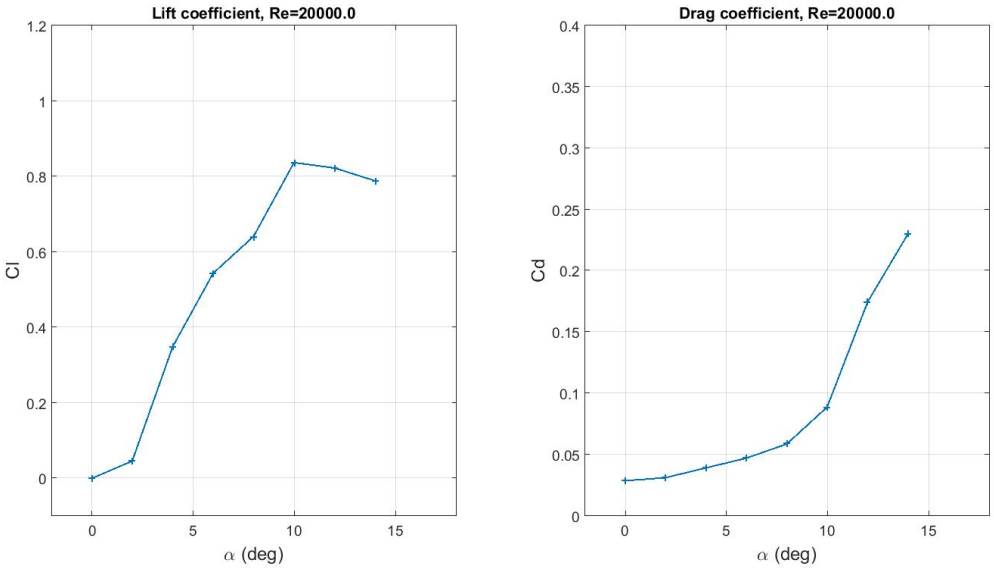

Figure A.8: Polars for NACA 0012, $Re = 2 \cdot 10^4$

Reynolds 40'000

Table A.9: Data for NACA 0012, $Re = 4 \cdot 10^4$

Reynolds = 40000.0

Alpha	CL	CD	Cl/Cd	Ct	number of iterations
0	-6.95E-05	0.021976	-0.00316	-0.02198	3420
2	0.20302	0.024397	8.3214	-0.0173	7341
4	0.44052	0.026347	16.7198	0.004446	6819
6	0.53382	0.030492	17.5067	0.025474	4969
8	0.65977	0.039503	16.702	0.052705	5218
10	0.86708	0.064165	13.5133	0.087377	4157
12	0.88879	0.1621	5.483	0.026232	10000
14	0.88585	0.25466	3.4786	-0.03279	10000

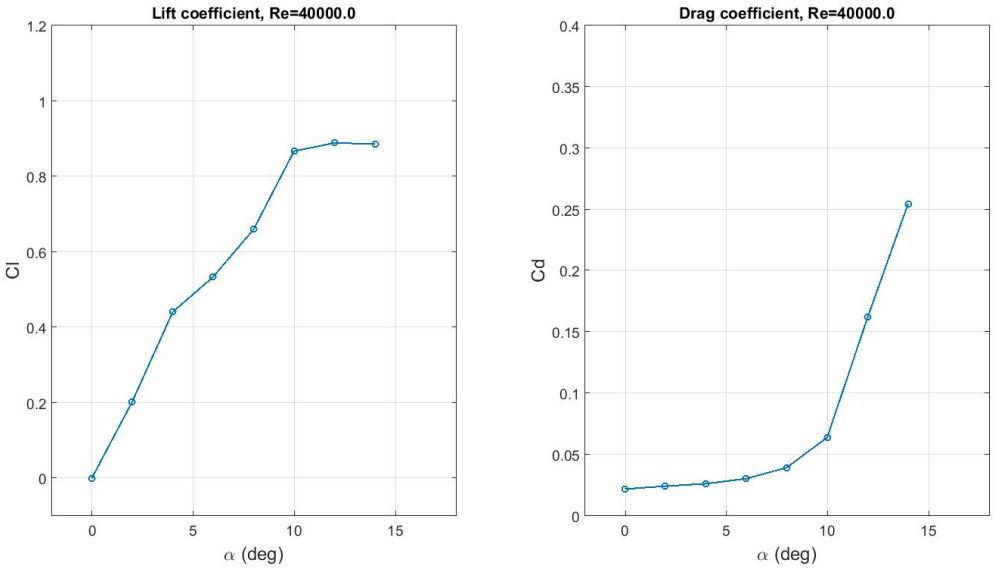

Figure A.9: Polars for NACA 0012, $Re = 4 \cdot 10^4$

A.4 NACA 0018

Reynolds 10'000

Table A.10: Data for NACA 0018, $Re = 10^4$

Reynolds = 10000.0

Alpha	CL	CD	Cl/Cd	Ct	number of iterations
0	3.33E-05	0.057298	0.00058	-0.0573	7743
2	-0.0009628	0.059652	-0.01614	-0.05965	10000
4	0.1467	0.069779	2.1024	-0.05938	10000
6	0.2479	0.08198	3.0239	-0.05562	10000
8	0.35201	0.10139	3.472	-0.05141	10000
10	0.44774	0.12767	3.507	-0.04798	10000
12	0.59696	0.1812	3.2945	-0.05312	8145
14	0.38233	0.18232	2.097	-0.08441	10000

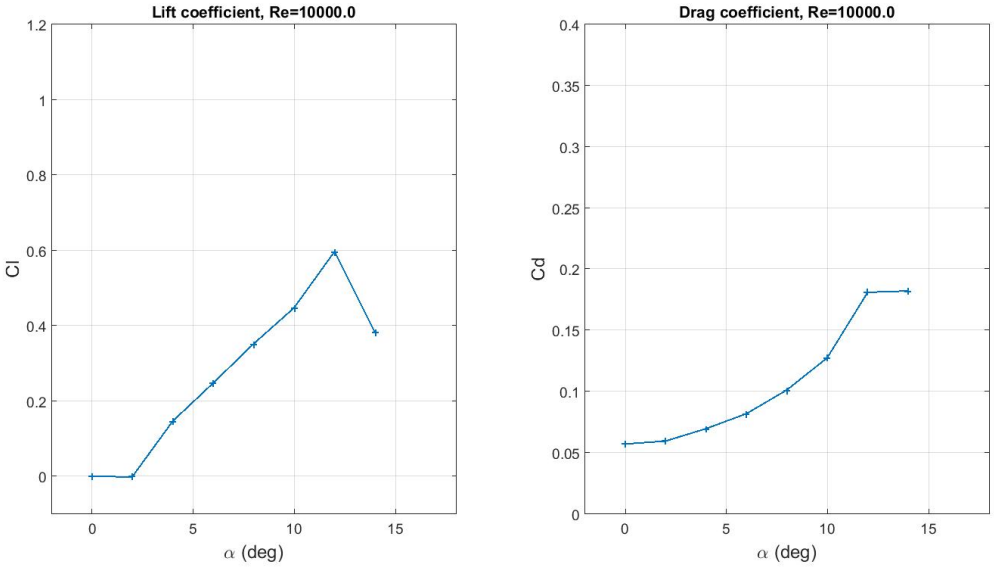

Figure A.10: Polars for NACA 0018, $Re = 10^4$

Reynolds 20'000

Table A.11: Data for NACA 0018, $Re = 2 \cdot 10^4$

Reynolds = 20000.0

Alpha	CL	CD	Cl/Cd	Ct	number of iterations
0	-0.00031	0.048605	-0.00642	-0.04861	4867
2	0.28012	0.0507	5.525	-0.04089	7798
4	0.33908	0.054373	6.2361	-0.03059	6910
6	0.41443	0.061341	6.7562	-0.01769	6076
8	0.53858	0.073996	7.2785	0.00168	5959
10	0.61146	0.10157	6.0203	0.006155	7970
12	0.59579	0.15106	3.9439	-0.02389	10000
14	0.67733	0.20981	3.2283	-0.03972	10000

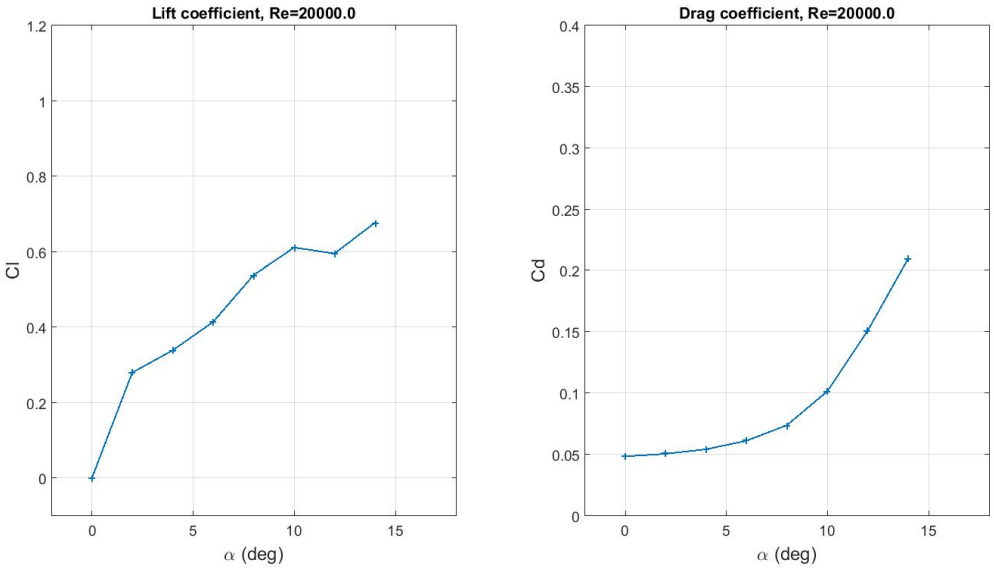

Figure A.11: Polars for NACA 0018, $Re = 2 \cdot 10^4$

Reynolds 40'000

Table A.12: Data for NACA 0018, $Re = 4 \cdot 10^4$

Reynolds = 40000.0

Alpha	CL	CD	Cl/Cd	Ct	number of iterations
0	0.071488	0.035375	2.0209	-0.03538	10000
2	0.34093	0.034724	9.8181	-0.02281	9917
4	0.50201	0.035872	13.9946	-0.00077	8228
6	0.5528	0.039302	14.0653	0.018696	10000
8	0.62304	0.04724	13.1889	0.039931	8147
10	0.70669	0.058763	12.0261	0.064846	5731
12	0.72385	0.09165	7.898	0.06085	10000
14	0.75291	0.18358	4.1012	0.004015	10000

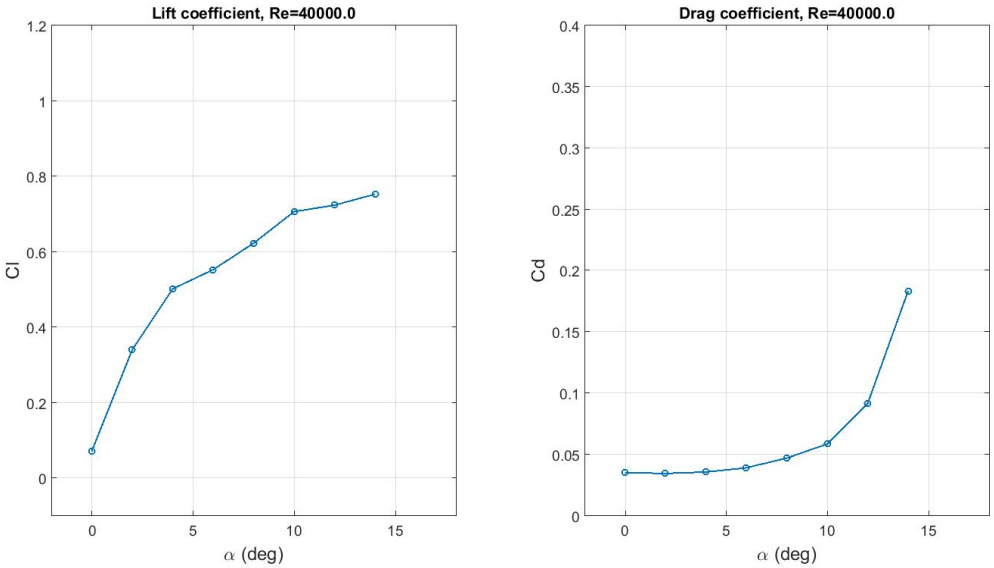

Figure A.12: Polars for NACA 0018, $Re = 4 \cdot 10^4$

A.5 NACA 0021

Reynolds 10'000

Table A.13: Data for NACA 0021, $Re = 10^4$

Reynolds = 10000.0

Alpha	CL	CD	Cl/Cd	Ct	number of iterations
0	3.84E-05	0.073461	0.000523	-0.07346	6286
2	0.043501	0.074656	0.582686	-0.07309	17506
4	0.13895	0.084065	1.652888	-0.07417	11519
6	0.17491	0.093077	1.8792	-0.07429	8206
8	0.18283	0.10684	1.7112	-0.08036	10000
10	0.27244	0.12793	2.1297	-0.07867	10000
12	0.38986	0.1554	2.5088	-0.07095	10000
14	0.50012	0.20233	2.4718	-0.07533	10000

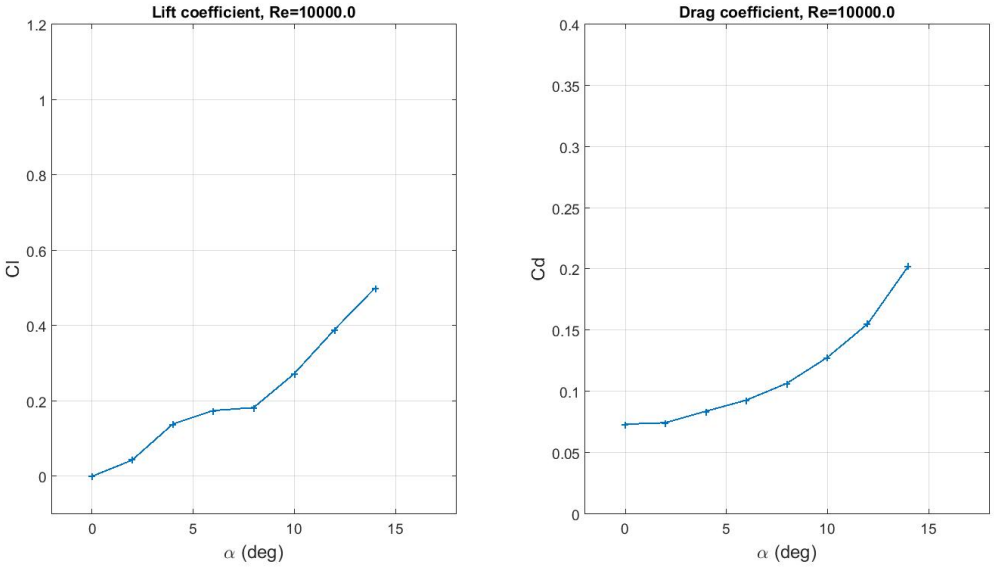

Figure A.13: Polars for NACA 0021, $Re = 10^4$

Reynolds 20'000

Table A.14: Data for NACA 0021, $Re = 2 \cdot 10^4$

Reynolds = 20000.0

Alpha	CL	CD	Cl/Cd	Ct	number of iterations
0	0.000444	0.060807	0.007305	-0.06081	5769
2	0.24884	0.061444	4.0498	-0.05272	6681
4	0.39341	0.065218	6.0323	-0.03762	8613
6	0.34181	0.07238	4.7225	-0.03626	6408
8	0.48838	0.086345	5.6562	-0.01754	4797
10	0.38008	0.11419	3.3286	-0.04645	10000
12	0.64007	0.16695	3.8339	-0.03022	10000
14	0.61388	0.21288	2.8837	-0.05805	10000

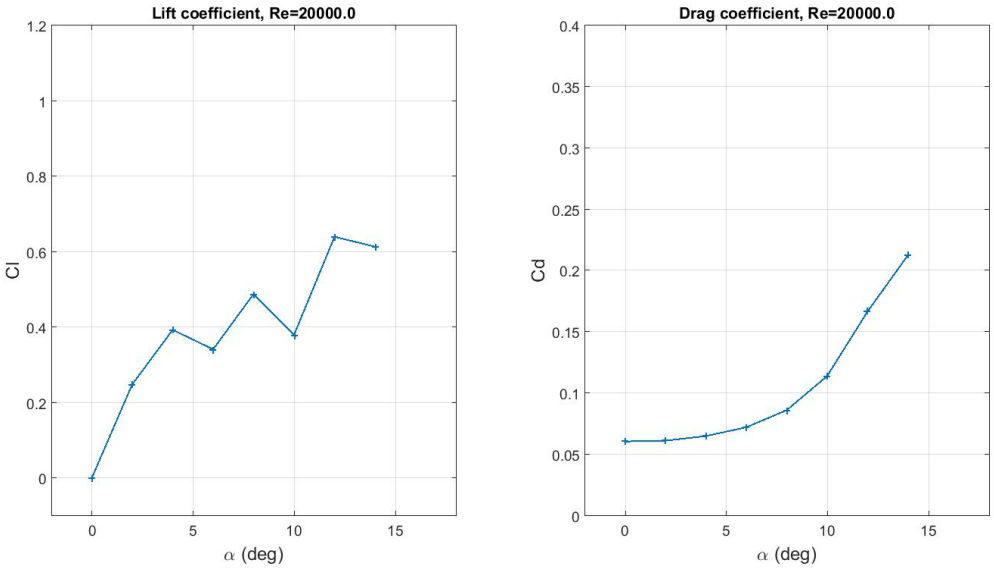

Figure A.14: Polars for NACA 0021, $Re = 2 \cdot 10^4$

Reynolds 40'000

Table A.15: Data for NACA 0021, $Re = 4 \cdot 10^4$

Reynolds = 40000.0

Alpha	CL	CD	Cl/Cd	Ct	number of iterations
0	0.000401	0.041072	0.009758	-0.04107	4737
2	0.23435	0.042005	5.5791	-0.0338	5624
4	0.42982	0.043447	9.893	-0.01336	4651
6	0.54796	0.046835	11.6998	0.010699	10000
8	0.55438	0.053249	10.4111	0.024424	5087
10	0.59766	0.07265	8.2265	0.032236	7832
12	0.60362	0.11539	5.2311	0.012631	10000
14	0.95991	0.21895	4.3842	0.01978	10000

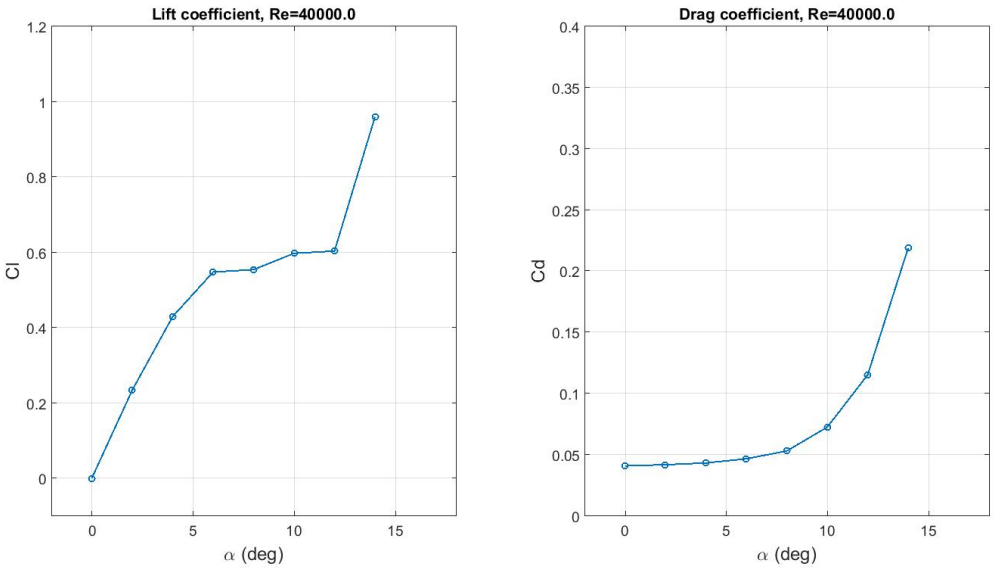

Figure A.15: Polars for NACA 0021, $Re = 4 \cdot 10^4$

A.6 NACA 0005-05

Reynolds 10'000

Table A.16: Data for NACA 0005-05, $Re = 10^4$

Reynolds = 10000.0

Alpha	CL	CD	Cl/Cd	Ct	number of iterations
0	9.86E-05	0.032493	0.003033	-0.03249	3828
2	0.18114	0.033377	5.4272	-0.02704	3322
4	0.40621	0.038024	10.6829	-0.0096	5299
6	0.61649	0.067203	9.1735	-0.00239	5524
8	0.82867	0.10927	7.5835	0.007119	5943
10	0.80542	0.15258	5.2786	-0.0104	10000
12	0.93736	0.21944	4.2716	-0.01975	10000
14	0.81217	0.22299	3.6422	-0.01988	10000

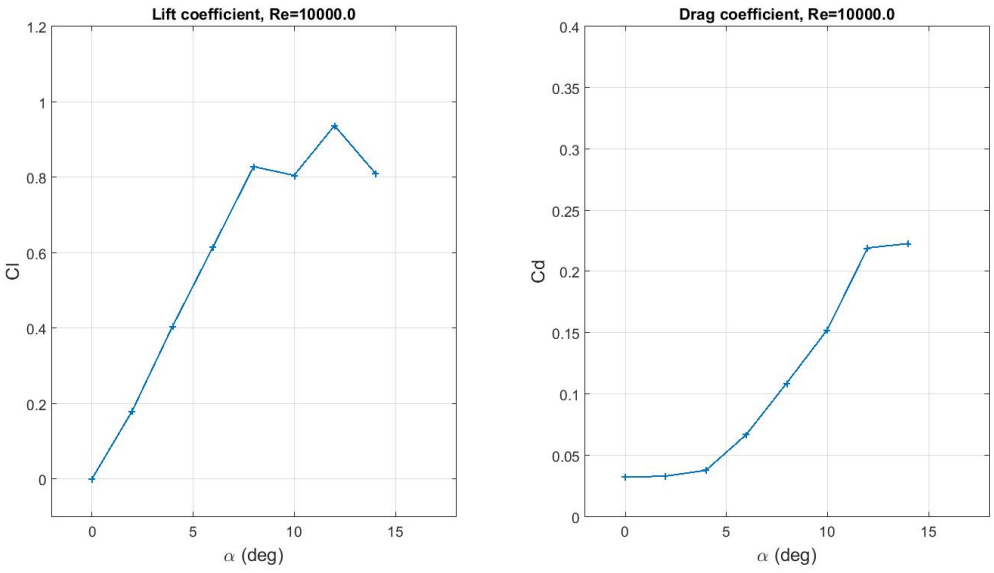

Figure A.16: Polars for NACA 0005-05, $Re = 10^4$

Reynolds 20'000

Table A.17: Data for NACA 0005-05, $Re = 2 \cdot 10^4$

Reynolds = 20000.0

Alpha	CL	CD	Cl/Cd	Ct	number of iterations
0	0.000101	0.022898	0.004402	-0.0229	2633
2	0.1658	0.023167	7.1568	-0.01737	3418
4	0.40297	0.036811	10.9469	-0.00861	4471
6	0.60353	0.061365	9.8351	0.002057	4796
8	0.79493	0.104	7.6435	0.007644	7841
10	0.81872	0.1568	5.2214	-0.01225	10000
12	0.73306	0.17707	4.1399	-0.02079	10000
14	0.13154	0.063841	2.0605	-0.03012	10000

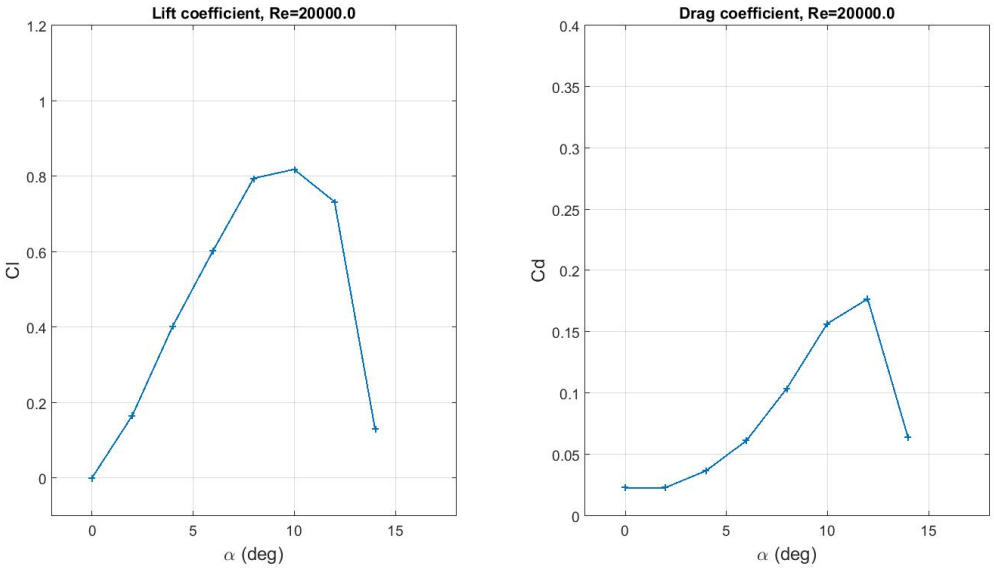

Figure A.17: Polars for NACA 0005-05, $Re = 2 \cdot 10^4$

Reynolds 40'000

Table A.18: Data for NACA 0005-05, $Re = 4 \cdot 10^4$

Reynolds = 40000.0

Alpha	CL	CD	Cl/Cd	Ct	number of iterations
0	0.000131	0.016375	0.008006	-0.01638	1665
2	0.15345	0.016593	9.2483	-0.01123	3735
4	0.40911	0.033735	12.127	-0.00512	3857
6	0.61707	0.057617	10.71	0.007201	4628
8	0.74101	0.10197	7.2671	0.002153	10000
10	0.83559	0.16107	5.1877	-0.01353	10000
12	0.83594	0.19549	4.2762	-0.01741	10000
14	-0.30118	-0.04045	7.445	-0.03361	10000

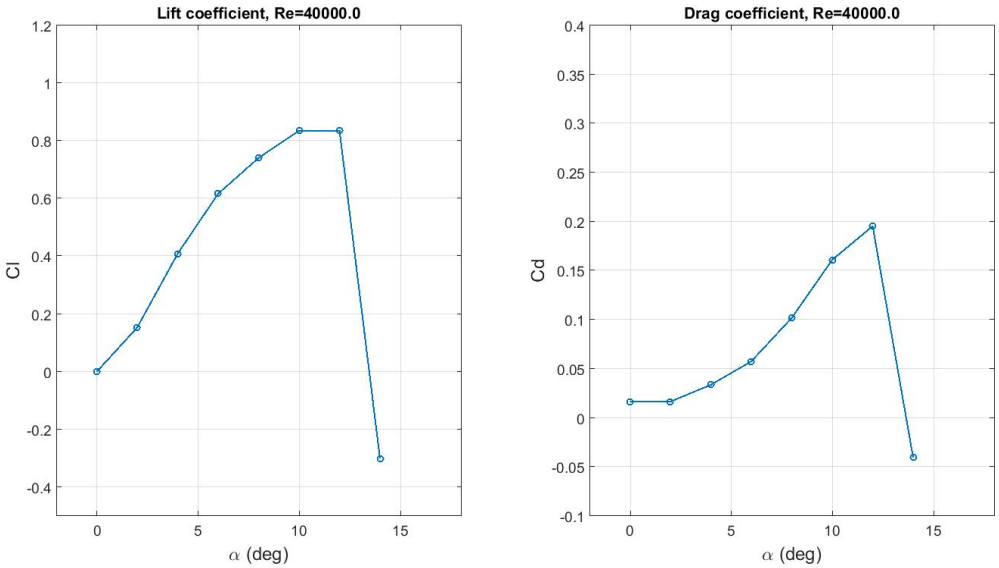

Figure A.18: Polars for NACA 0005-05, $Re = 4 \cdot 10^4$

A.7 NACA 0009-05

Reynolds 10'000

Table A.19: Data for NACA 0009-05, $Re = 10^4$

Reynolds = 10000.0

Alpha	CL	CD	Cl/Cd	Ct	number of iterations
0	-1.51E-05	0.037282	-0.0004	-0.03728	4835
2	0.10968	0.037764	2.9042	-0.03391	4389
4	0.22525	0.039233	5.7413	-0.02343	4522
6	0.55302	0.054639	10.1214	0.003467	6134
8	0.69911	0.083931	8.3296	0.014183	5795
10	0.76879	0.12569	6.1168	0.009723	8126
12	0.73548	0.17873	4.1151	-0.02191	10000
14	0.89132	0.25239	3.5316	-0.02926	10000

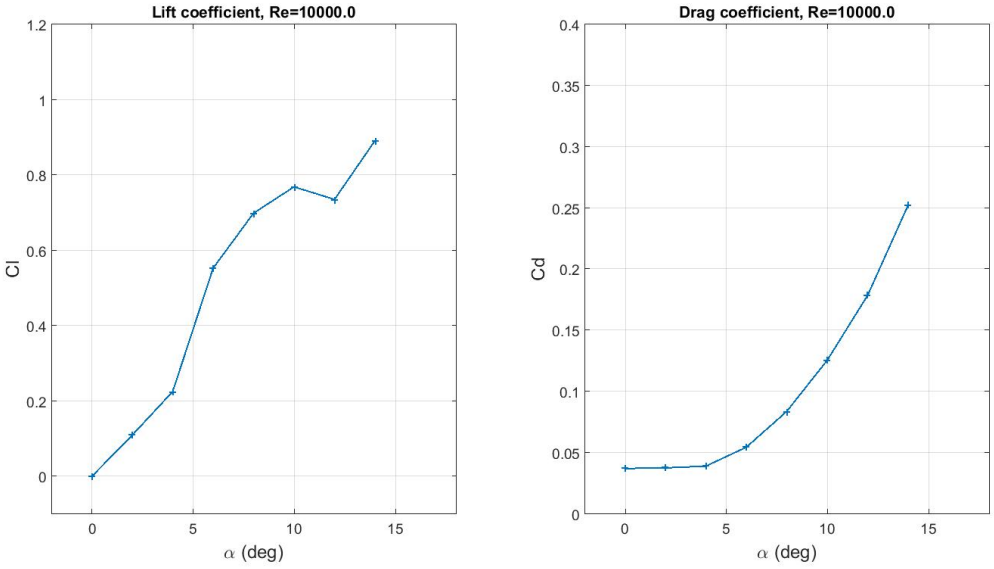

Figure A.19: Polars for NACA 0009-05, $Re = 10^4$

Reynolds 20'000

Table A.20: Data for NACA 0009-05, $Re = 2 \cdot 10^4$

Reynolds = 20000.0

Alpha	CL	CD	Cl/Cd	Ct	number of iterations
0	-5.00E-05	0.02746	-0.00182	-0.02746	4461
2	0.087916	0.02823	3.1143	-0.02514	3781
4	0.19528	0.03141	6.217	-0.01771	10000
6	0.53201	0.050088	10.6216	0.005797	4972
8	0.70939	0.077716	9.1279	0.021768	4793
10	0.67224	0.1182	5.6874	0.000331	10000
12	0.73591	0.1822	4.0391	-0.02521	10000
14	0.48706	0.1626	2.9955	-0.03994	10000

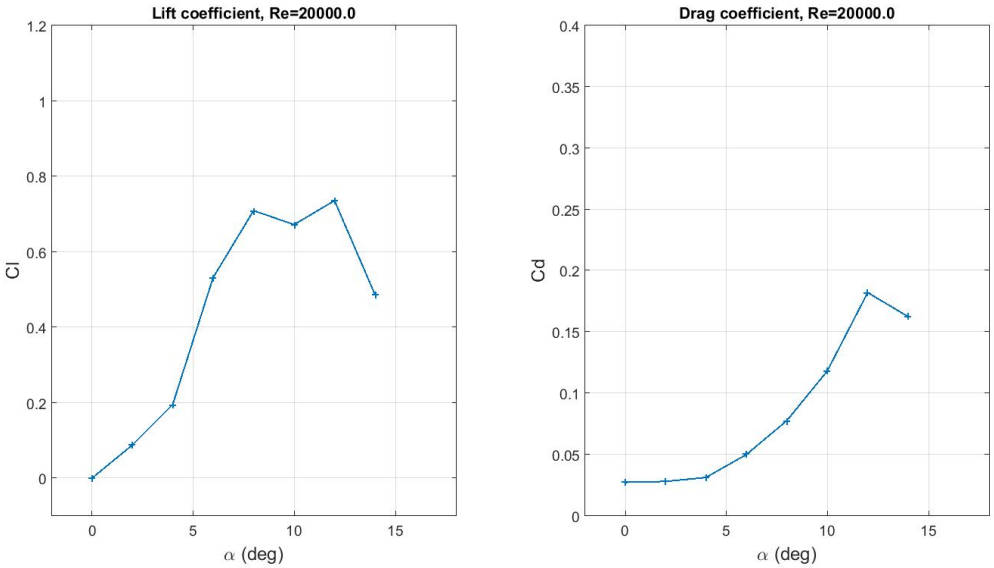

Figure A.20: Polars for NACA 0009-05, $Re = 2 \cdot 10^4$

Reynolds 40'000

Table A.21: Data for NACA 0009-05, $Re = 4 \cdot 10^4$

Reynolds = 40000.0

Alpha	CL	CD	Cl/Cd	Ct	number of iterations
0	-0.00013	0.021091	-0.00619	-0.02109	3558
2	0.071073	0.023043	3.0843	-0.02055	10000
4	0.41199	0.030864	13.3484	-0.00205	6905
6	0.5596	0.046707	11.9811	0.012043	3952
8	0.65192	0.071775	9.0828	0.019653	7463
10	0.7095	0.13083	5.423	-0.00564	10000
12	0.72797	0.18621	3.9095	-0.03079	10000
14	0.82254	0.23724	3.4671	-0.03121	10000

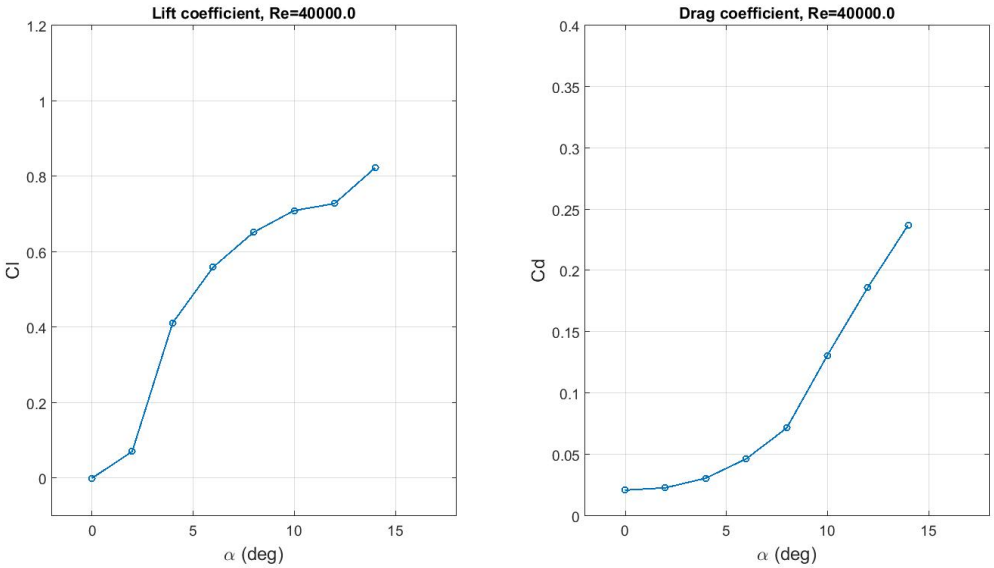

Figure A.21: Polars for NACA 0009-05, $Re = 4 \cdot 10^4$

A.8 NACA 0012-05

Reynolds 10'000

Table A.22: Data for NACA 0012-05, $Re = 10^4$

Reynolds = 10000.0

Alpha	CL	CD	Cl/Cd	Ct	number of iterations
0	-2.02E-05	0.043593	-0.00046	-0.04359	6182
2	0.065334	0.044517	1.4676	-0.04221	5572
4	0.15118	0.047056	3.2127	-0.0364	10000
6	0.24432	0.053426	4.5729	-0.0276	10000
8	0.61873	0.071511	8.6523	0.015296	6369
10	0.74859	0.10683	7.0074	0.024786	5927
12	0.70827	0.15664	4.5216	-0.00596	9184
14	0.68858	0.21522	3.1995	-0.04224	10000

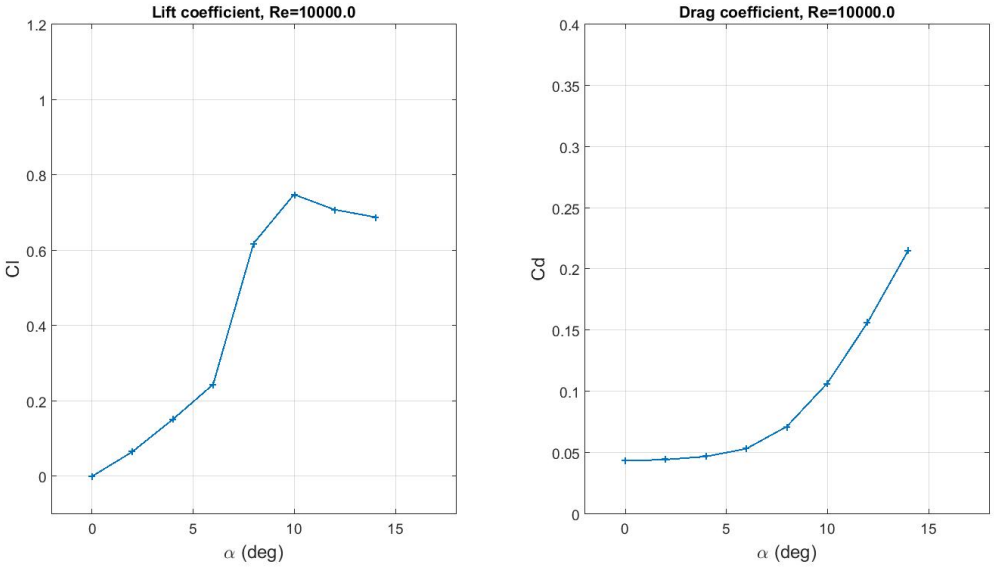

Figure A.22: Polars for NACA 0012-05, $Re = 10^4$

Reynolds 20'000

Table A.23: Data for NACA 0012-05, $Re = 2 \cdot 10^4$

Reynolds = 20000.0

Alpha	CL	CD	Cl/Cd	Ct	number of iterations
0	-2.46E-05	0.034376	-0.00072	-0.03438	5156
2	0.083321	0.035524	2.3454	-0.0326	10000
4	0.1599	0.039455	4.0526	-0.02821	10000
6	0.48166	0.044753	10.7626	0.005839	9669
8	0.60857	0.065852	9.2414	0.019485	5102
10	0.69384	0.097277	7.1326	0.024685	6966
12	0.63443	0.15451	4.1061	-0.01923	10000
14	0.59877	0.19348	3.0947	-0.04288	10000

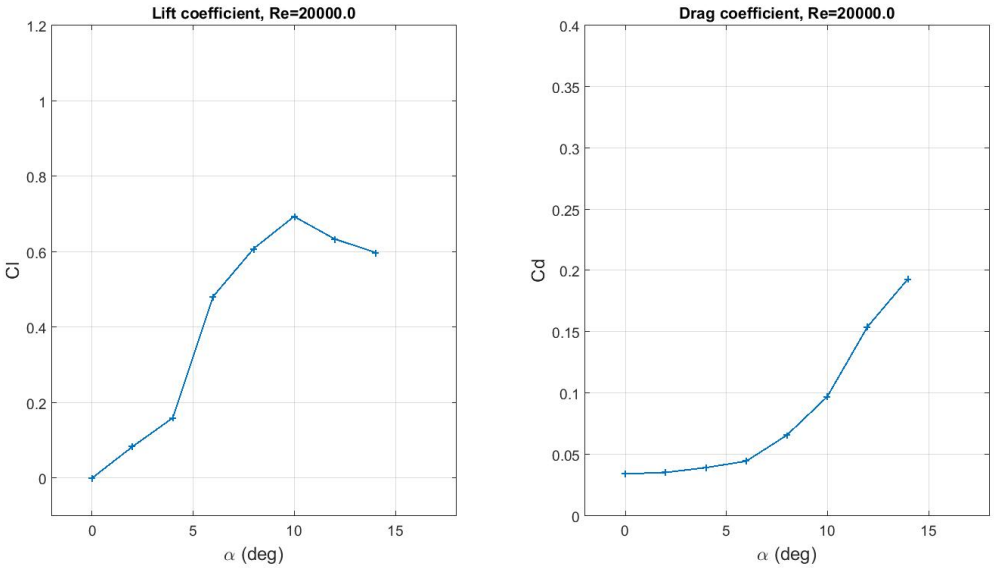

Figure A.23: Polars for NACA 0012-05, $Re = 2 \cdot 10^4$

Reynolds 40'000

Table A.24: Data for NACA 0012-05, $Re = 4 \cdot 10^4$

Reynolds = 40000.0

Alpha	CL	CD	Cl/Cd	Ct	number of iterations
0	0.000167	0.028454	0.005862	-0.02845	4076
2	0.11301	0.029281	3.8595	-0.02532	7092
4	0.2832	0.031911	8.8748	-0.01208	10000
6	0.49878	0.0422	11.8195	0.010168	7506
8	0.59828	0.060262	9.928	0.023589	6025
10	0.58438	0.091908	6.3583	0.010964	9975
12	0.65509	0.16872	3.8828	-0.02883	10000
14	0.70154	0.22428	3.1279	-0.0479	10000

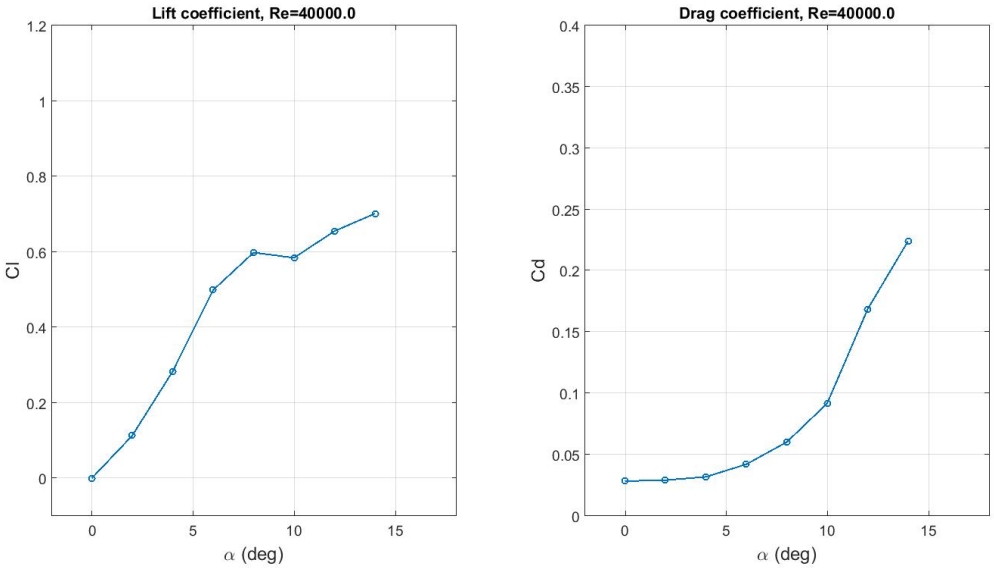

Figure A.24: Polars for NACA 0012-05, $Re = 4 \cdot 10^4$

A.9 NACA 5505

Reynolds 10'000

Table A.25: Data for NACA 5505, $Re = 10^4$

Reynolds = 10000.0

Alpha	CL	CD	Cl/Cd	Ct	number of iterations
0	0.25275	0.038928	6.4927	-0.03893	2281
2	0.4365	0.043015	10.1476	-0.02776	2324
4	0.61048	0.050379	12.1179	-0.00767	2346
6	0.75428	0.062623	12.0447	0.016563	10000
8	0.8891	0.088845	10.0073	0.035759	10000
10	0.99959	0.12768	7.8292	0.047842	10000
12	1.0032	0.16716	6.0015	0.045072	10000
14	0.98405	0.20994	4.6874	0.034363	10000

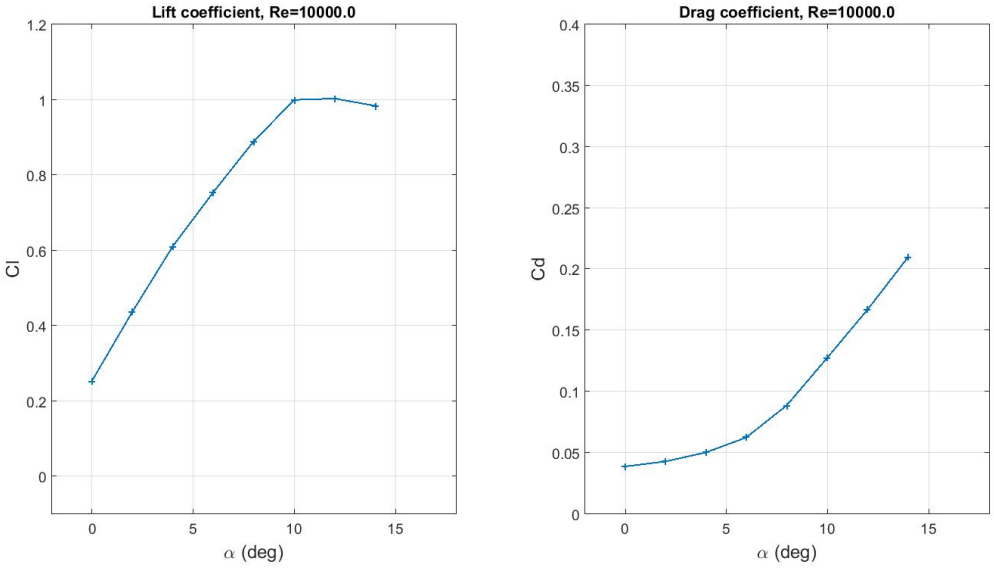

Figure A.25: Polars for NACA 5505, $Re = 10^4$

Reynolds 20'000

Table A.26: Data for NACA 5505, $Re = 2 \cdot 10^4$

Reynolds = 20000.0

Alpha	CL	CD	Cl/Cd	Ct	number of iterations
0	0.27916	0.030185	9.2483	-0.03019	2265
2	0.48507	0.034671	13.9904	-0.01772	2232
4	0.65996	0.042488	15.5328	0.003652	10000
6	0.82515	**0.056019**	14.7299	0.03054	10000
8	1.0111	0.067005	15.0898	0.074364	10000
10	1.0489	0.10288	10.1947	0.080812	3074
12	0.97879	0.15432	6.3426	0.052555	10000
14	**0.93798**	0.20115	4.6632	0.031747	10000

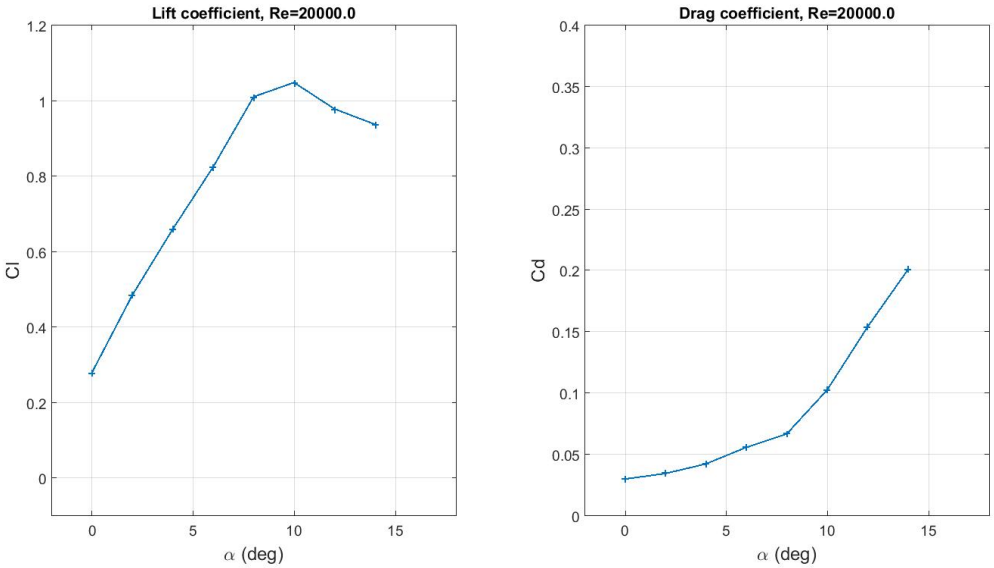

Figure A.26: Polars for NACA 5505, $Re = 2 \cdot 10^4$

Reynolds 40'000

Table A.27: Data for NACA 5505, $Re = 4 \cdot 10^4$

Reynolds = 40000.0

Alpha	CL	CD	Cl/Cd	Ct	number of iterations
0	**0.32123**	**0.024782**	12.9524	-0.02478	10000
2	**0.54081**	**0.028849**	18.762	-0.00993	10000
4	0.73086	0.03568	20.4841	0.01539	10000
6	**0.95309**	**0.038357**	24.8477	0.061478	10000
8	1.0412	**0.059739**	17.4289	0.085746	10000
10	1.0449	0.094385	11.071	0.0885	8477
12	0.94258	0.15344	6.1429	0.045884	10000
14	**0.91613**	0.19899	4.6037	0.028545	10000

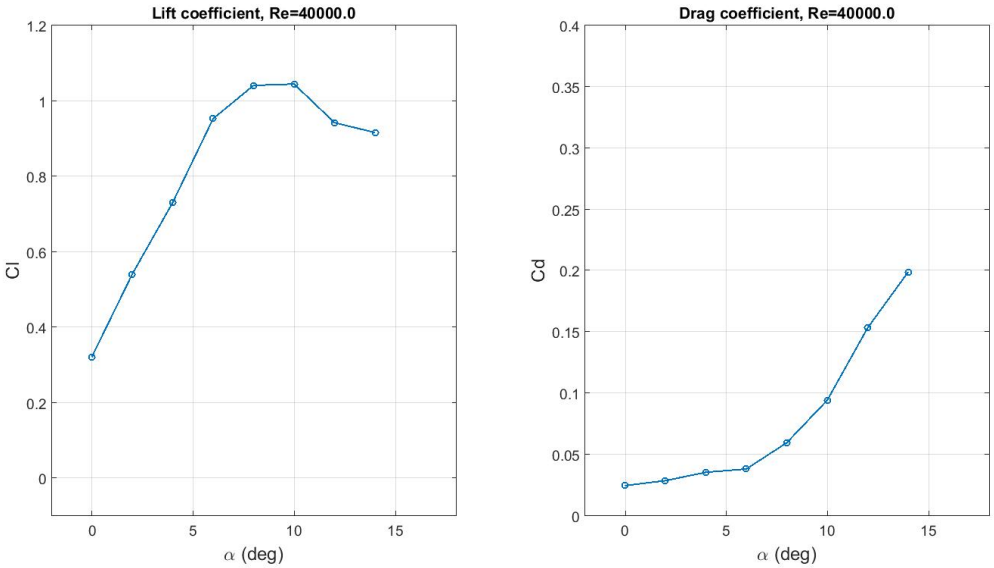

Figure A.27: Polars for NACA 5505, $Re = 4 \cdot 10^4$

A.10 NACA 5510

Reynolds 10'000

Table A.28: Data for NACA 5510, $Re = 10^4$

Reynolds = 10000.0

Alpha	CL	CD	Cl/Cd	Ct	number of iterations
0	**0.13498**	**0.047224**	2.8624	-0.04729	10000
2	0.32121	0.053123	6.0465	-0.04188	10000
4	0.49526	0.06259	7.9127	-0.02789	10000
6	0.65369	0.075837	8.6196	-0.00709	10000
8	0.79273	0.094932	8.3505	0.016319	10000
10	0.88994	0.12355	7.203	0.032862	10000
12	0.93006	0.1627	5.7165	0.034229	10000
14	0.93121	0.20176	4.6155	0.029517	10000

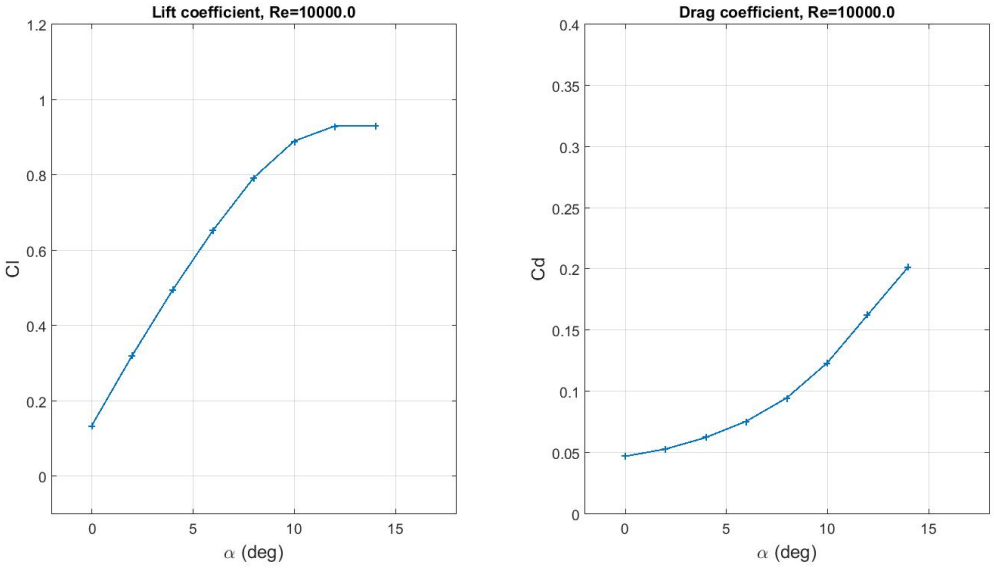

Figure A.28: Polars for NACA 5510, $Re = 10^4$

Reynolds 20'000

Table A.29: Data for NACA 5510, $Re = 2 \cdot 10^4$

Reynolds = 20000.0

Alpha	CL	CD	Cl/Cd	Ct	number of iterations
0	0.18986	0.038619	4.9163	-0.03862	10000
2	0.40038	0.044592	8.9788	-0.03059	10000
4	0.57154	**0.052973**	10.7891	-0.01298	10000
6	0.70847	0.06541	10.8312	0.009003	10000
8	0.80419	0.08499	9.4622	0.027759	10000
10	0.86269	0.11517	7.4907	0.036387	10000
12	0.91812	0.15707	5.8451	0.037246	10000
14	0.89302	0.19513	4.5766	0.026711	10000

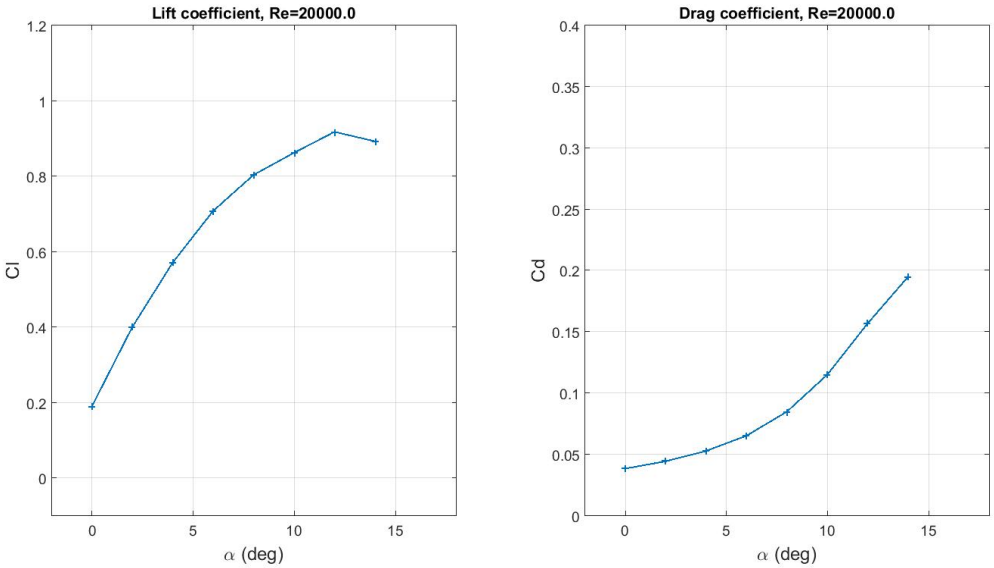

Figure A.29: Polars for NACA 5510, $Re = 2 \cdot 10^4$

Reynolds 40'000

Table A.30: Data for NACA 5510, $Re = 4 \cdot 10^4$

Reynolds = 40000.0

Alpha	CL	CD	Cl/Cd	Ct	number of iterations
0	0.24841	**0.032715**	7.5934	-0.03271	10000
2	0.45471	**0.036324**	12.518	-0.02043	10000
4	0.6188	0.04384	14.1152	-0.00057	10000
6	0.8101	0.04749	17.0584	0.037449	10000
8	0.93109	0.059457	15.6599	0.070704	10000
10	1.0213	0.075302	13.5622	0.10318	10000
12	0.93803	0.13855	6.7705	0.059509	10000
14	0.8763	0.18528	4.7296	0.032219	10000

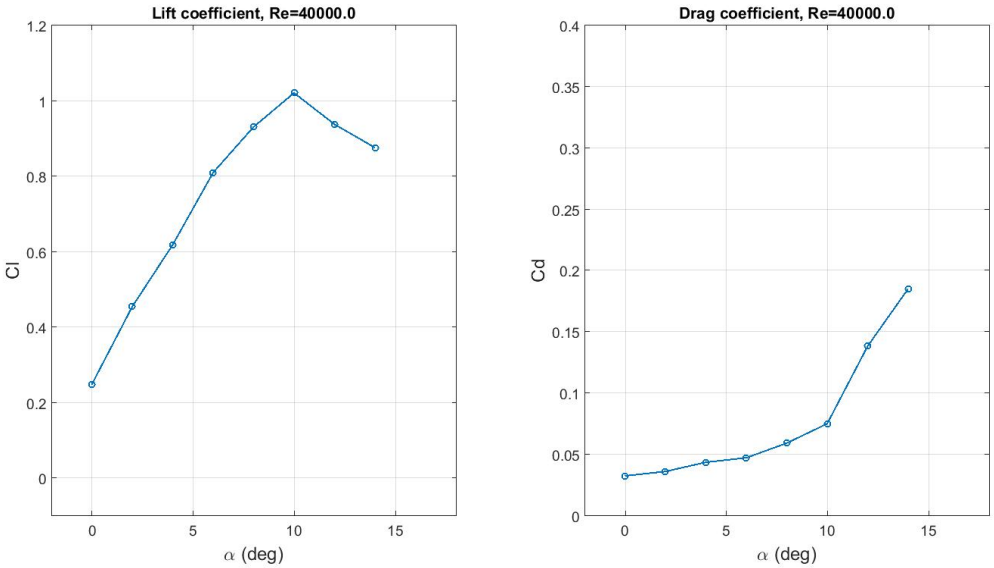

Figure A.30: Polars for NACA 5510, $Re = 4 \cdot 10^4$

A.11 E387

Reynolds 10'000

Table A.31: Data for E387, $Re = 10^4$

Reynolds = 10000.0

Alpha	CL	CD	Cl/Cd	Ct	number of iterations
0	0.10068	0.040931	2.4596	-0.04093	1653
2	0.26353	0.046764	5.6352	-0.03754	1709
4	0.43415	0.056294	7.7122	-0.02587	10000
6	0.59467	0.069723	8.5291	-0.00718	10000
8	0.7293	0.089271	8.1695	0.013097	10000
10	0.78234	0.11654	6.7129	0.021079	10000
12	0.80561	0.15259	5.2796	0.018241	10000
14	0.83614	0.1917	4.3617	0.016273	10000

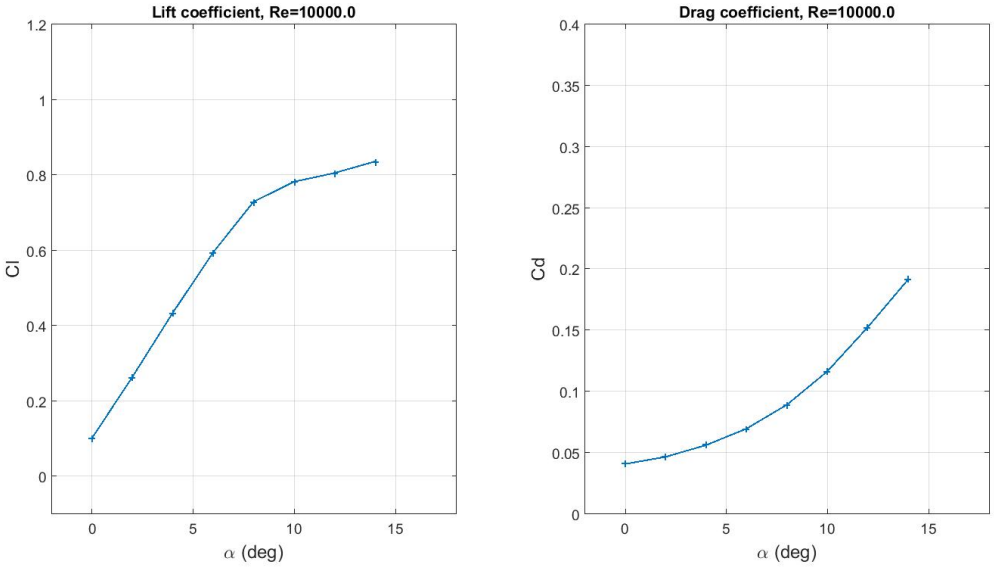

Figure A.31: Polars for E387, $Re = 10^4$

Reynolds 20'000

Table A.32: Data for E387, $Re = 2 \cdot 10^4$

Reynolds = 20000.0

Alpha	CL	CD	Cl/Cd	Ct	number of iterations
0	0.15457	0.032565	4.7465	-0.03257	1463
2	0.36192	0.038357	9.4356	-0.0257	10000
4	0.53158	0.046975	11.3163	-0.00978	10000
6	0.65351	0.059654	10.9549	0.008983	10000
8	0.72381	**0.080566**	8.9841	0.020953	10000
10	0.74861	0.10993	6.81	0.021737	10000
12	0.78253	0.14422	5.4258	0.021626	10000
14	0.82552	0.18729	4.4077	0.017982	10000

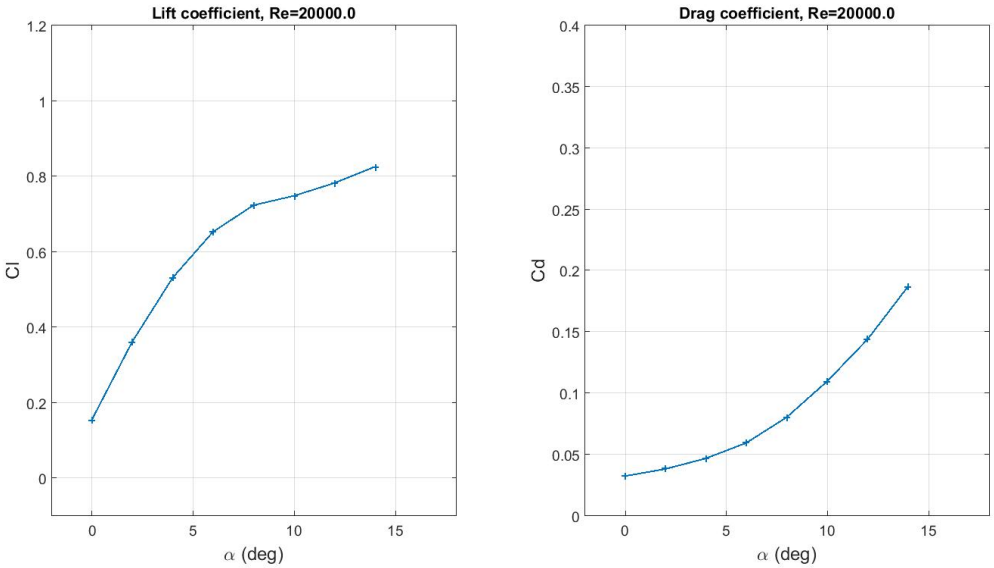

Figure A.32: Polars for E387, $Re = 2 \cdot 10^4$

Reynolds 40'000

Table A.33: Data for E387, $Re = 4 \cdot 10^4$

Reynolds = 40000.0

Alpha	CL	CD	Cl/Cd	Ct	number of iterations
0	0.2733	0.024233	11.2781	-0.02423	10000
2	0.48115	0.026939	17.861	-0.01013	10000
4	0.63041	0.034337	18.3595	0.009722	1595
6	0.76385	0.04134	18.4773	0.038731	3513
8	0.74446	0.070571	10.549	0.033724	10000
10	0.78472	0.096611	8.1224	0.041121	10000
12	0.87348	0.1537	5.683	0.031264	10000
14	0.95532	0.21756	4.391	0.020012	10000

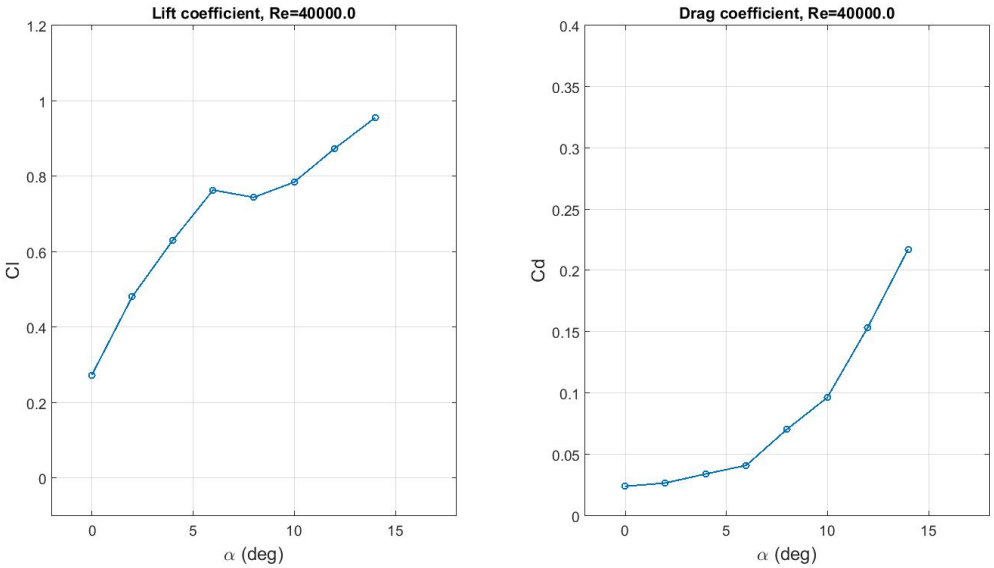

Figure A.33: Polars for E387, $Re = 4 \cdot 10^4$

A.12 S1223

Reynolds 10'000

Table A.34: Data for S1223, $Re = 10^4$

Reynolds = 10000.0

Alpha	CL	CD	Cl/Cd	Ct	number of iterations
0	0.18008	0.091671	1.9644	-0.091671	2127
2	0.48412	0.086263	5.6122	-0.069315	10000
4	0.77615	0.10032	7.7365	-0.045937	10000
6	0.91457	0.12172	7.5139	-0.025452	10000
8	0.98657	0.14673	6.7238	-0.0079958	10000
10	1.0405	0.1749	5.9488	0.0084291	10000
12	1.1515	0.21854	5.269	0.025643	10000
14	1.2216	0.26308	4.6435	0.040272	10000

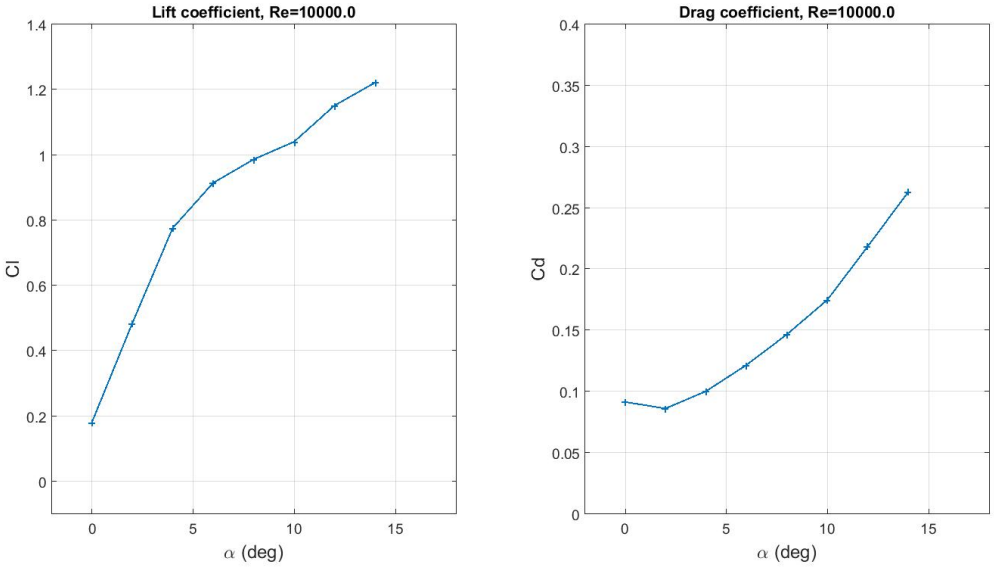

Figure A.34: Polars for S1223, $Re = 10^4$

Reynolds 20'000

Table A.35: Data for S1223, $Re = 2 \cdot 10^4$

Reynolds = 20000.0

Alpha	CL	CD	Cl/Cd	Ct	number of iterations
0	0.33512	0.077395	4.33	-0.077395	2265
2	0.67124	0.07344	9.1401	-0.049969	10000
4	0.86682	0.084929	10.2064	-0.024256	10000
6	0.93795	0.11053	8.4861	-0.01188	10000
8	0.97639	0.13811	7.0694	-0.00088407	10000
10	1.0559	0.15933	6.6269	0.02644	10000
12	1.1442	0.20244	5.6519	0.039871	10000
14	1.3472	0.28907	4.6603	0.045424	10000

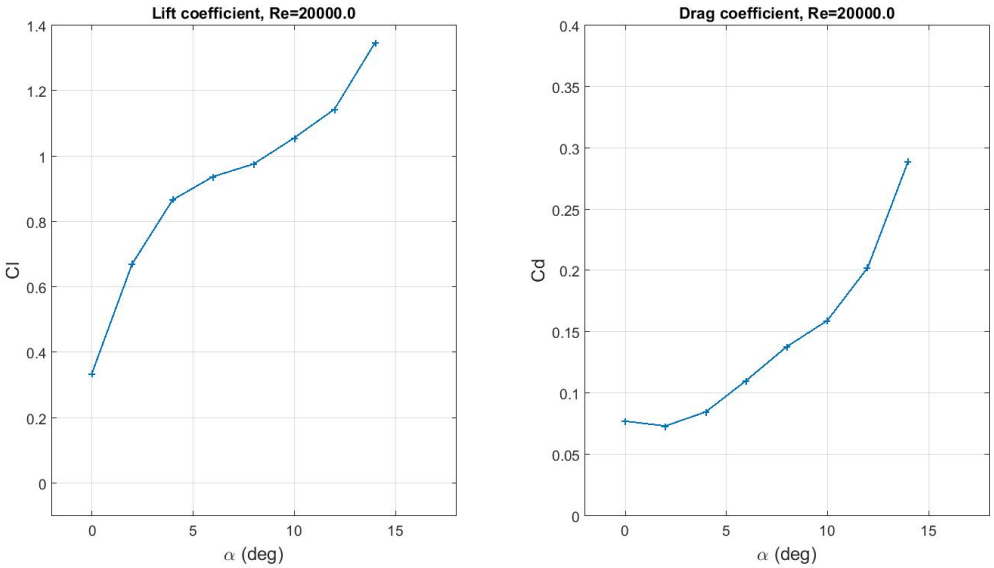

Figure A.35: Polars for S1223, $Re = 2 \cdot 10^4$

Reynolds 40'000

Table A.36: Data for S1223, $Re = 4 \cdot 10^4$

Reynolds = 40000.0

Alpha	CL	CD	Cl/Cd	Ct	number of iterations
0	0.57649	0.049819	11.5717	-0.049819	10000
2	0.96822	0.042987	22.5232	-0.009171	10000
4	1.108	0.05421	20.4387	0.023211	10000
6	0.93392	0.10583	8.8247	-0.007629	10000
8	0.97918	0.13275	7.3759	0.0048139	10000
10	1.0696	0.16172	6.6139	0.02647	10000
12	1.181	0.20575	5.7401	0.044295	10000
14	1.3434	0.29809	4.5068	0.035767	10000

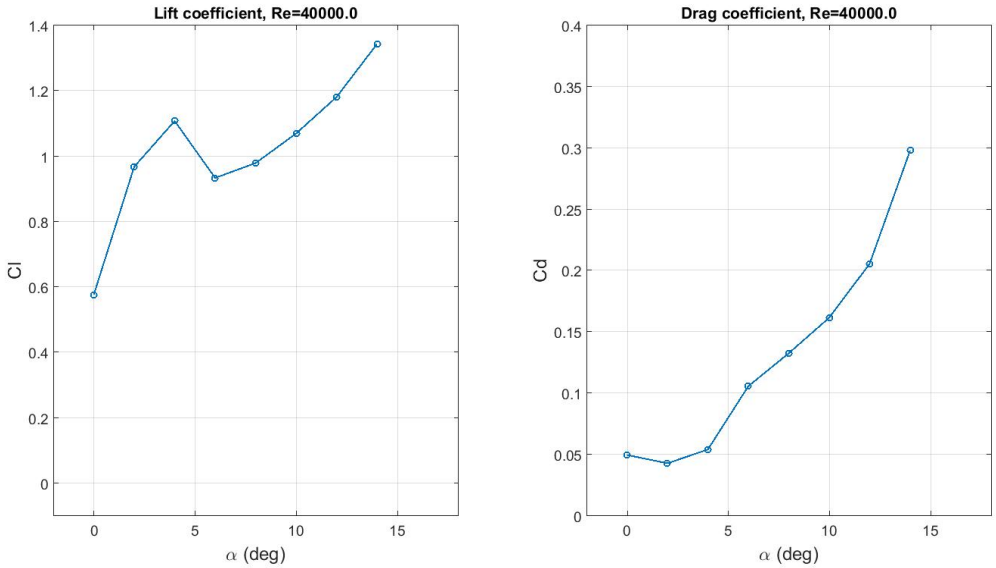

Figure A.36: Polars for S1223, $Re = 4 \cdot 10^4$

A.13 BW3

Reynolds 10'000

Table A.37: Data for BW3, $Re = 10^4$

Reynolds = 10000.0

Alpha	CL	CD	Cl/Cd	Ct	number of iterations
0	0.28681	0.04331	6.6222	-0.04331	1928
2	0.48034	0.04965	9.6746	-0.032856	1837
4	0.65657	0.061426	10.6888	-0.015476	1912
6	0.82137	0.080258	10.2341	0.0060383	10000
8	0.92483	0.1047	8.8335	0.025035	10000
10	0.99479	0.13738	7.2413	0.037453	10000
12	1.0193	0.17748	5.7435	0.038333	10000
14	1.0142	0.21775	4.6577	0.034079	10000

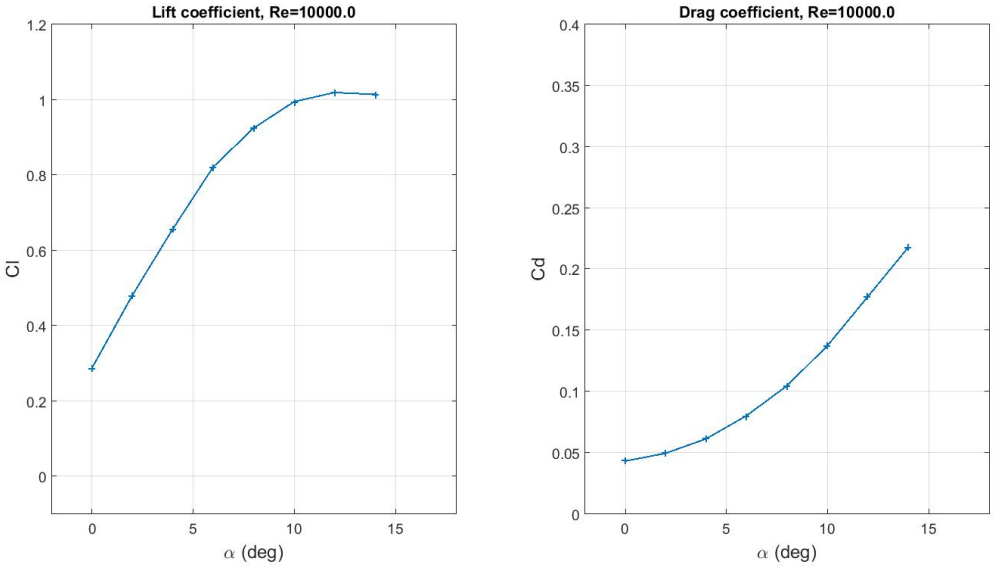

Figure A.37: Polars for BW3, $Re = 10^4$

Reynolds 20'000

Table A.38: Data for BW3, $Re = 2 \cdot 10^4$

Reynolds = 20000.0

Alpha	CL	CD	Cl/Cd	Ct	number of iterations
0	0.33847	0.037694	8.9793	-0.037694	10000
2	0.56163	0.040956	13.7132	-0.02133	10000
4	0.7443	0.051871	14.349	0.0001749	10000
6	0.88989	0.066577	13.3663	0.026806	10000
8	0.96007	0.089532	10.7232	0.044955	10000
10	0.9587	0.12794	7.4931	0.040476	10000
12	0.96128	0.17306	5.5547	0.030586	10000
14	0.97177	0.21242	4.5753	0.028992	10000

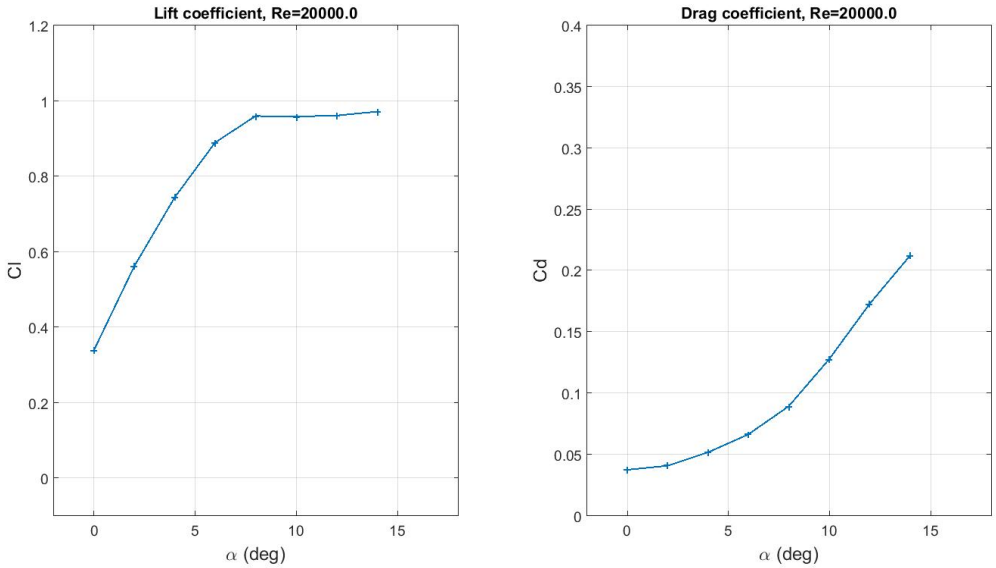

Figure A.38: Polars for BW3, $Re = 2 \cdot 10^4$

Reynolds 40'000

Table A.39: Data for BW3, $Re = 4 \cdot 10^4$

Reynolds = 40000.0

Alpha	CL	CD	Cl/Cd	Ct	number of iterations
0	0.42614	0.031551	13.5063	-0.031551	10000
2	0.64819	0.032593	19.8875	-0.0099514	10000
4	0.88518	0.032668	27.0963	0.029159	10000
6	1.0453	0.040372	25.8915	0.069112	10000
8	**1.1097**	0.059858	18.5396	0.095172	10000
10	0.93964	0.12365	7.5995	0.0414	10000
12	0.93725	0.17235	5.4383	0.026282	10000
14	0.95283	0.21026	4.5305	0.026467	10000

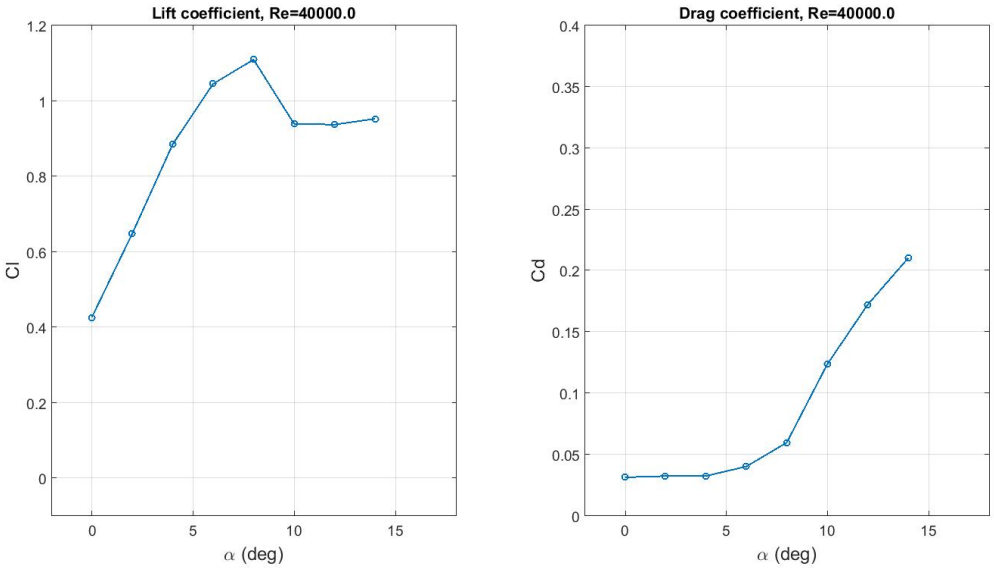

Figure A.39: Polars for BW3, $Re = 4 \cdot 10^4$

B Comparison with existing data (additional content)

B.1 Data from Kumar

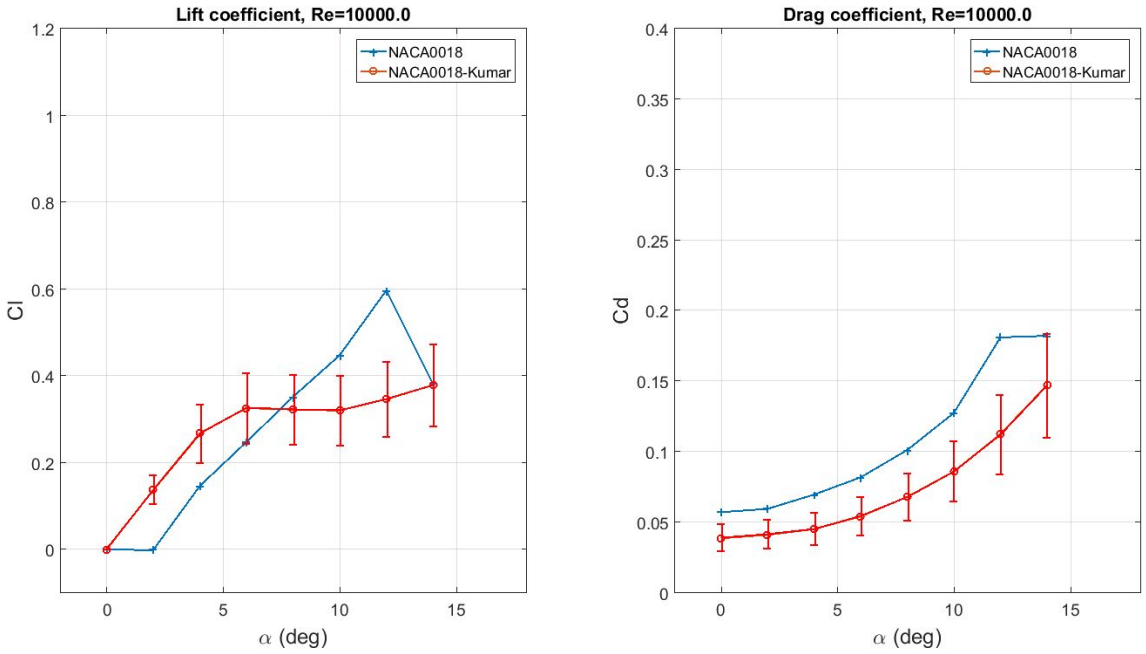

Figure B.1: Comparison of lift coefficients of NACA 0018 with Kumar, $Re = 10^4$

B.2 Data from Sheldahl

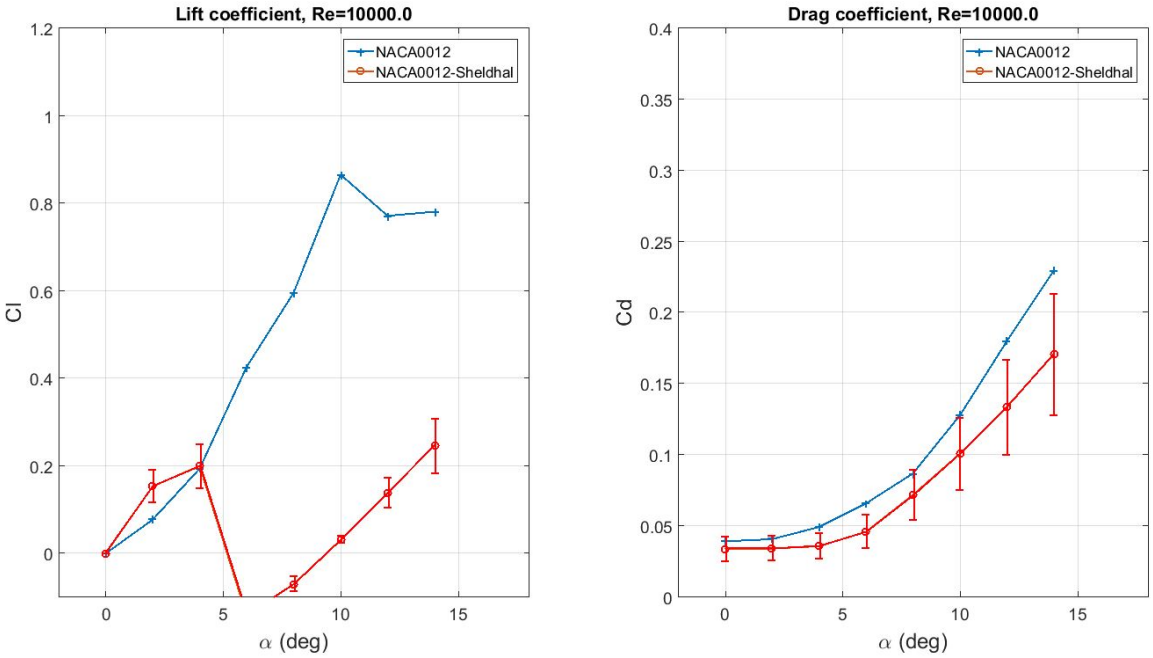

Figure B.2: Comparison of lift coefficients of NACA 0012 with Sheldahl, $Re = 10^4$

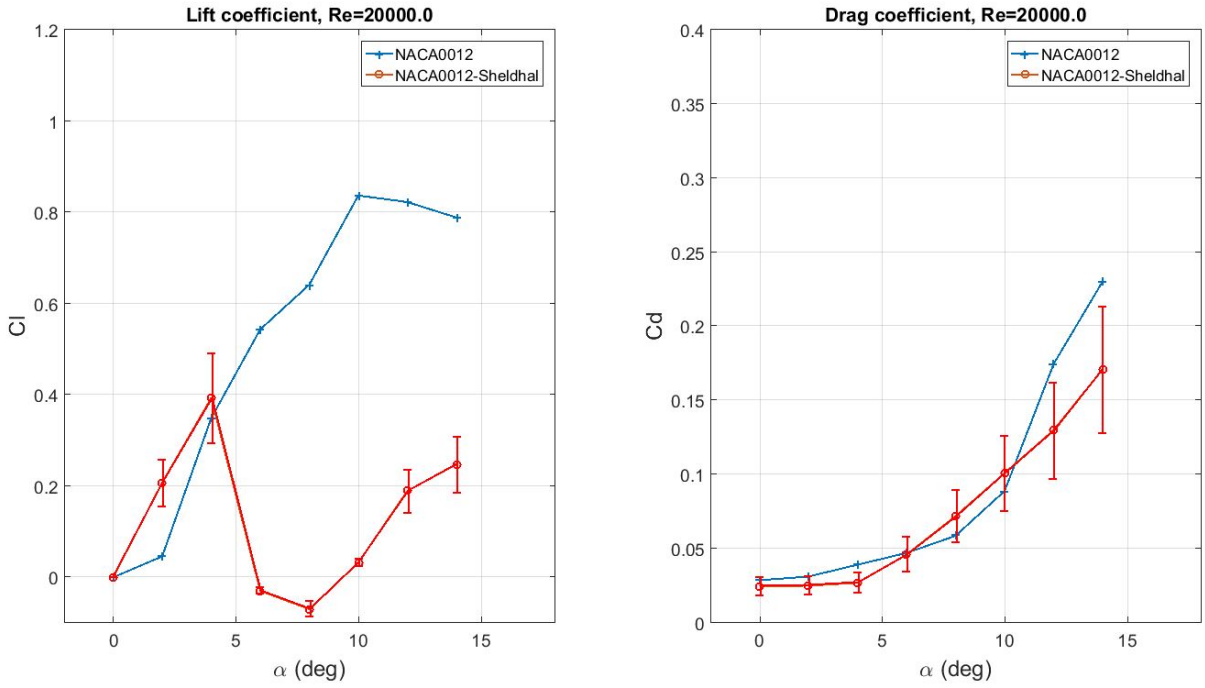

Figure B.3: Comparison of lift coefficients of NACA 0012 with Sheldahl, $Re = 2 \cdot 10^4$

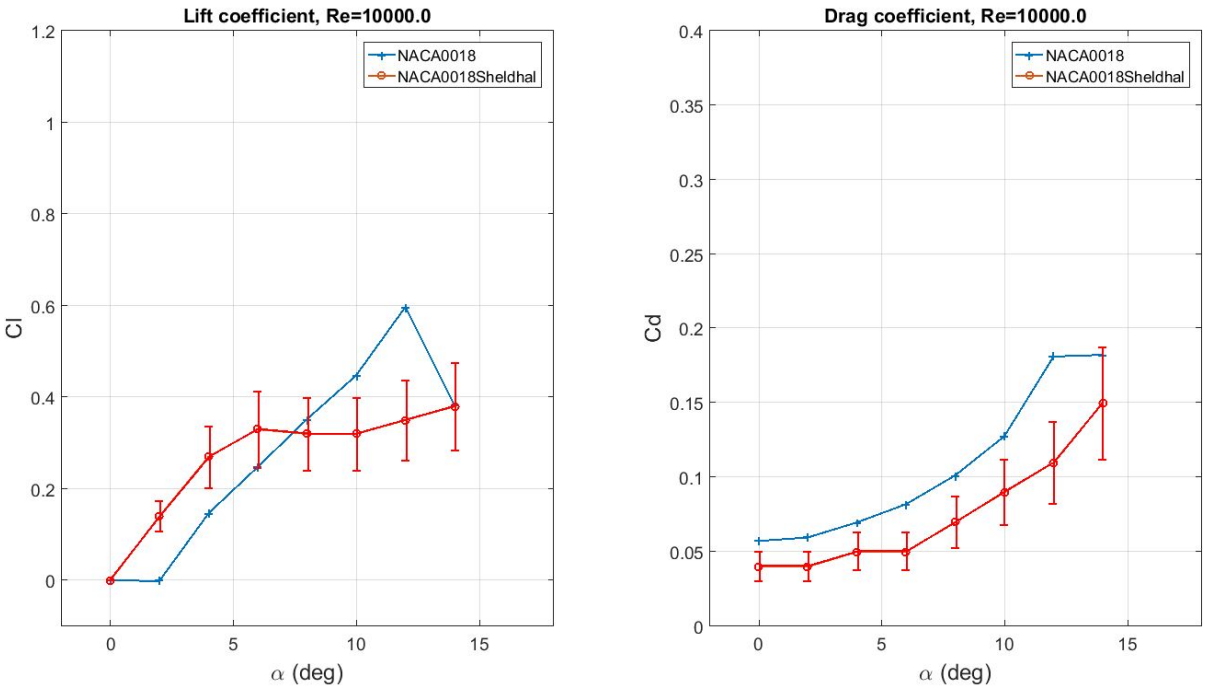

Figure B.4: Comparison of lift coefficients of NACA 0018 with Sheldahl, $Re = 10^4$

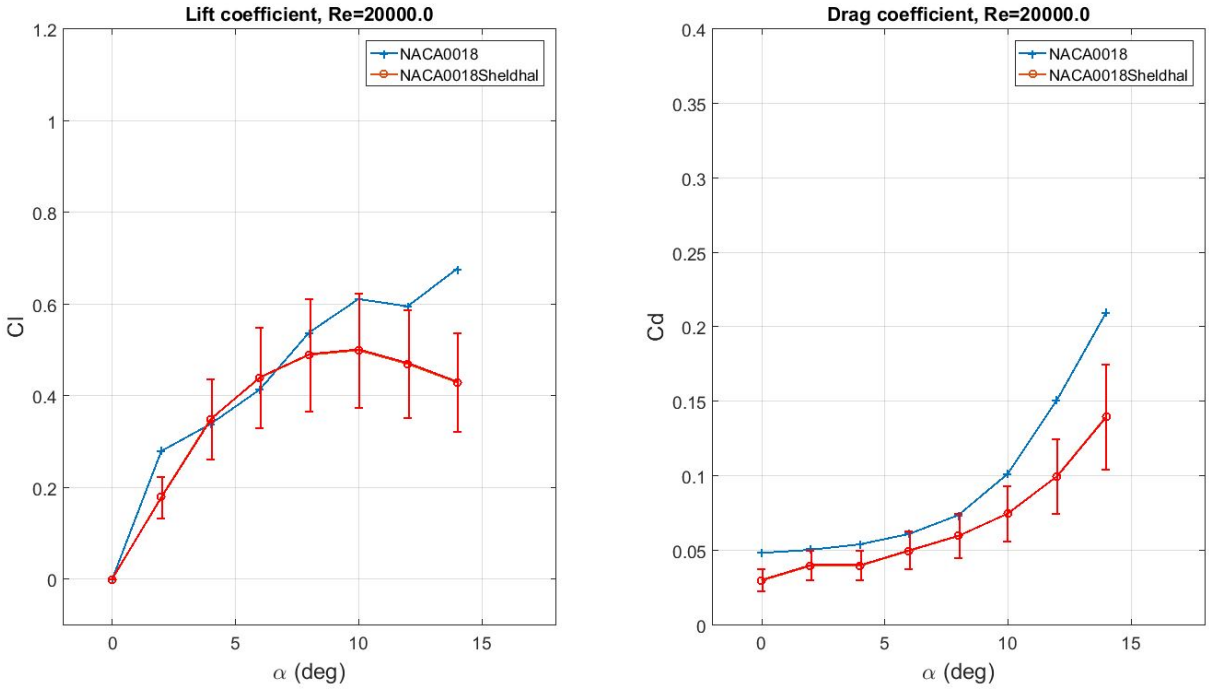

Figure B.5: Comparison of lift coefficients of NACA 0018 with Sheldahl, $Re = 2 \cdot 10^4$

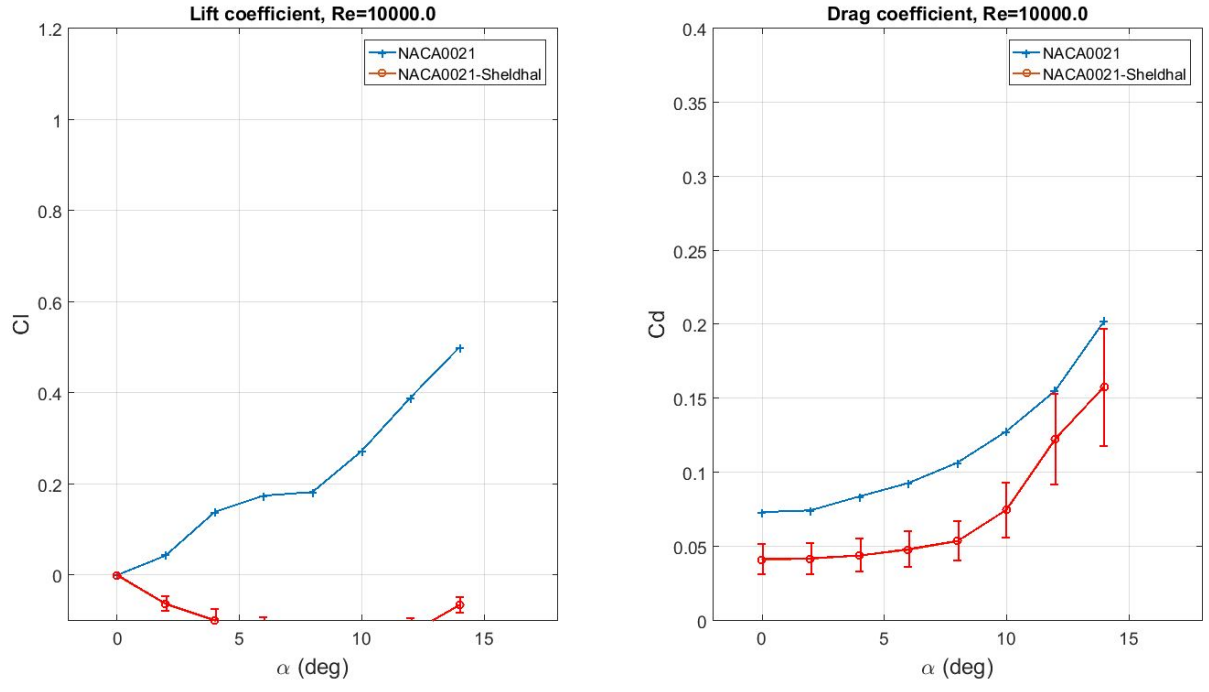

Figure B.6: Comparison of lift coefficients of NACA 0021 with Sheldahl, $Re = 10^4$

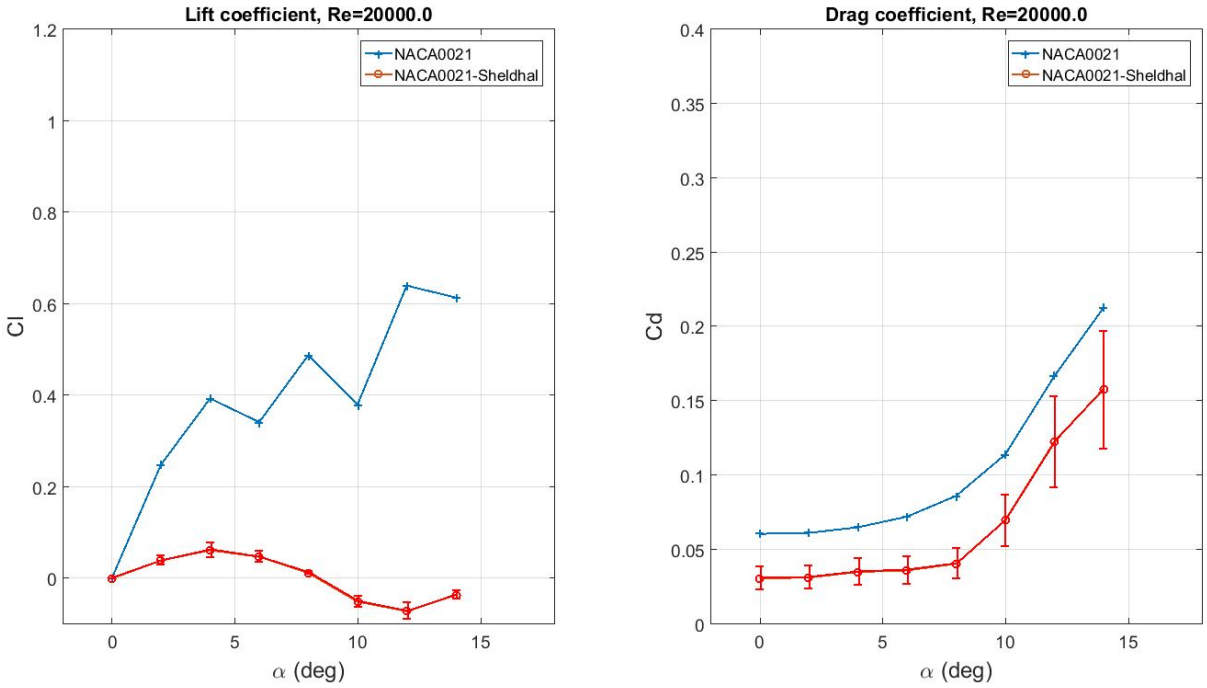

Figure B.7: Comparison of lift coefficients of NACA 0021 with Sheldahl, $Re = 2 \cdot 10^4$

C Comparison between simulations (additional content)

C.1 Addition of a camber

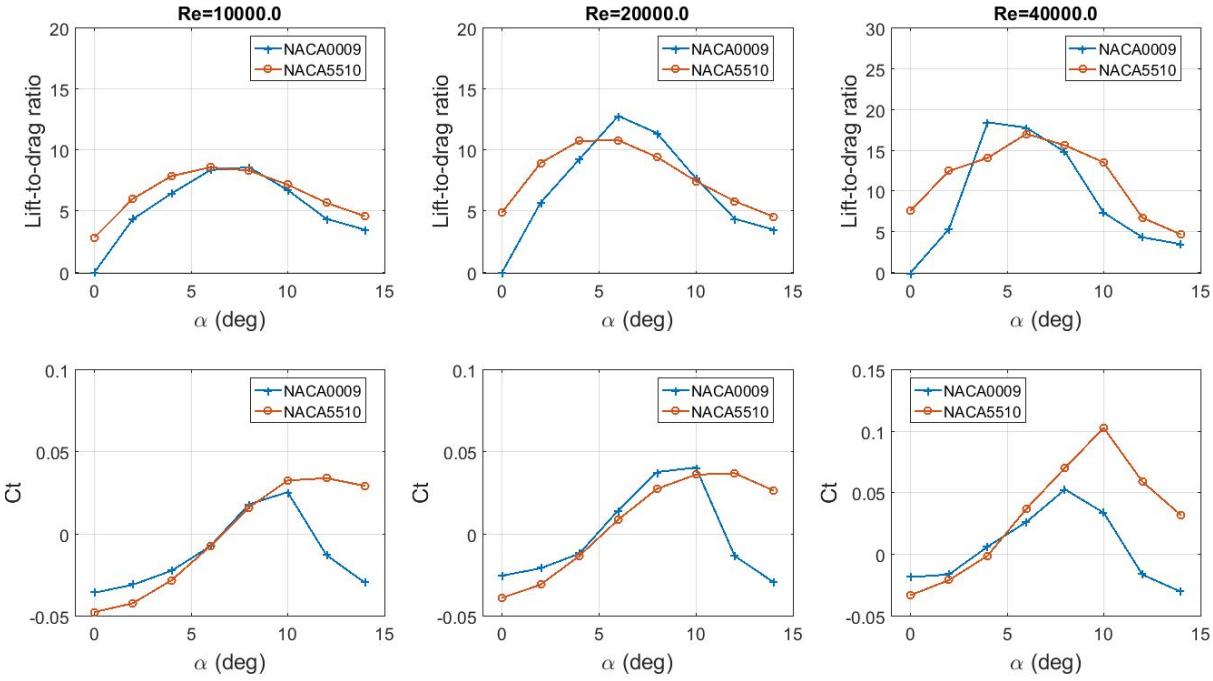

Figure C.8: Comparison between NACA 0009 and NACA 5510

C.2 Specific airfoils

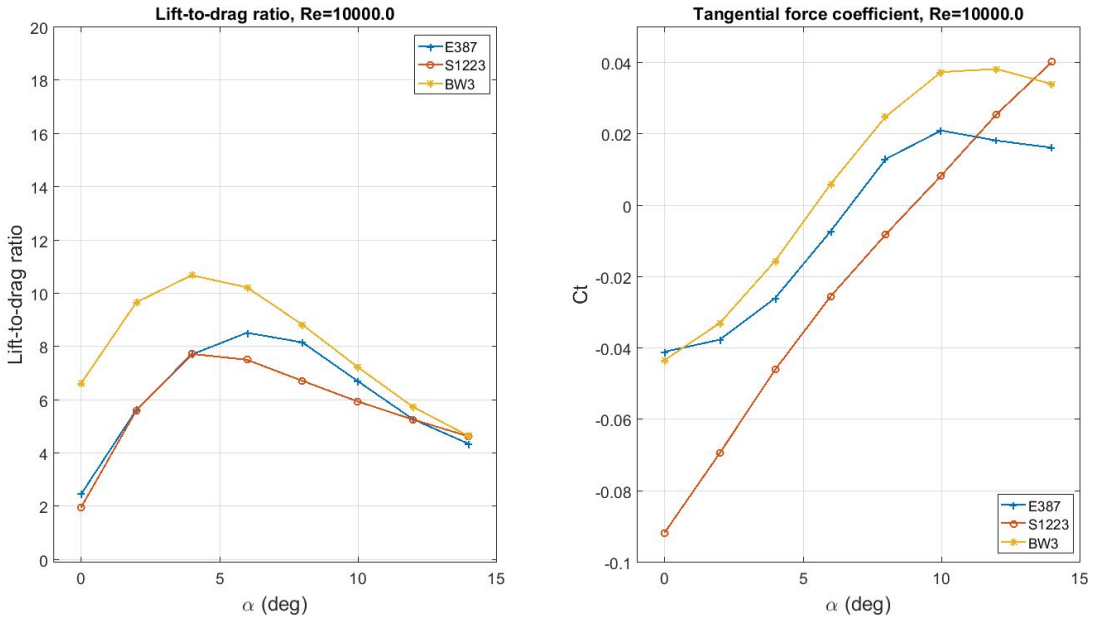

Figure C.9: Comparison of E387, S1223 and BW3 at $Re = 10^4$

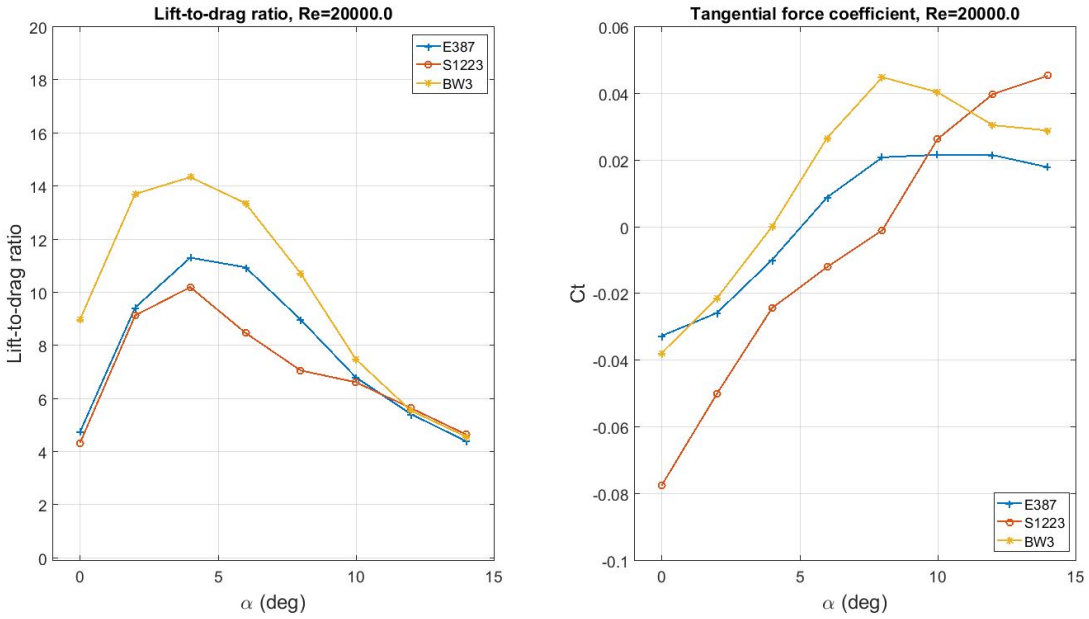

Figure C.10: Comparison of E387, S1223 and BW3 at $Re = 2 \cdot 10^4$

D Matlab scripts

All the Matlab scripts presented in this section were written for this project. They were used for post processing oh the data after the simulations were completed.

The first one is reading the lift and drag histories from Fluent and creates the tables presented in A. Three Excel tables are created per airfoil, one for each Reynolds number. For each angle of attack, the script is writing down the number of iterations, the C_l and C_d coefficients and is additionally computing the lift-to-drag ratio as well as the tangential force coefficients. This script is presented in Appendix D.1.

The second script is reading the values from the previously created Excel tables. It is then plotting the lift and drag polars for each Reynolds number of a given airfoil. It is presented in Appendix D.2.

The last one is comparing the airfoils amongst them. Many versions of this scripts exist (for existing data as well) for the principle remains always the same. The lift-to-drag ratios and the tangential force coefficients are taken from the Excel files and plotted for the comparison. A version of this script is presented in Appendix D.3.

D.1 Script "read.m"

```
function[] = read(fileOut1)
% Collect and read all the Cl and Cd files to extract the last iterations
% of each file in order to have for each Reynolds and each alpha, the Cl
% and Cd corresponding.

type = 'BW3';

%Range of Reynolds and alpha
aoa = {'0','2','4','6','8','10','12','14'};
Re={'10000.0','20000.0','40000.0'};

name_Cd={'','','';'','','';'','','';'','','';'','','';'','','';'','','';...
    '',''};
name_Cl={'','','';'','','';'','','';'','','';'','','';'','','';'','','';...
    '',''};

% Vectors Cl and Cd for Re = 10000.0
a1 = zeros(8,1);
a2 = zeros(8,1);

% Vectors Cl and Cd for Re = 20000.0
b1 = zeros(8,1);
b2 = zeros(8,1);

% Vectors Cl and Cd for Re = 40000.0
c1 = zeros(8,1);
c2 = zeros(8,1);
```

```
% Name of each files :
for i=1:8
    for j=1:3
        name_Cd{i,j}= strcat('CD-',type,'-sst_stdInit_convE-5-a',aoa{i},...
            'Re',Re{j},'.txt');
        name_Cl{i,j}= strcat('CL-',type,'-sst_stdInit_convE-5-a',aoa{i},...
            'Re',Re{j},'.txt');
    end
end

%Storing number of iterations for each simulation:
n=zeros(8,3); %1 column per Reynolds and 1 line per alpha

%Reading the values of each file and extracting the last one for
%Reynolds = 10000.0
for i=1:8
    temp1 = dlmread(name_Cl{i,1},'',2,1);
    a1(i)=temp1(length(temp1));
    n(i,1)=length(temp1);
    temp2 = dlmread(name_Cd{i,1},'',2,1);
    a2(i)=temp2(length(temp2));
    length(temp2)
end
%Reading the values of each file and extracting the last one for
%Reynolds = 20000.0
for i=1:8
    temp1 = dlmread(name_Cl{i,2},'',2,1);
    b1(i)=temp1(length(temp1));
    n(i,2)=length(temp1);
    temp2 = dlmread(name_Cd{i,2},'',2,1);
    b2(i)=temp2(length(temp2));
    length(temp2)
end
%Reading the values of each file and extracting the last one for
%Reynolds = 40000.0
for i=1:8
    temp1 = dlmread(name_Cl{i,3},'',2,1);
    c1(i)=temp1(length(temp1));
    n(i,3)=length(temp1);
    temp2 = dlmread(name_Cd{i,3},'',2,1);
    c2(i)=temp2(length(temp2));
    length(temp2)
end

A = {'Reynolds = 10000.0','','','','','';'Alpha','CL','CD','Cl/Cd','Ct',...
    'number of iterations';'','','','','','';'','','','','','';'','','',...
    '','','';'','','','','','';'','','','','','';'','','','','','';'','',...
```

```
    '','','','';'','','','','','',''};
B = {'Reynolds = 20000.0','','','','','';'Alpha','CL','CD','Cl/Cd','Ct',...
    'number of iterations';'','','','','','';'','','','','','';'','','',...
    '','','';'','','','','','';'','','','','','';'','','','','','';'','',...
    '','','','';'','','','','',''};
C = {'Reynolds = 40000.0','','','','','';'Alpha','CL','CD','Cl/Cd','Ct',...
    'number of iterations';'','','','','','';'','','','','','';'','','',...
    '','','';'','','','','','';'','','','','','';'','','','','','';'','',...
    '','','','';'','','','','',''};

%Calcul de Ct = Cl*sin(aoa) - Cd*cos(aoa)
for i=1:8
    alpha=str2num(aoa{i});
    Ct1(i)=a1(i)*sin(alpha*pi()/180)-a2(i)*cos(alpha*pi()/180);
    Ct2(i)=b1(i)*sin(alpha*pi()/180)-b2(i)*cos(alpha*pi()/180);
    Ct3(i)=c1(i)*sin(alpha*pi()/180)-c2(i)*cos(alpha*pi()/180);
end

% Grouping of the values for each Reynolds
for i=1:8
    A{i+2,1} = aoa{i};   % For Re = 10000.0
    A{i+2,2}=num2str(a1(i));
    A{i+2,3}=num2str(a2(i));
    A{i+2,4}=num2str(a1(i)/a2(i));
    A{i+2,5}=num2str(Ct1(i));
    A{i+2,6}=num2str(n(i,1));

    B{i+2,1} = aoa{i};   % For Re = 20000.0
    B{i+2,2}=num2str(b1(i));
    B{i+2,3}=num2str(b2(i));
    B{i+2,4}=num2str(b1(i)/b2(i));
    B{i+2,5}=num2str(Ct2(i));
    B{i+2,6}=num2str(n(i,2));

    C{i+2,1} = aoa{i};   % For Re = 40000.0
    C{i+2,2}=num2str(c1(i));
    C{i+2,3}=num2str(c2(i));
    C{i+2,4}=num2str(c1(i)/c2(i));
    C{i+2,5}=num2str(Ct3(i));
    C{i+2,6}=num2str(n(i,3));
end

%Writing the tables
xlswrite(fileOut1,A);
xlswrite(fileOut1,B,2);
xlswrite(fileOut1,C,3);
```

D.2 Script "plotClCd.m"

```
function[] = plotClCd(xls1)

% extract and plot lift and drag coefficients from excel file
% The files should contain one Reynolds per sheet
% and the value should go from the range A3 to F10.
type = xls1;
% Angles
aoa = [0 2 4 6 8 10 12 14];
%Reading the files for each Reynolds (one per sheet) and each alpha (8 in
%total)
cont11 = xlsread(type,1,'A3:E10'); %Reynolds 1 (10000)
cont12 = xlsread(type,2,'A3:E10'); %Reynolds 2 (20000)
cont13 = xlsread(type,3,'A3:E10'); %Reynolds 3 (40000)
for i =1:8
    Cl11(i)=cont11(i,2);
    Cl12(i)=cont12(i,2);
    Cl13(i)=cont13(i,2);
    Cd11(i)=cont11(i,3);
    Cd12(i)=cont12(i,3);
    Cd13(i)=cont13(i,3);
    ratio11(i) = cont11(i,4);
    ratio12(i) = cont12(i,4);
    ratio13(i) = cont13(i,4);
    Ct11(i)=cont11(i,5);
    Ct12(i)=cont12(i,5);
    Ct13(i)=cont13(i,5);
end
% plotting Polars for Reynolds 1 : (10000.0)
fig1 = figure('color','white');
% plotting Cl
subplot(1,2,1);
plot(aoa,Cl11,'-+','LineWidth',1.5)
set(gca,'fontsize',14,'LineWidth',1.2)
grid on
ylim([-0.1 1.2])
xlim([-2 18])
xlabel('\alpha (deg)','fontsize',18)
ylabel('Cl','fontsize',18)
title('Lift coefficient, Re=10000.0')
% plotting Cd
subplot(1,2,2);
plot(aoa,Cd11,'-+','LineWidth',1.5)
set(gca,'fontsize',14,'LineWidth',1.2)
grid on
ylim([0 0.4])
xlim([-2 18])
```

```
xlabel('\alpha (deg)','fontsize',18)
ylabel('Cd','fontsize',18)
title('Drag coefficient, Re=10000.0')

% plotting Polars for Reynolds 2 : (20000.0)
fig2 = figure('color','white');
% plotting Cl
subplot(1,2,1);
plot(aoa,Cl12,'-+','LineWidth',1.5)
set(gca,'fontsize',14,'LineWidth',1.2)
grid on
ylim([-0.1 1.2])
xlim([-2 18])
xlabel('\alpha (deg)','fontsize',18)
ylabel('Cl','fontsize',18)
title('Lift coefficient, Re=20000.0')
% plotting Cd
subplot(1,2,2);
plot(aoa,Cd12,'-+','LineWidth',1.5)
set(gca,'fontsize',14,'LineWidth',1.2)
grid on
ylim([0 0.4])
xlim([-2 18])
xlabel('\alpha (deg)','fontsize',18)
ylabel('Cd','fontsize',18)
title('Drag coefficient, Re=20000.0')

% plotting Polars for Reynolds 3 : (40000.0)
fig3 = figure('color','white');
% plotting Cl
subplot(1,2,1);
plot(aoa,Cl13,'-o','LineWidth',1.5)
set(gca,'fontsize',14,'LineWidth',1.2)
grid on
ylim([-0.1 1.2])
xlim([-2 18])
xlabel('\alpha (deg)','fontsize',18)
ylabel('Cl','fontsize',18)
title('Lift coefficient, Re=40000.0')
% plotting Cd
subplot(1,2,2);
plot(aoa,Cd13,'-o','LineWidth',1.5)
set(gca,'fontsize',14,'LineWidth',1.2)
grid on
ylim([0 0.4])
xlim([-2 18])
xlabel('\alpha (deg)','fontsize',18)
ylabel('Cd','fontsize',18)
```

```
title('Drag coefficient, Re=40000.0')
```

D.3 Script "compareLD-v2.m"

```
function[] = compareLD-v2(xls1,xls2,xls3,xls4)%,xls5,xls6)

% extract and plot some lift and drag coefficient from excel files
% in order to compare them. The files should contain one Reynolds per sheet
% and The value should go from the range A3 to F10.

% Number of file to compare
N = nargin;

% Range of Y axis
ysupRatio1=20;
ysupRatio2=20;
ysupRatio3=30;
ysupCt1=0.1;
ysupCt2=0.1;
ysupCt3=0.1;

%Name of the files (entered)
fileName = {xls1,xls2,xls3,xls4};%,xls5,xls6};

% Angles
aoa = [0 2 4 6 8 10];% 12 14];

%allocating space
contRe1 = zeros(6,(4*N));
contRe2 = zeros(6,(4*N));
contRe3 = zeros(6,(4*N));

Cl1=zeros(6,4);
Cl2=zeros(6,4);
Cl3=zeros(6,4);

Cd1=zeros(6,4);
Cd2=zeros(6,4);
Cd3=zeros(6,4);

ratio1=zeros(6,4);
ratio2=zeros(6,4);
ratio3=zeros(6,4);

Ct1=zeros(6,4);
Ct2=zeros(6,4);
Ct3=zeros(6,4);
```

```
for j=1:N
    %position of the coefficient (8x5 tab) for this airfoils (j)
    li = 1;
    lf = 8;
    ri = 4*(j-1)+1;
    rf = 4*(j-1)+4;

    % for xls j
    contRe1(li:lf,ri:rf) = xlsread(fileName{j},1,'B3:E10'); %Reynolds 1 (10000)
    contRe2(li:lf,ri:rf) = xlsread(fileName{j},2,'B3:E10'); %Reynolds 2 (20000)
    contRe3(li:lf,ri:rf) = xlsread(fileName{j},3,'B3:E10'); %Reynolds 3 (40000)
end

for i=1:6
    for j=1:N
        %position des Cl
        rCl = 4*(j-1)+1;

        Cl1(i,j)=contRe1(i,rCl);
        Cl2(i,j)=contRe2(i,rCl);
        Cl3(i,j)=contRe3(i,rCl);

        %position des Cd
        rCd = 4*(j-1)+2;

        Cd1(i,j)= contRe1(i,rCd);
        Cd2(i,j)= contRe2(i,rCd);
        Cd3(i,j)= contRe3(i,rCd);

        %Position des ratios Cl/Cd
        rRatio = 4*(j-1)+3;

        ratio1(i,j) = contRe1(i,rRatio);
        ratio2(i,j) = contRe2(i,rRatio);
        ratio3(i,j) = contRe3(i,rRatio);

        %Position des Ct
        rCt = 4*(j-1)+4;

        Ct1(i,j)= contRe1(i,rCt);
        Ct2(i,j)= contRe2(i,rCt);
        Ct3(i,j)= contRe3(i,rCt);
    end
end

% plotting Reynolds 1 : (10000.0)
% plotting Cl/Cd ratio
```

```
fig1 = figure('color','white');
subplot(1,2,1);
plot(aoa,ratio1(:,1),'-+',aoa,ratio1(:,2),'-o',aoa,ratio1(:,3),'-*',...
    aoa,ratio1(:,4),'-x','LineWidth',1.5)%aoa,ratio1(:,5),'-s',aoa,
    %ratio1(:,6),'-d','LineWidth',1.5)%,aoa,ratio1(:,6),'-d',aoa,ratio1(:,7)
    %,'-h','LineWidth',1.5)
set(gca,'fontsize',14,'LineWidth',1.2)
grid on
ylim([-0.1 ysupRatio1])
xlim([-1 11])
xlabel('\alpha (deg)','fontsize',18)
ylabel('Lift-to-drag ratio','fontsize',18)
title('Lift-to-drag ratio, Re=10000.0')
%legend(xls1,xls2,xls3,xls4,xls5,'Location','best')
legend('NACA 0012','NACA 5505','E387','BW3','Location','best')

% plotting Ct comparison
subplot(1,2,2);
plot(aoa,Ct1(:,1),'-+',aoa,Ct1(:,2),'-o',aoa,Ct1(:,3),'-*',aoa,...
    Ct1(:,4),'-x','LineWidth',1.5)
    %aoa,Ct1(:,5),'-s',aoa,Ct1(:,6),'-d','LineWidth',1.5)
set(gca,'fontsize',14,'LineWidth',1.2)
grid on
ylim([-0.1 ysupCt1])
xlim([-1 11])
xlabel('\alpha (deg)','fontsize',18)
ylabel('Ct','fontsize',18)
title('Tangential force coefficient, Re=10000.0')

legend('NACA 0012','NACA 5505','E387','BW3','Location','best')

% plotting Reynolds 2 : (20000.0)
% plotting Cl/Cd ratio
fig2 = figure('color','white');
subplot(1,2,1);
plot(aoa,ratio2(:,1),'-+',aoa,ratio2(:,2),'-o',aoa,ratio2(:,3),'-*',...
    aoa,ratio2(:,4),'-x','LineWidth',1.5)
    %aoa,ratio2(:,5),'-s',aoa,ratio2(:,6),'-d','LineWidth',1.5)%,aoa,
    %ratio2(:,6),'-d',aoa,ratio2(:,7),'-h')'LineWidth',1.5)
set(gca,'fontsize',14,'LineWidth',1.2)
grid on
ylim([-0.1 ysupRatio2])
xlim([-1 11])
xlabel('\alpha (deg)','fontsize',18)
ylabel('Lift-to-drag ratio','fontsize',18)
title('Lift-to-drag ratio, Re=20000.0')
%legend(xls1,xls2,xls3,xls4,xls5,'Location','best')
legend('NACA 0012','NACA 5505','E387','BW3','Location','best')
```

```
% plotting Ct comparison
subplot(1,2,2);
plot(aoa,Ct2(:,1),'-+',aoa,Ct2(:,2),'-o',aoa,Ct2(:,3),'-*',aoa,Ct2(:,4),...
    '-x','LineWidth',1.5)%aoa,Ct2(:,5),'-s',aoa,Ct2(:,6),'-d','LineWidth',
    %1.5),aoa,Ct2(:,6),'-d',aoa,Ct2(:,7),'-h')'LineWidth',1.5)
set(gca,'fontsize',14,'LineWidth',1.2)
grid on
ylim([-0.1 ysupCt2])
xlim([-1 11])
xlabel('\alpha (deg)','fontsize',18)
ylabel('Ct','fontsize',18)
title('Tangential force coefficient, Re=20000.0')
%legend(xls1,xls2,xls3,xls4,xls5,'Location','best')
legend('NACA 0012','NACA 5505','E387','BW3','Location','best')

% plotting Reynolds 3 : (40000.0)
fig3 = figure('color','white');
% plotting Cl/Cd ratio

subplot(1,2,1);
plot(aoa,ratio3(:,1),'-+',aoa,ratio3(:,2),'-o',aoa,ratio3(:,3),'-*',...
    aoa,ratio3(:,4),'-x','LineWidth',1.5)%aoa,ratio3(:,5),'-s',aoa,
    %ratio3(:,6),'-d','LineWidth',1.5)%,aoa,ratio3(:,6),'-d',aoa,
    %ratio3(:,7),'-h')'LineWidth',1.5)

set(gca,'fontsize',14,'LineWidth',1.2)
grid on
ylim([-0.1 ysupRatio3])
xlim([-1 11])
xlabel('\alpha (deg)','fontsize',18)
ylabel('Lift-to-drag ratio','fontsize',18)
title('Lift-to-drag ratio, Re=40000.0')
%legend(xls1,xls2,xls3,xls4,xls5,'Location','best')

% plotting Ct comparison
subplot(1,2,2);
plot(aoa,Ct3(:,1),'-+',aoa,Ct3(:,2),'-o',aoa,Ct3(:,3),'-*',aoa,Ct3(:,4),...
    '-x','LineWidth',1.5)%aoa,Ct3(:,5),'-s',aoa,Ct3(:,6),'-d','LineWidth',
    %1.5),aoa,Ct3(:,6),'-d',aoa,Ct3(:,7),'-h')
set(gca,'fontsize',14,'LineWidth',1.2)
grid on
ylim([-0.1 ysupCt3])
xlim([-1 11])
xlabel('\alpha (deg)','fontsize',18)
ylabel('Ct','fontsize',18)
title('Tangential force coefficient, Re=40000.0')
```